Architecture Definition Document

Written by	
Di Tommaso Umberto	Written on 19/12/2023 09:18
Verified By	
Musso Giorgio	Verified on 19/12/2023 09:21
Cavaglia' Rosetta	Verified on 19/12/2023 09:53
Di Tommaso Umberto	Verified on 19/12/2023 09:22
Approved By	
Musso Giorgio	Approved on 19/12/2023 13:52
Released By	
Cavaglia' Rosetta	Released on 19/12/2023 14:15

Approval evidence is kept within the documentation management system.

SBSP Pre-Phase A System Study

Architecture Definition Document

DRL: TN 4

Written by	***Responsibility*** + handwritten signature if no electronic workflow tool
U. Di Tommaso	Author
Verified by	
F. Massobrio	Checker
R. Cavaglià	Configuration Manager
U. Di Tommaso	Systems Engineer
Approved by	
G. Musso	Program Manager
Documentation Manager	
R. Cavaglià	Configuration Administrator

Approval evidence is kept within the document management system

Change Records

ISSUE	DATE	§ CHANGE RECORDS	AUTHOR
01	03/11/2023	Issue 1	SBSP Team
02	19/12/2023	Updated §2.4, §24.1.2, §4.2.4.2, §4.2.4.3, §4.2.5, §4.3.1, §4.4, §5.2, §7, §10.1, §10.2, §10.3, §10.4, §10.5, §10.6 and §12.1	SBSP Team

Table of contents

1 Introduction

1.1 Scope and purpose

This document elaborates the SBSP system architecture, selected at the ASR, by means of detailed analyses and design development.

The optimization approach adopted, which leverages the use of MATLAB & Simulink, is presented and used to assess the architecture and form the basis of the system perfomance simulations.

Energy and system cost analyses have been performed to assess the economic feasibility. The SPS critical areas and technology needs have been investigated from a technical standpoint.

The potential environmental impact of the proposed solution has been considered togheter with the business case confirmation, the roadmap and a preliminary risk analysis.

Regarding the MBSE approach the ARCADIA method[1] has been adopted and all the developed models are provided in A.1.

[1] For further details refer to https://www.eclipse.org/capella/arcadia.html

1.2 Applicable documents

Internal code / DRL	Reference	Issue	Title	Location of record
[AD1]			Orbit Analyses for Commercial-Scale Space-Based Solar Power Systems	
[AD2]			ESSB-HB-U-005 Space system Life Cycle Assessment (LCA) Guidelines iss.1.0	
[AD3]			ESA LCA Database	
[AD4]			ECSS-U-AS-10C Rev.1 – Adoption Notice of ISO 24113: Space systems – Space debris mitigation requirements (3 December 2019)	
[AD5]			Study Report(s) from ESA Future Launchers Preparatory Programme activity titled “euroPean Reusable and cOsT Effective heavy lIft transport investigation” (PROTEIN)	
[AD6]			ESA-TECSF-SOW-2022-003590 - Statement of Work Pre-Phase A System Study of a Commercial-Scale Space-Based Solar Power (SBSP) System for Terrestrial Needs	

1.3 Reference documents

Internal code / DRL	Reference	Issue	Title	Location of record
[RD1]			Final Deliverables from Frazer-Nash Consultancy for ESA-funded study titled “Cost-Benefit Analysis of Space-Based Solar Power Generation for Terrestrial Energy Needs” https://ec.europa.eu/eurostat/cache/infographs/energy/bloc-2a.html https://esamultimedia.esa.int/docs/technology/frazer-nash-consultancy-SBSP-cost-benefit-study-full-deliverables.zip	
[RD2]			Final Deliverables from Roland Berger for ESA-funded study titled “Cost-Benefit Analysis of Space-Based Solar Power Generation for Terrestrial Energy Needs” https://esamultimedia.esa.int/docs/technology/roland-berger-SBSP-cost-benefit-study-full-deliverables.zip	
[RD3]			SPS-ALPHA: The First Practical Solar Power Satellite via Arbitrarily Large Phased Array (A 2011-2012 NASA NIAC Phase 1 Project)	
[RD4]			Mankins, John C. "New Developments in Space Solar Power." NSS Space Settlement Journal (2017): 1-30.	
[RD5]			Space Solar Power: An Overview – John C. Mankins (Presentation at ISDC 2022)	
[RD6]			Cash, Ian. "CASSIOPeiA–A new paradigm for space solar power." Acta Astronautica 159 (2019): 170-178.	

Internal code / DRL	Reference	Issue	Title	Location of record
			https://doi.org/10.1016/j.actaastro.2019.03.063	
[RD7]			Cash, Ian. "CASSIOPeiA solar power satellite." 2017 IEEE International Conference on Wireless for Space and Extreme Environments (WiSEE). IEEE, 2017. 10.1109/WiSEE.2017.8124908	
[RD8]			UK Patent: GB2571383 - Solar concentrator: https://www.ipo.gov.uk/p-ipsum/Case/PublicationNumber/GB2571383	
[RD9]			UK Patent: GB2563574 - A phased array antenna and apparatus incorporating the same https://www.ipo.gov.uk/p-ipsum/Case/PublicationNumber/GB2563574	
[RD10]			CASSIOPEIA SPS: Advantages for Commercial Power, I Cash (Presentation at ISDC 2022)	
[RD11]			Space Solar Power development in China and MR-SPS, 4th SPS Symposium 2018, Kyoto, Japan https://www.sspss.jp/MR-SPS4.pdf	
[RD12]			Fraas, Lewis M. "Mirrors in space for low-cost terrestrial solar electric power at night." 2012 38th IEEE Photovoltaic Specialists Conference. IEEE, 2012.	
[RD13]			Fraas, Lewis M., Geoffrey A. Landis, and Arthur Palisoc. "Mirror satellites in polar orbit beaming sunlight to terrestrial solar fields at dawn and dusk." 2013 IEEE 39th Photovoltaic Specialists Conference (PVSC). IEEE, 2013.	
[RD14]			Çelik, Onur, et al. "Enhancing terrestrial solar power using orbiting solar reflectors." Acta Astronautica 195 (2022): 276-286.	
[RD15]			Çelik, Onur, and Colin R. McInnes. "An analytical model for solar energy reflected from space with selected applications." Advances in Space Research 69.1 (2022): 647-663.	
[RD16]			ESSB-ST-U-004 ESA Re-entry Safety Requirements iss.1.0	
[RD17]			FNC 011337 53514R Space Based Solar Power End of Life Study Final Report (Frazer-Nash Consultancy) Issue 1	
[RD18]			FNC 011337 53615R Space Based Solar Power End of Life Study Summary Report (Frazer-Nash Consultancy) Issue 1	
[RD19]			Sala, Serenella, et al. "Global normalisation factors for the environmental footprint and life cycle assessment." Publications Office of the European Union: Luxembourg (2017): 1-16	
[RD20]			Attitude and Orbit Control of a Very Large Geostationary Solar Power Satellite Bong Wie - Arizona State University, Tempe, Arizona 85287-6106 Carlos M. Roithmayr - NASA Langley Research Center, Hampton, Virginia 23681-2199	
[RD21]			MODELING THE COMPLETED SPACE STATION A THREE DIMENSIONAL RIGID-FLEXIBLE DYNAMIC MODEL TO PREDICT MODES OF VIBRATION	

Internal code / DRL	Reference	Issue	Title	Location of record
			AND STRESS ANALYSIS José J. Granda, Louis Nguyen, Sukhbir S Hundal California State University, Sacramento. Department of Mechanical Engineering Sacramento, California, 95819 NASA Johnson Space Center Integrated Navigation, Guidance and Control Analysis Branch, Houston, TX 77058	
[RD22]			Formulas for Natural Frequency and Mode Shape – Robert D.Blevins	
[RD23]			Telescoping Solar Array Concept for Achieving High Packaging Efficiency Martin Mikulas1 National Institute of Aerospace, Hampton, VA 23666 and Richard Pappa, Jay Warren, Geoff Rose NASA Langley Research Center, Hampton, VA 23681	
[RD24]			Design and Performance of the Telescopic Tubular Mast Mehran Mobrem and Chris Spier Astro Aerospace – Northrop Grumman Aerospace Systems, Carpinteria, CA	
[RD25]			ECSS-M-ST-80C, Space Project Management - Risk Management (31 July 2008)	
[RD26]			K Ch Sri Kavya & al., "Beam pointing accuracy of phased arrays for Satellite communication", Journal of Theoretical and Applied Information Technology, 31st May 2017. Vol.95. No 10	
[RD27]			Shi Tang, Stefania Peracchi et al. “Effect of Hole Transport Materials and Their Dopants on the Stability and Recoverability of Perovskite Solar Cells on Very Thin Substrates after 7 MeV Proton Irradiation.” 22 May 2023	
[RD28]			“Testing of Thermal Runaway Tolerant Battery Designs Utilizing High Energy Density 18650 Lithium Ion Cells” Kyle Adam - Blake Cardwell - Joshua Fedders	
[RD29]			Teledyne HV FEP Wire Datasheet	
[RD30]			“POWER PROCESSING UNIT ACTIVITIES IN AIRBUS DS SPACE EQUIPMENTS” Fernando PINTÓ - Javier PALENCIA -Nicoletta WAGNER - Guillaume GLORIEUX	
[RD31]			Preliminary Elements on European Reusable and Cost-Effective Heavy Lift Transportation (PROTEIN) – PRO-RFA-IED-B Issue 0.9	
[RD32]			Coordinated Orbit–Attitude–Vibration Control of a Sun-Facing Solar Power Satellite, Qingjun Li and Zichen Deng, Journal of Guidance, Control, and Dynamics, Vol. 42, No. 8, August 2019	

Internal code / DRL	Reference	Issue	Title	Location of record
[RD33]			Optimal Attitude Sensors Placement for a Solar Power Satellite Considering Control–Structure Interaction, AIAA Journal, Vol. 57, No. 10, October 2019	

1.4 Definitions and Acronyms

Acronym/Abbreviation	Definition
AC	Alternating Current
ARCADIA	Architecture Analysis & Design Integrated Approach
ASR	Architecture Selection Review
CAPEX	Capital Expenditure
CER	Cost Estimation Relationships
ConOps	Concept of Operations
CFRP	Carbon Fiber Reinforced Polymer
CSI	Current Source Inverter
DLR	Deutsches Zentrum für Luft- und Raumfahrt
DC	Direct Current
DM	Digital Model
EES	Electrical Energy Storage
EESS	Electrical Energy Storage Systems
EHLL	European Heavy Lift Launcher
EPBT	Energy PayBack Time
ERoEI	Energy Return on Energy Investment
ESA	European Space Agency
FOAK	First Of A Kind
GCPC	Grid-Connected Power Converters
GEO	Geostationary Orbit
GHG	GreenHouse Gas
GPS	Ground Power Station
GWP	Global Warming Potential
HMI	Human Machine Interface
HV	High Voltage
IEC	International Electrotechnical Commission
IED	Inter-Activity Exchange Document
LC	Learning Curve
LCA	Life Cycle Assessment
LCE	Life Cycle Emissions
LCOE	Levelized Cost Of Energy
LV	Low Voltage
MBSE	Model Based Systems Engineering
MC	Main Controller
MV	Medium Voltage
NASA	National Aeronautics and Space Administration
NOAK	N-Of A Kind
OM	Operations & Maintenance
OPEX	Operational Expenditure
PCU	Power Control Unit
POC	Point Of Connection
PV	Photovoltaic
PVA	Photovoltaic Assembly
RF	Radio Frequency
RR	Risk Register
RRL	Ranked Risk Log
RTLS	Return To Launch Site
SARJ	Solar Alpha Rotary Joint
SBSP	Space-Based Solar Power
S/C	Spacecraft
SPS	Solar Power Satellite

SSDS	Strathclyde Space Systems Database
TAS	Thales Alenia Space
TSTO	Two Stage To Orbit
VSI	Voltage Source Inverter

2 Concept of Operations

2.1 Mission Phases

The SBSP mission phases are summarized below:

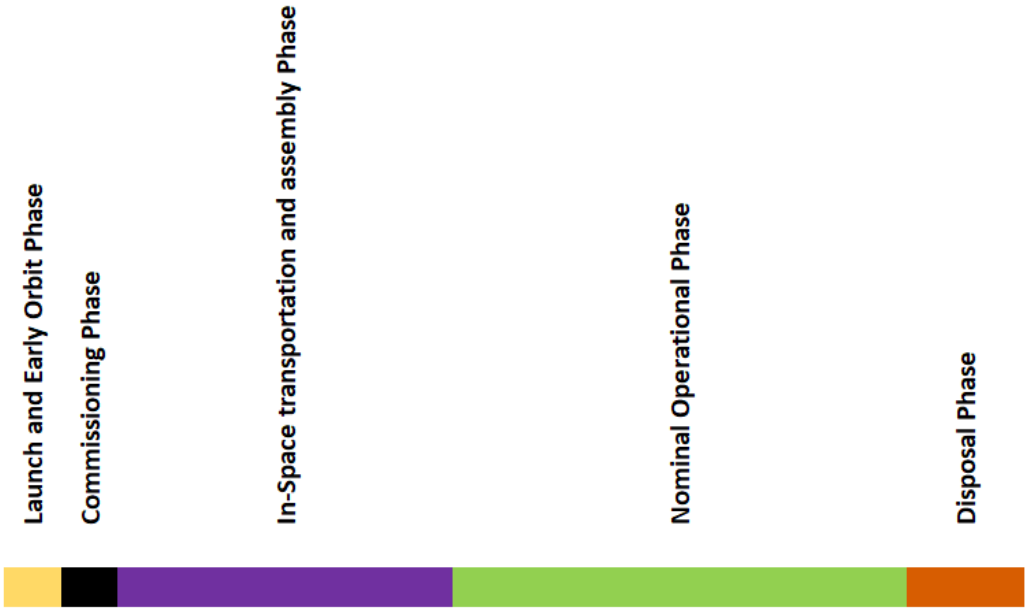

Figure 2-1 SBSP mission phases

and a pictorial overview is provided in Figure 2-2.

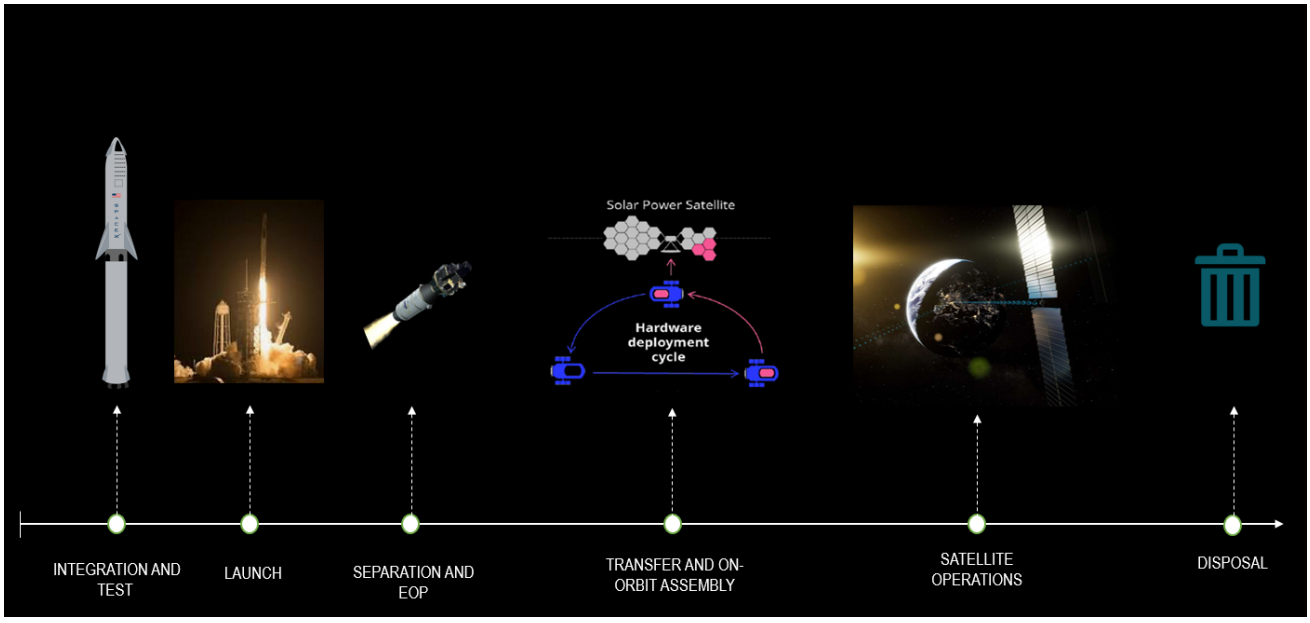

Figure 2-2 SBSP mission phases overview

2.2 Launch, Deployment & Assembly

For SPS launch, deployment and assembly three options have been analysed. The selected one is shown in Figure 2-3.

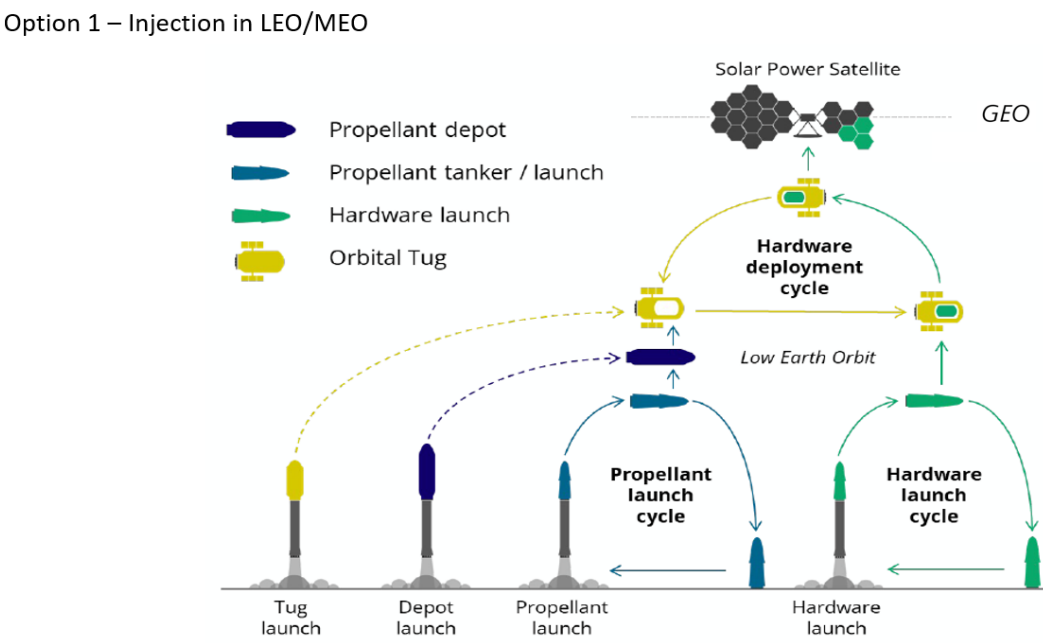

Figure 2-3 SPS launch, deployment and assembly

The concept foresees a modular in-orbit assembly for the antenna and the solar arrays, with several launches to LEO with cargos. Once in LEO, an orbital tug will be used to move the hardware from LEO to GEO. A propellant depot will be needed to refuel the tug during the mission.

Once in GEO, the hardware will be assembled thanks to the contribution of automated devices called In-Orbit Services. The concept foresees the capability to operate the SPS in a reduced power mode before the complete assembly take place. This will grant solar power beaming from early stage of the mission allowing in orbit test and refinements.

2.3 Communications Strategy

The Communications strategy, similar to the standard GEO satellites, is summarized in Figure 2-4.

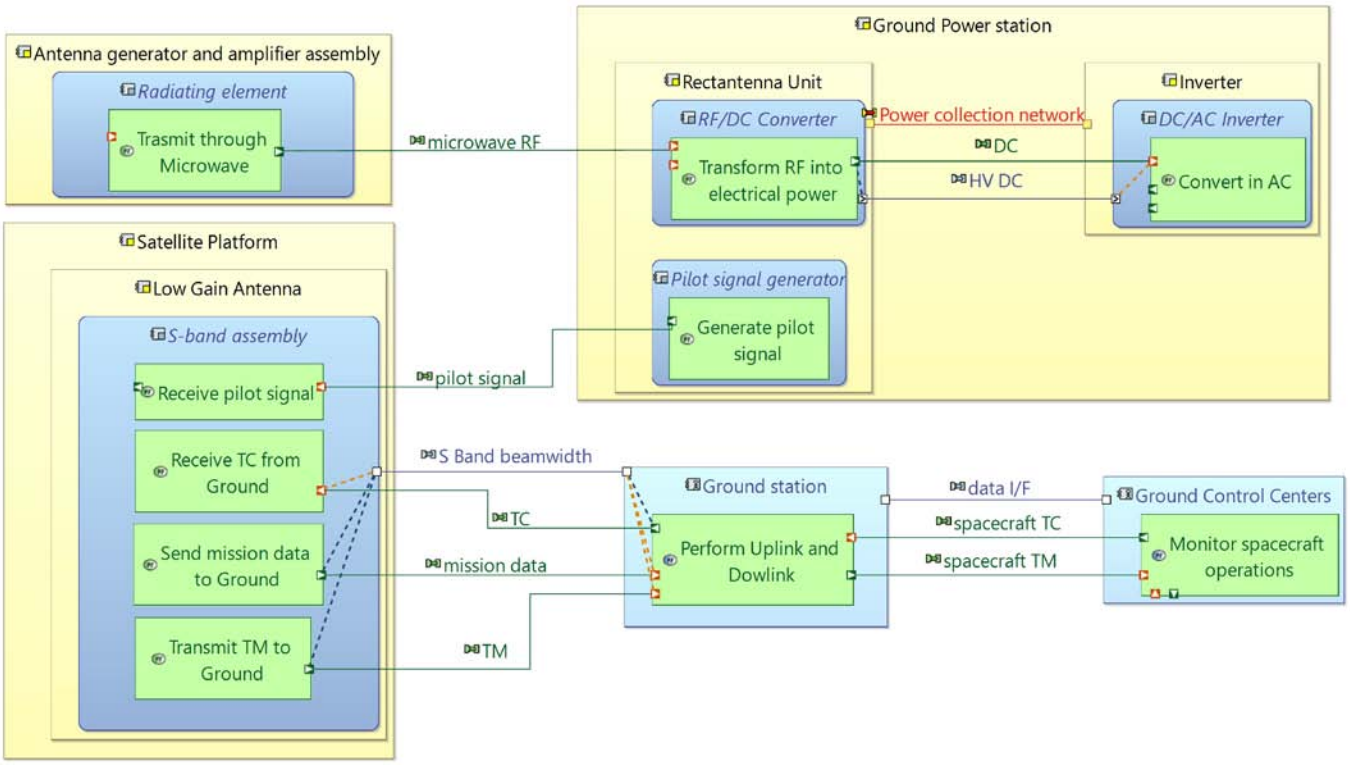

Figure 2-4 SBSP Communications strategy

The SPS is equipped with an S-band low gain antenna to communicate with ground and to receive the retrodirective beaming signal, essential for a precise pointing of the power beam.

2.4 Decommissioning Strategy

As the graveyard orbit is not compliant with the Zero Debris policy the SPS will be disassembled with the help of the robotic systems and then recycled. Two options are proposed:

- *Lunar recycling* (Figure 2-5): the robotic systems disassemble a small hardware part from the SPS and the orbital tug, after being refueled, transfers it to the Moon. This hardware decommissioning cycle is then repeated. The Orbital Tug is capable to perform GEO to Moon orbit and back trip as the Delta V required is similar to the LEO to GEO transfer;
- *In-situ recycling*: the SPS will be disassembled and then recycled in GEO via in-orbit manufacturing.

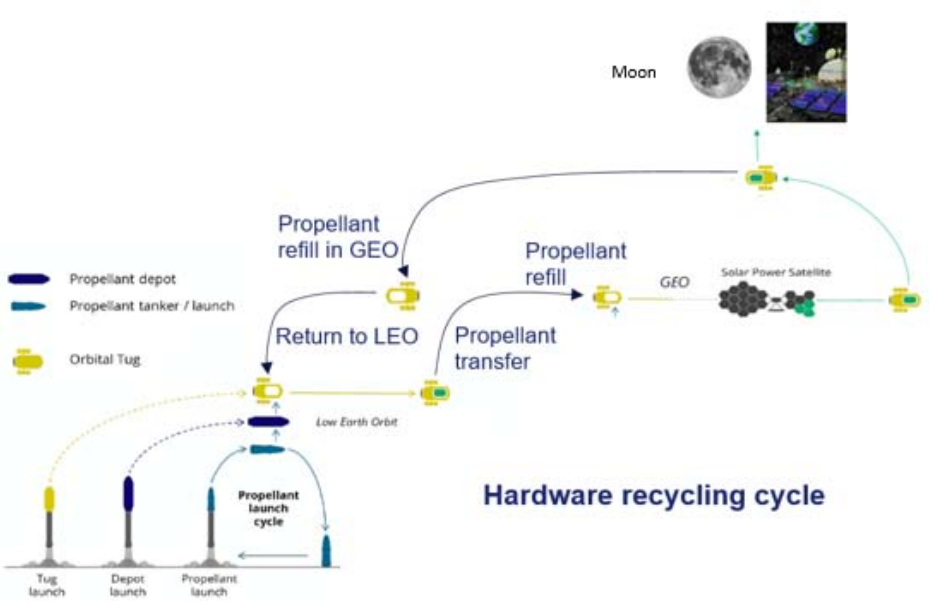

Figure 2-5 SPS Moon disassembly and decommissioning

3 System Area Optimization

3.1 Optimization Approach & System Driving Parameters

The main mathematical model, presented in TN3 and containing the power link budget, has been implemented in an SBSP digital framework (for details refer to chapter 9) following a methodology similar to the one adopted to make decisions for frequency trade-offs. This integration aims to shed light on the potential impact of variations in key design parameters related to the three principal SBSP domains: GPS area, solar panels area and on-board antenna area.

Each of these values have been inserted in an objective function to be minimized by the optimization model with the correspondent weight factors, which could be changed arbitrarily to observe the possible impact on the optimized solutions.

Optimization Weights List

Pameter Name	Parameter Value
WGoundStation	1
WAntenna	50
WSolarPanel	50

Figure 3-1 Possible combination of weight factors for the optimization model

The main parameters affecting the system (in terms of the three areas), with the corresponding possible options and implications, have been implemented inside the tool and are listed below (considering GEO orbit and 1GW power provision as baseline for the solution):

Parameter	Options	Main impact on the SBSP System
Cell technology	Thin Film 3 Junctions (Expected cell efficiency: 36 %)	Cell technology and the associated cell efficiency significantly influence the size of PVA (though factors like cost and weight remain equally relevant).
	CIGS (Expected cell efficiency: 29 %)	
	Perovskite (Expected cell efficiency: 29%)	
Frequency	2.45 GHz	Considering the GEO orbit as baseline and a fixed GPS location, the frequency remains the only parameter affecting the product of the GPS area and the on-orbit antenna area (higher frequencies lead to lower product values)
	5.8 GHz	

GPS location	Spain (Latitude: 40.2°)	Considering the GEO orbit as baseline and a fixed value of frequency, an higher GPS area is needed when considering higher latitudes (because of the power footprint stretching)
	Germany (Latitude: 51.1°)	
	Sweden (Latitude: 60.1°)	

Table 3-1 Main mathematical model implementation: parameters and possible options

3.2 Main Mathematical Model Results

Three analyses have been conducted to examine the variations in results stemming from various weight factor combinations (1-1-1, 1-30-30, 1-50-50, 1-200-200). Furthermore, for each individual analysis, all viable option combinations have been assessed and are outlined in the following tables.
In addition to the summary results table two graphical representations have been added for each simulation:

- A scatter plot for a visual representation of optimized area values corresponding to the given weight factor combination.
- A bivariate histogram illustrating the multiplicity of solutions that involve precise couplings between on-board antenna area and GPS area. This graph provides insights into the multiplicity of couplings between the antenna area and the GPS area in the simulations. A higher occurrence of coupling with a specific solution multiplicity indicates that, for the corresponding weight factor combinations, that solution emerges as the most credible and well-optimized choice across a wide range of parameter options.

In particular, for the 1-200-200 weight factor combination, the baseline solution highlighted presents the following values:

System area	Area value [km2]
GPS area	34
PVA area	6.2
On-board antenna area	0.44

Table 3-2 Optimized area values for the selected architecture

All the simulation results are displayed below.

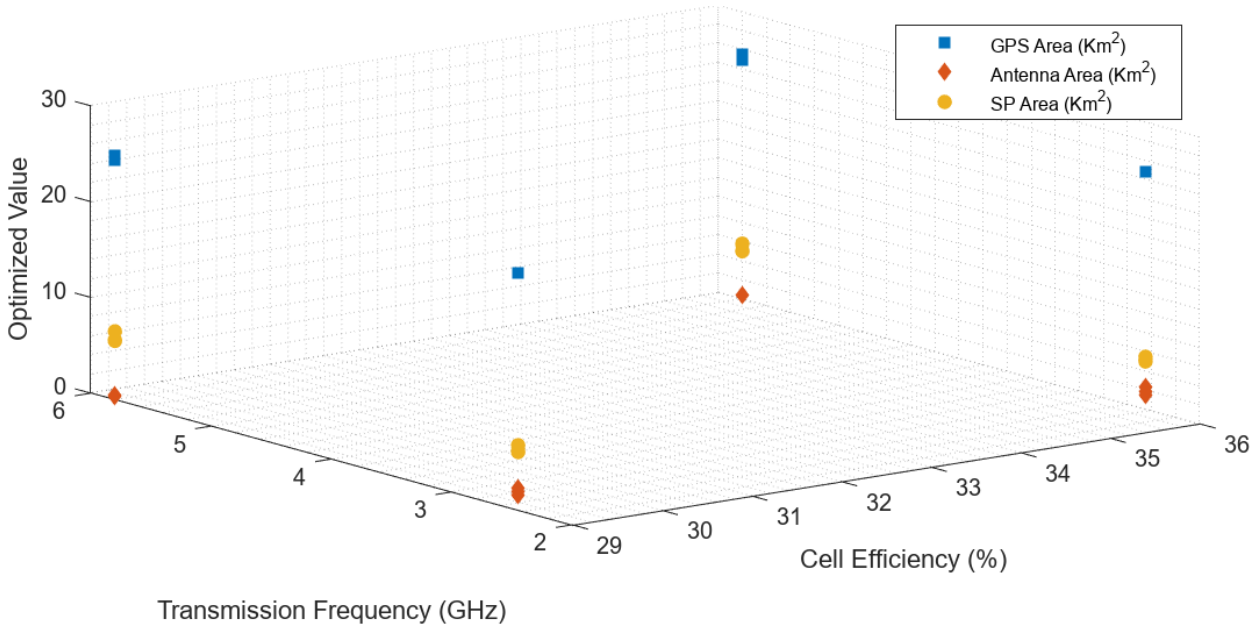

Figure 3-2 Optimized area values for 1-1-1 weight factors combination

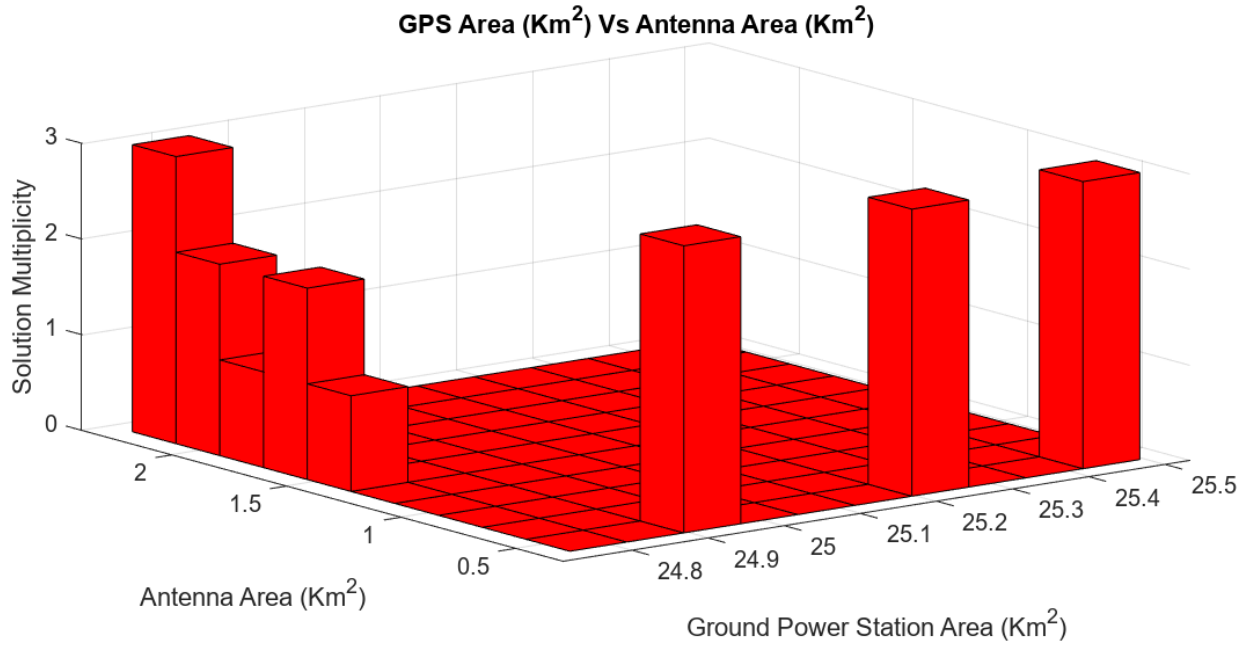

Figure 3-3 Solutions multiplicity for the GPS-antenna area coupling for 1-1-1 weight factors combination

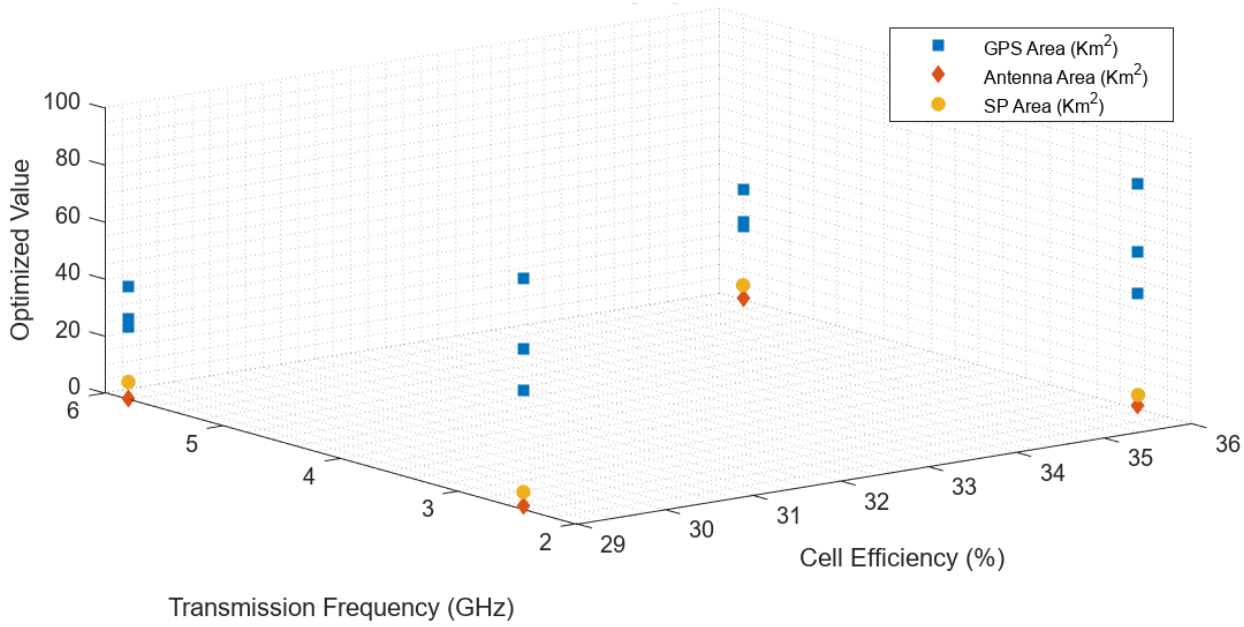

Figure 3-4 Optimized area values for 1-30-30 weight factors combination

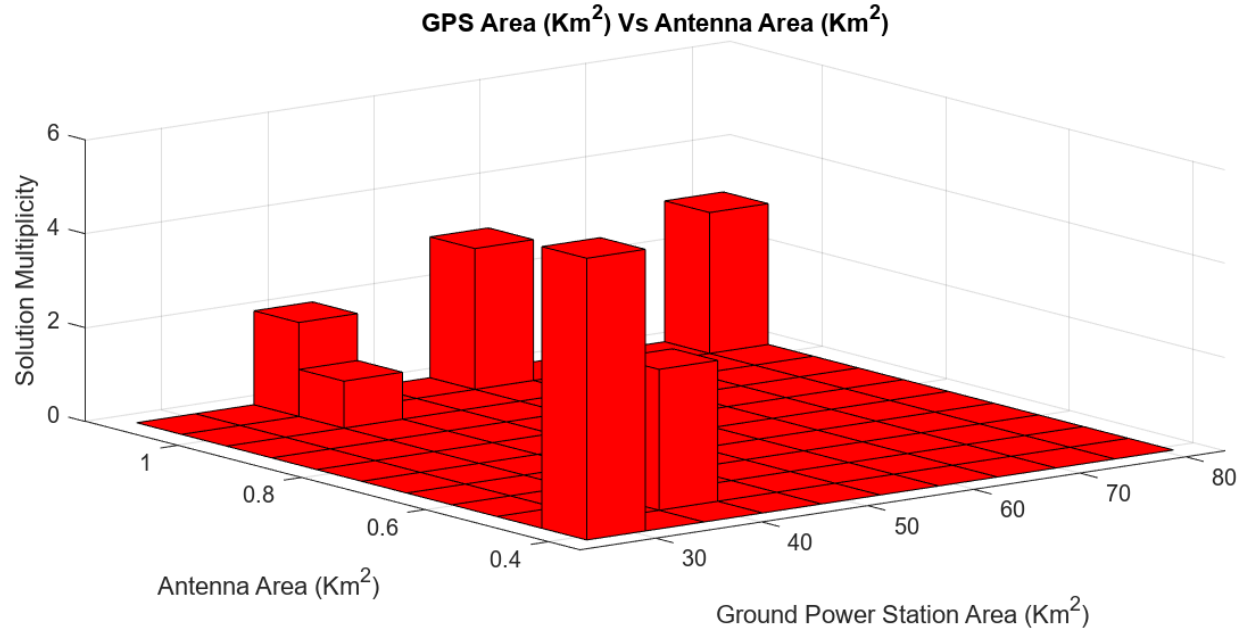

Figure 3-5 Solutions multiplicity for the GPS-antenna area coupling for 1-30-30 weight factors combination

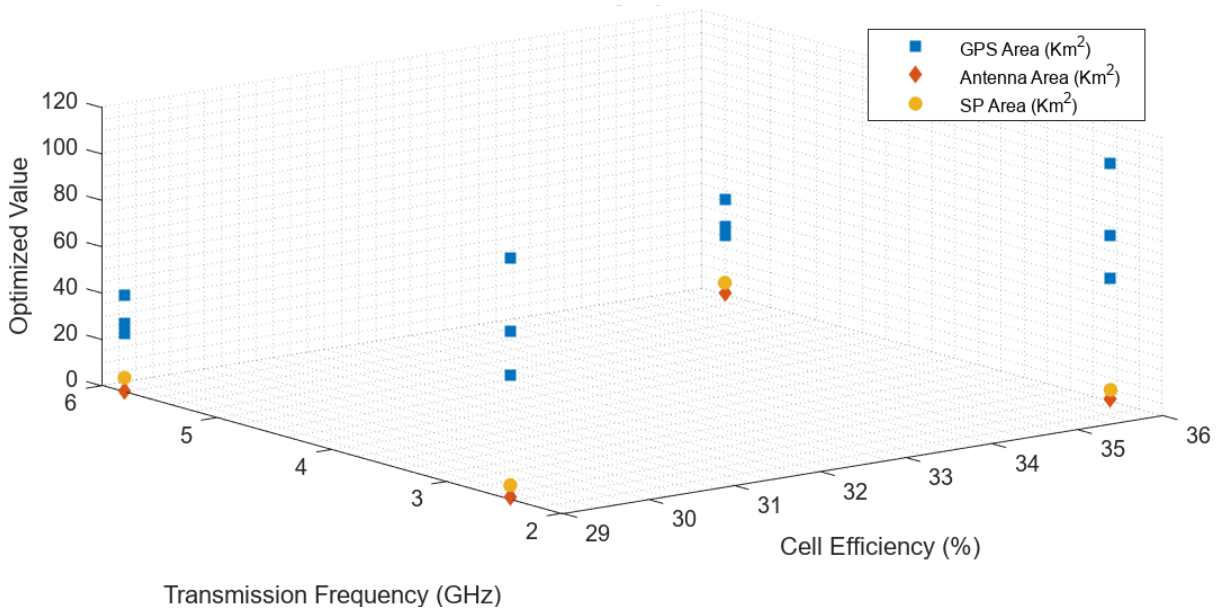

Figure 3-6 Optimized area values for 1-50-50 weight factors combination

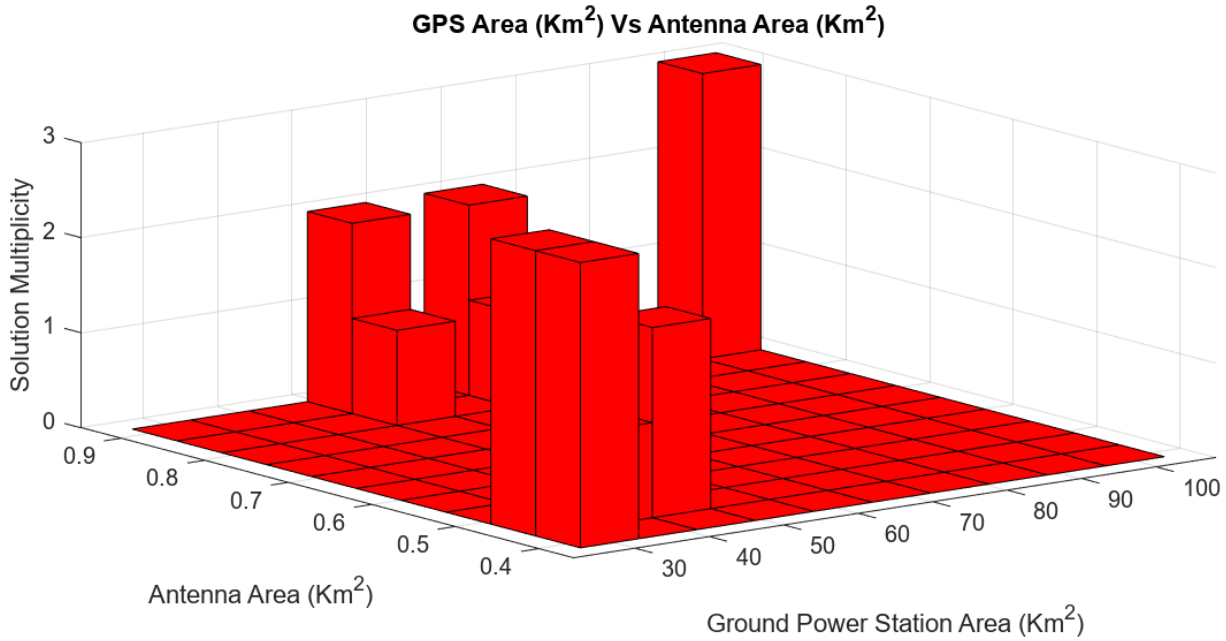

Figure 3-7 Solutions multiplicity for the GPS-antenna area coupling for 1-50-50 weight factors combination

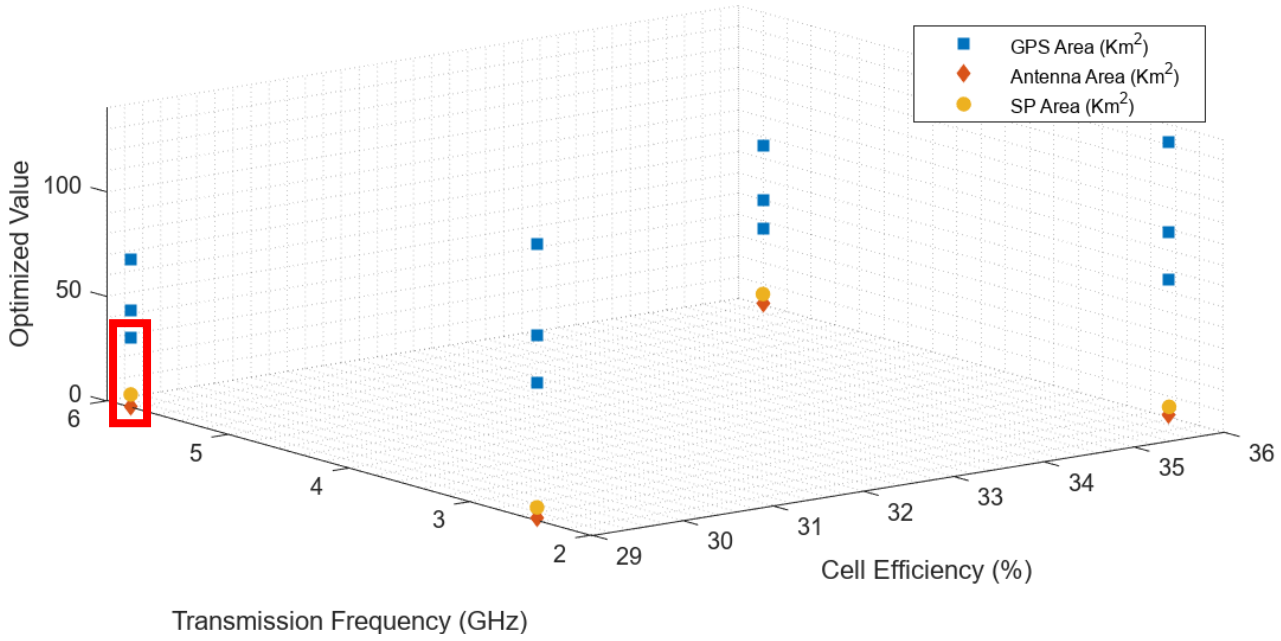

Figure 3-8: Optimized area values for 1-200-200 weight factors combination (with baseline solution selected)

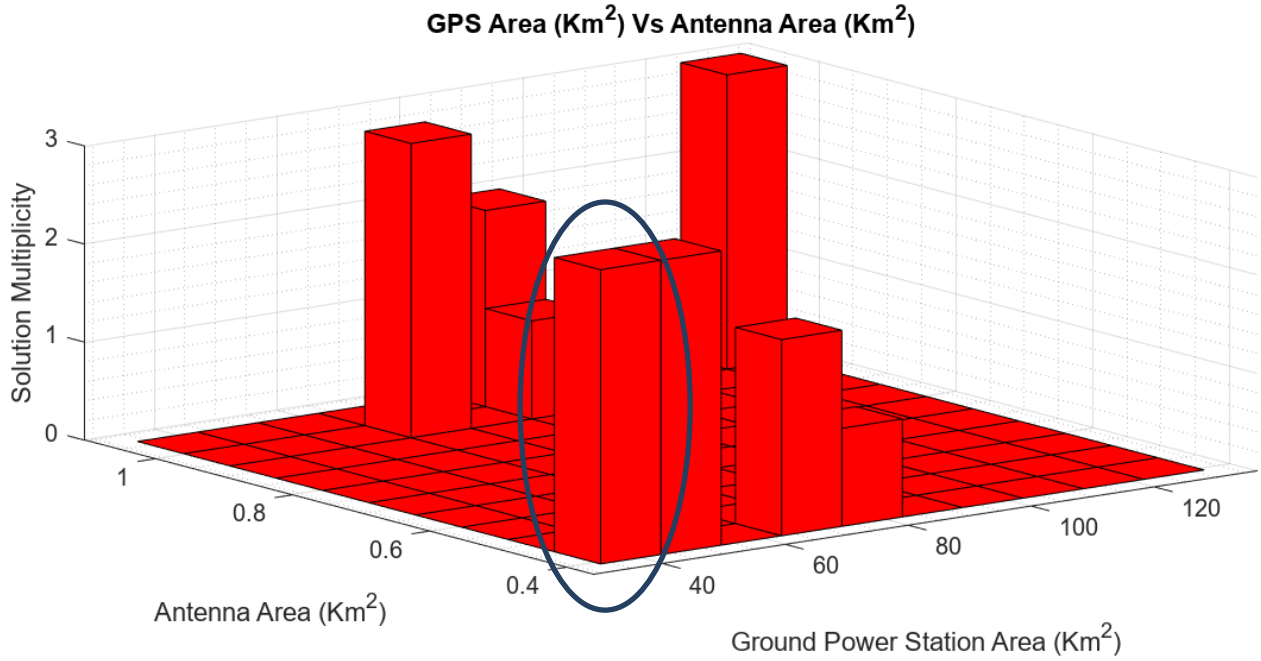

Figure 3-9: Solutions multiplicity for the GPS-antenna area coupling for 1-200-200 weight factors combination

4 System Definition

This chapter describes the SBSP System, starting from mission analysis considerations. The following topics are subsequently addressed:

- Space Segment (section 4.2);
- Ground Segment (section 4.3);
- Launch Segment (section 4.4).

4.1 Mission Analyses

The Geostationary orbit has been chosen (refer to TN3) as operative orbit due to its advantages in terms of amount of required satellites (only one), GPS area and ease of operations. In the following sections the effects of the chosen orbit in terms of perturbations have been analyzed.

4.1.1 Effect of the ecliptic plane

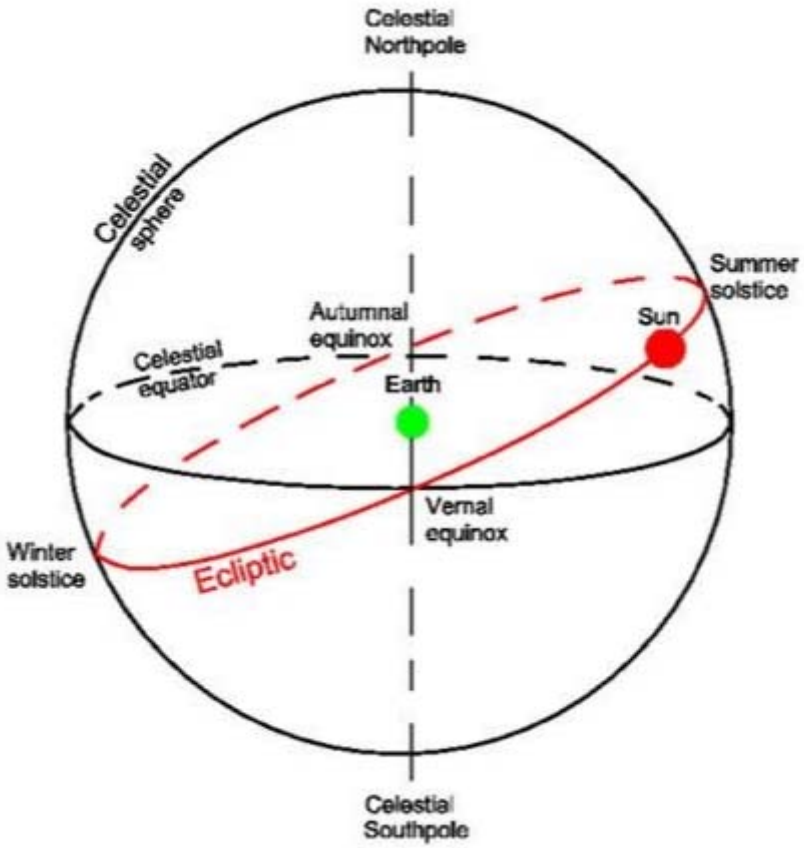

Figure 4-1 Ecliptic and equator relative position

Due to the inclination between the ecliptic and the equator plane, the inclination of the Sun vector w.r.t. the solar arrays will change over time, from a minimum of 0 deg during the equinoxes to a maximum of 23.44 deg during the solstices, resulting in a small decrease of performances of around 8%. During equinoxes there are eclipses of a duration of up to 71 minutes, which causes a loss of energy delivered during the eclipses. The effect on the system of both these events are shown in chapter 9.

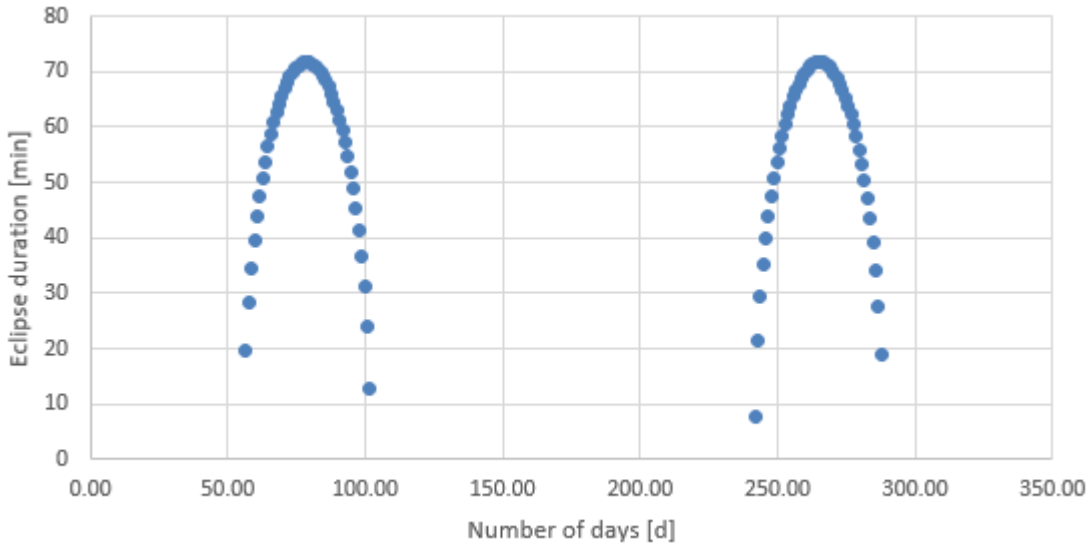

Figure 4-2 Eclipse duration during a year

4.1.2 Station-keeping considerations

Considering the GEO orbit baseline, preliminary station-keeping considerations are needed to perform the sizing of the thrusters for AOCS.

Amongst the perturbations suffered by the SPS in GEO orbit, the solar pressure is prominent due to the high area of the SPS. For a conservative approach, a cannonball model has been utilized to evaluate the solar radiation force with the considered values reported below:

Solar panels	6.2 km^2
Scaling coefficient C_R	2

Table 4-1 Input values for the Solar Radiation Force

The output values for the SPS in GEO with a propagation time of one year is shown in the following figure:

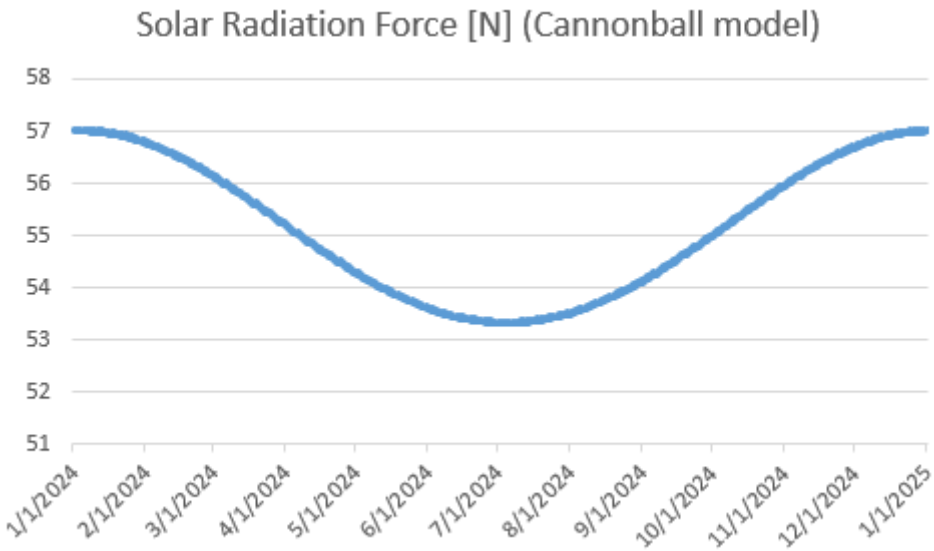

Figure 4-3 Solar Radiation Force in a year

So the dimensioning value is of 57N. As the effect is continuous during the year, the proposed station-keeping approach to contrast this perturbation is to have thrusters that continuously burn in the opposite direction of the solar radiation force with the same force to even out the forces. Due to the inclination of the ecliptic a force along the satellite x-axis is required to contrast the solar radiation pressure when getting nearer the solstice.

Another perturbation to consider is the luni-solar effects, mainly affecting the orbit's inclination. The station-keeping for this disturbance is called North-South stationkeeping as the thrust shall be applied in the out-of-plane direction, along the satellite x-axis. The DeltaV tipically required to compensate for this disturbance is of 50 m/s per year. The time required to perform this DeltaV change based on the total thrust is shown:

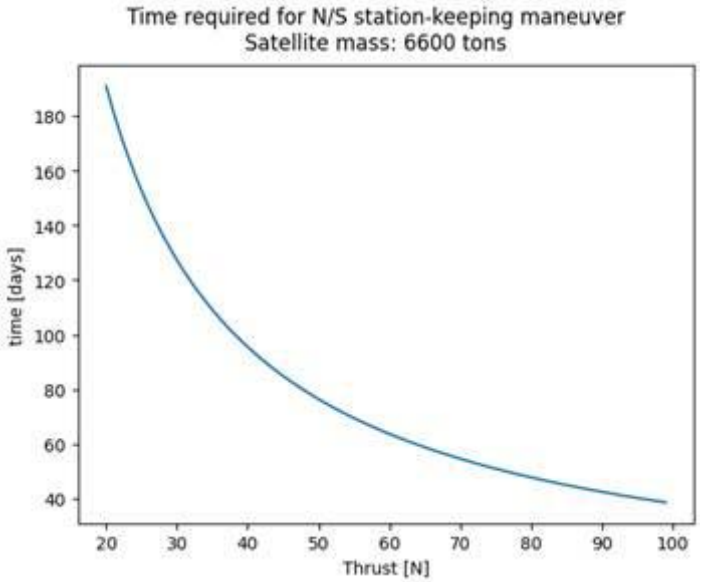

Figure 4-4 Continuous burn time for N/S station-keeping based on total thrust

To maximise the thruster usage this effect shall be contrasted when the satellite is near the equinoxes, as the effect of the solar radiation pressure is lower along the x-axis thus there are more thrusters available.

The last considered perturbation is the Earth triaxiality which affect the satellite's longitude. The station-keeping for this disturbance is called East-West station-keeping as the thrust shall be applied in the in-plane direction. The DeltaV tipically required to compensate for this disturbance is of 2 m/s per year. As before, the time required to obtain this DeltaV is shown:

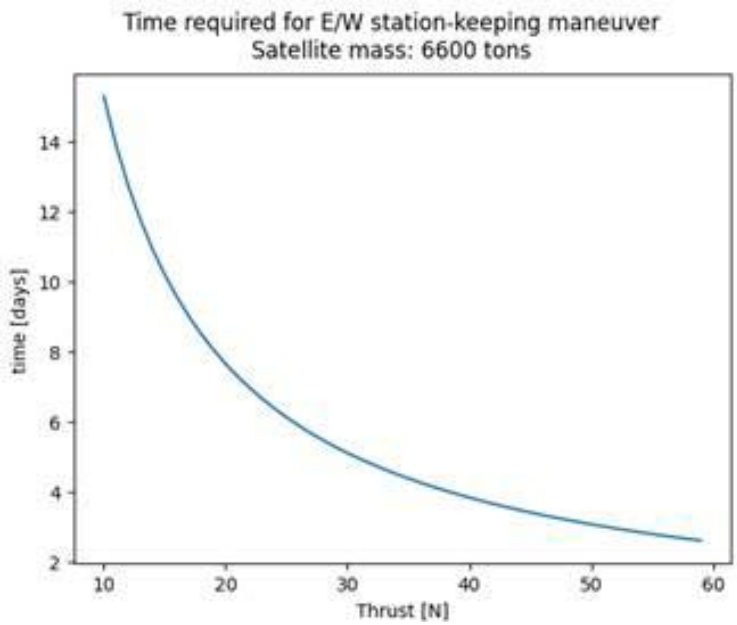

Figure 4-5 Continuous burn time for E/W station-keeping based on total thrust

During nominal operation, the spacecraft absorbs solar photons but re-emits microwave photons towards Earth. This megawatt microwave beam could also produce a propulsive force in the opposite direction (i.e. towards zenith) due to the photon pressure.

The force emitted can be evaluated as:

$$F_{emitted} = P_{emitted} * Area = \frac{Transmitted\ Power}{speed\ of\ light\ in\ vacuum} = 2.058\ GW * 3.34\ \left(\frac{N}{GW}\right) = 6.87\ N$$

This effect cannot be neglected and is tackled in the AOCS section.

4.2 Space Segment

4.2.1 SPS Configuration

The SPS is composed of 4 main elements:

1. Roll-out Module (Figure 4-6 and Figure 4-7)
2. Truss Module (Figure 4-8)
3. Node Module (Figure 4-9)
4. Active Truss Module (Figure 4-10)

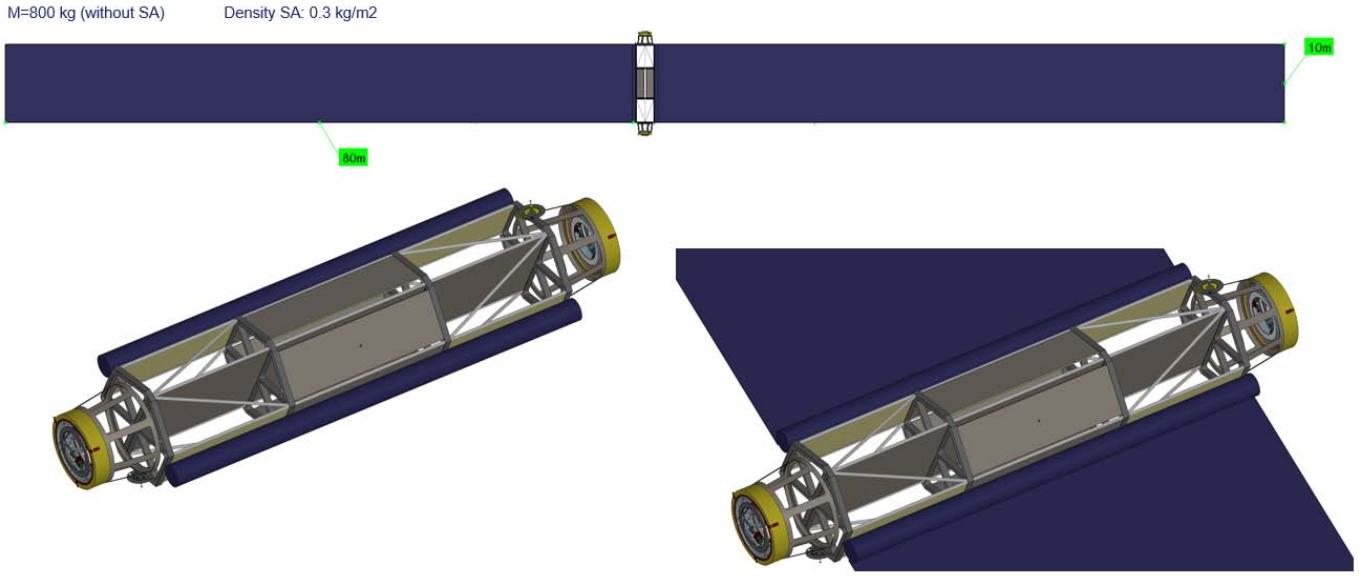

Figure 4-6 Roll-out Module (1/2)

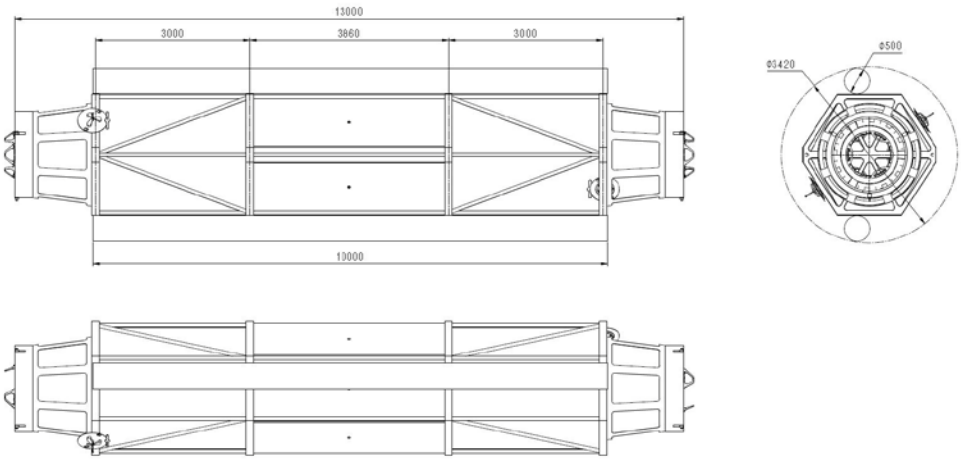

Figure 4-7 Roll-out Module (2/2)

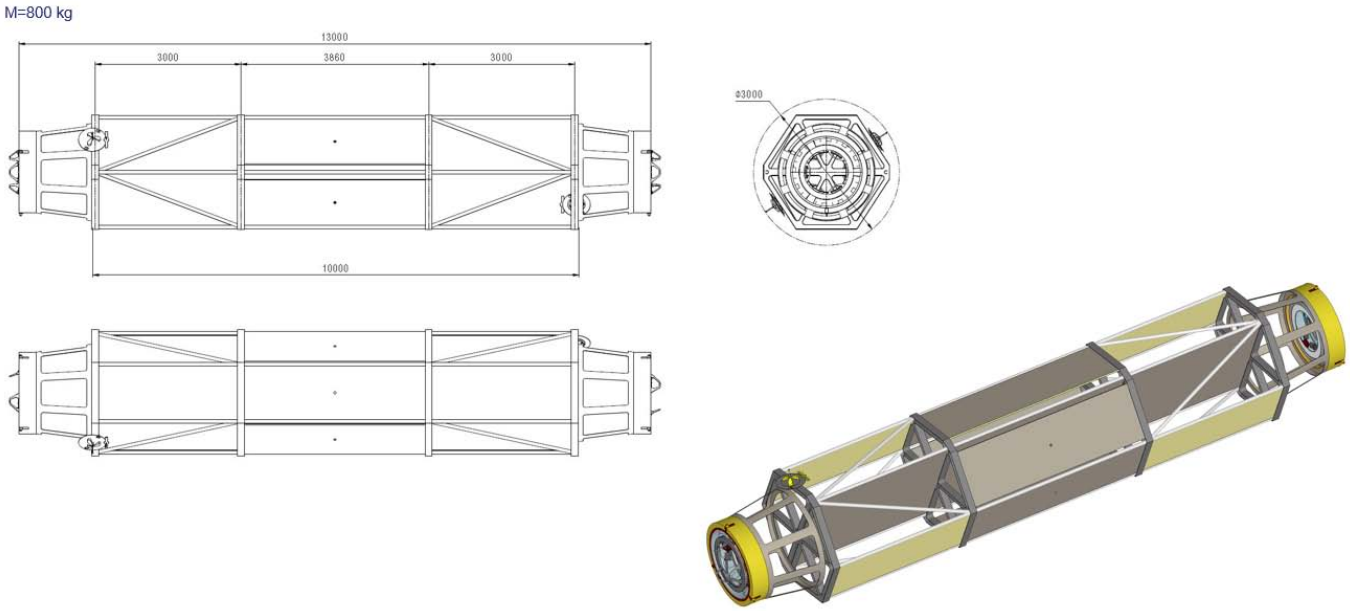

Figure 4-8 Truss Module

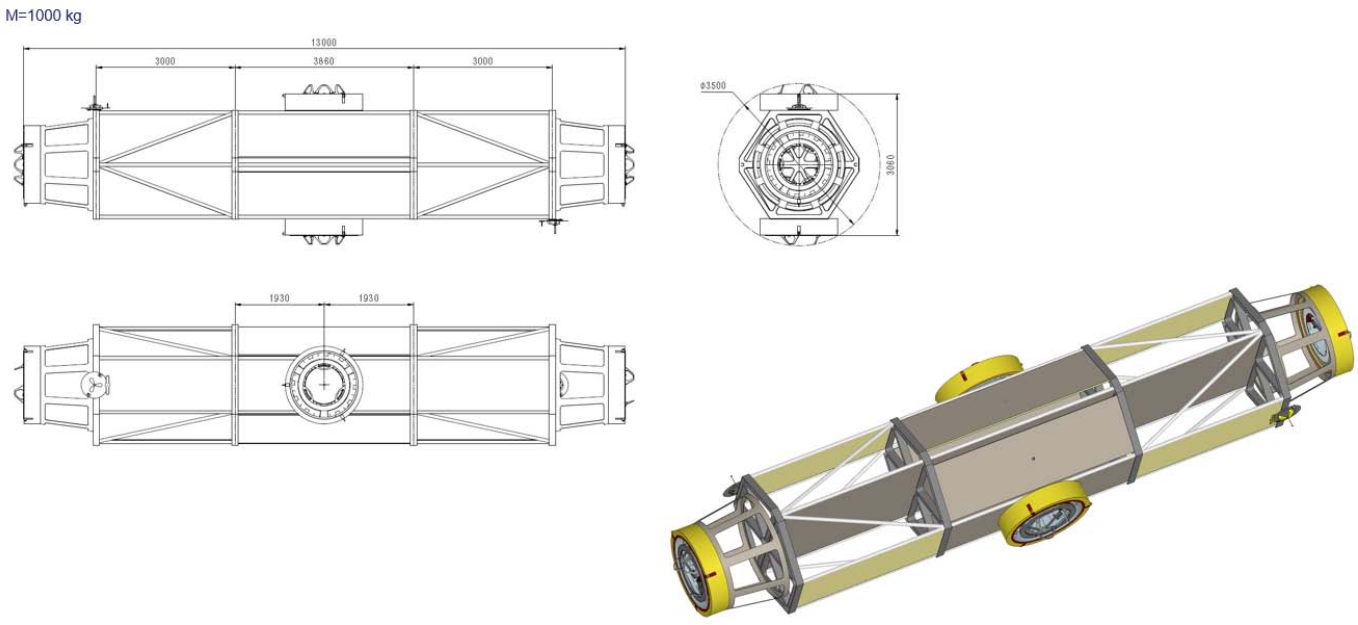

Figure 4-9 Node Module

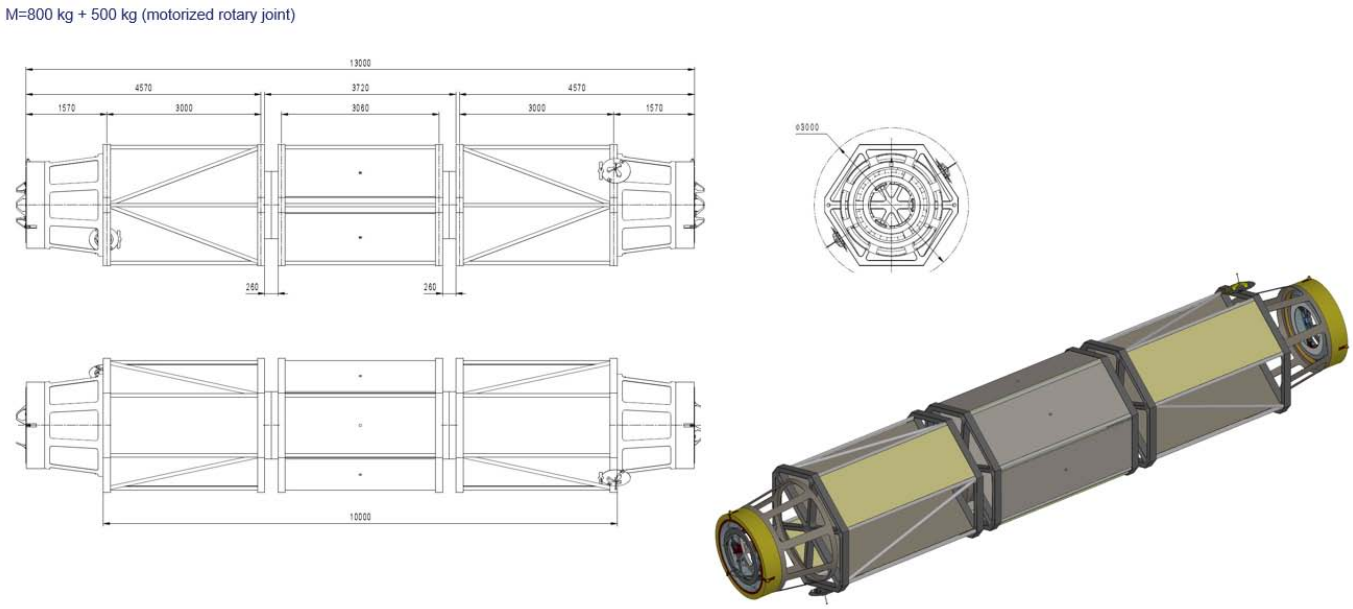

Figure 4-10 Active Truss Module

An SPS overview is provided in Figure 4-11.

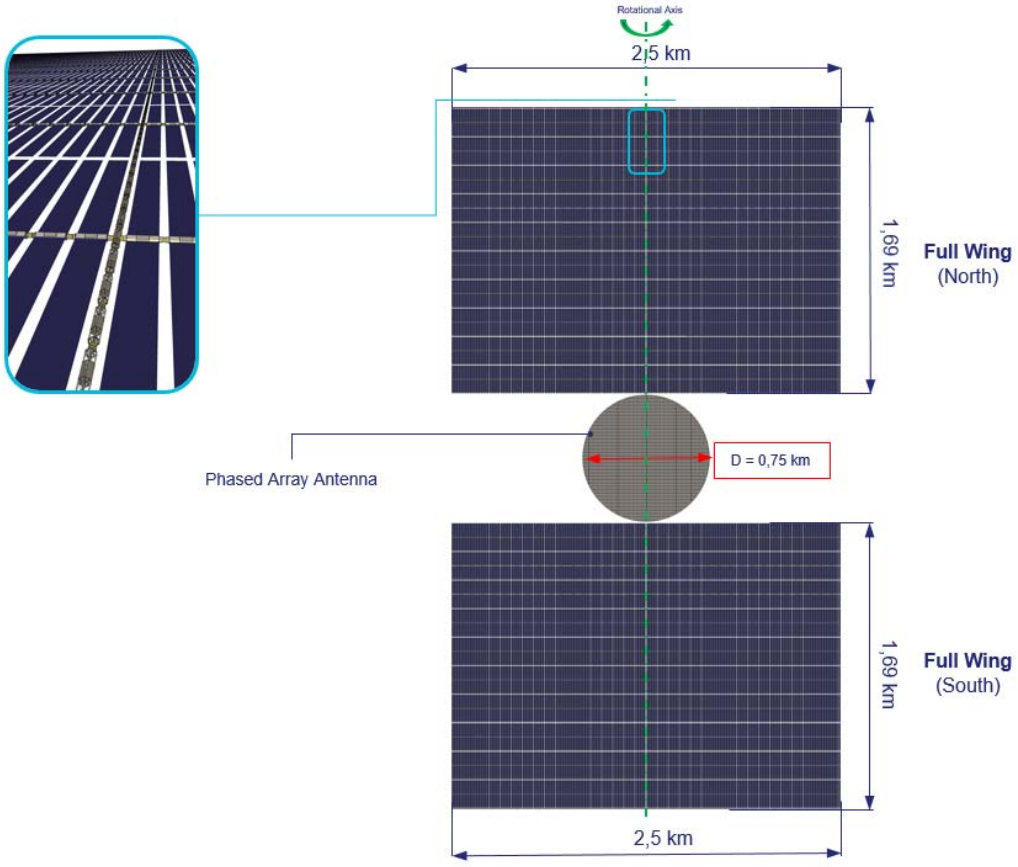

Figure 4-11 SPS overview

Each Full Wing (North & South) is composed of 10 Single Wing of (97+97) Roll-out Module as shown in Figure 4-12.

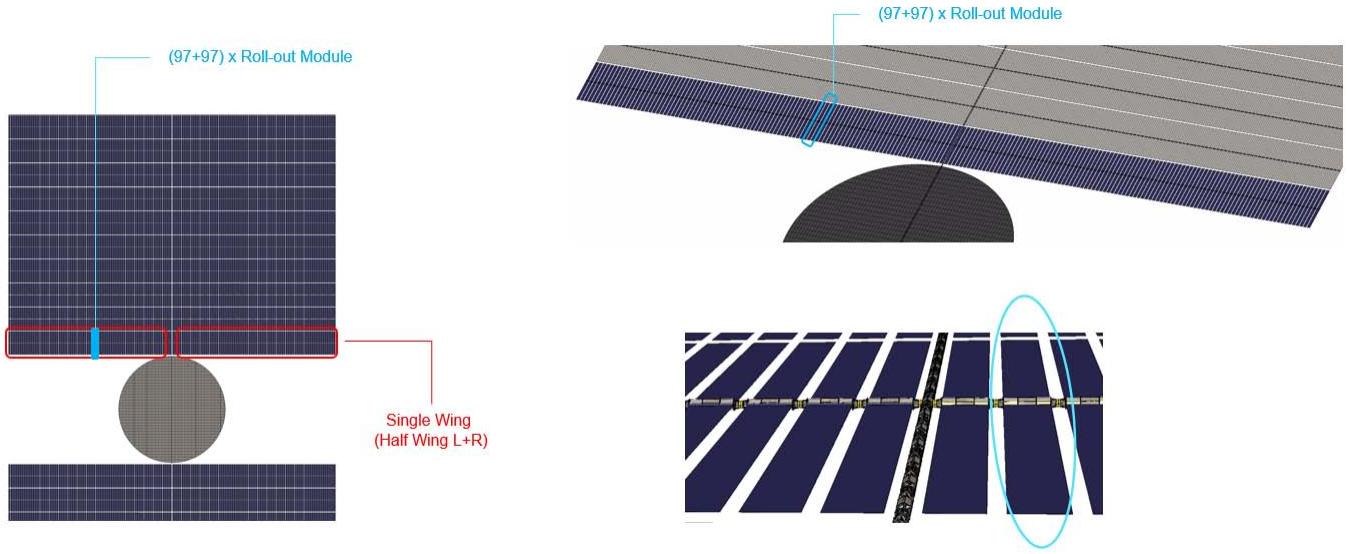

Figure 4-12 Single Wing details

Details of the Central Truss composed, for each Full Wing, of 120 Truss Module + 10 Node Module, are shown in Figure 4-13.

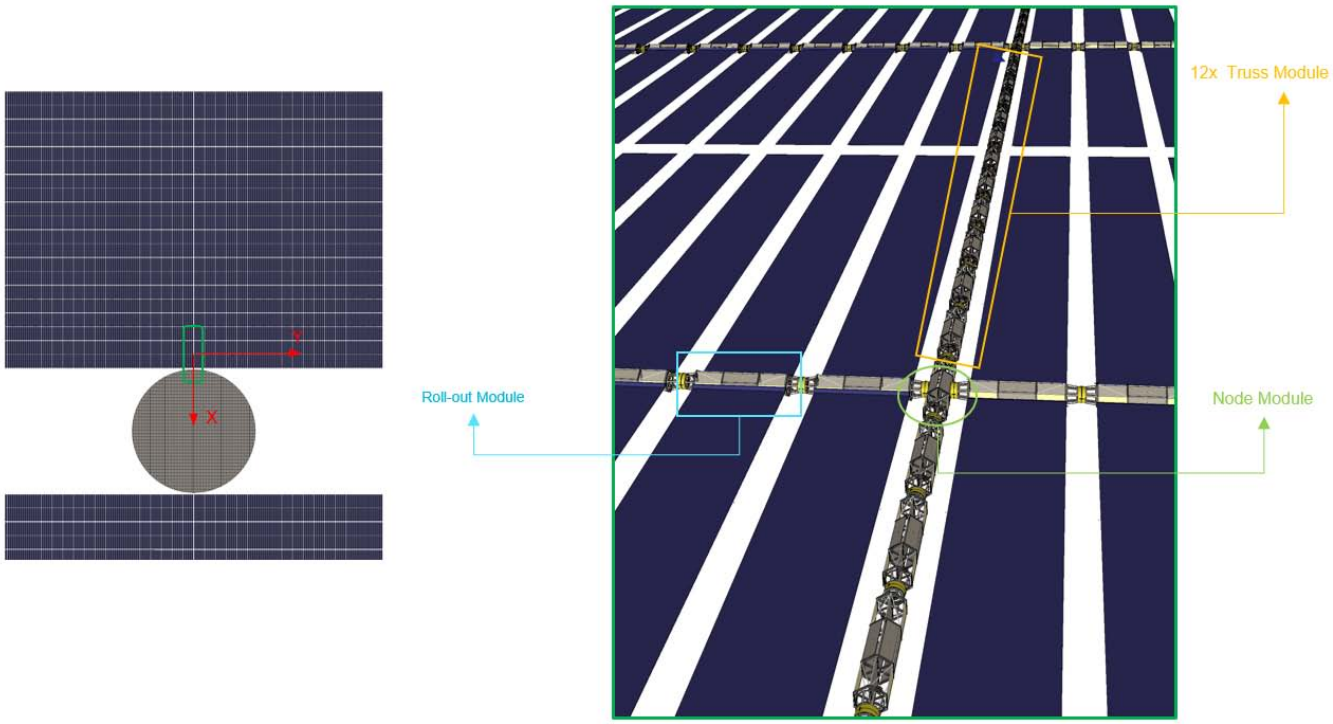

Figure 4-13 Central Truss details

The Phased Array Antenna Structure composed of 59 Active Truss Modules is shown in Figure 4-14.

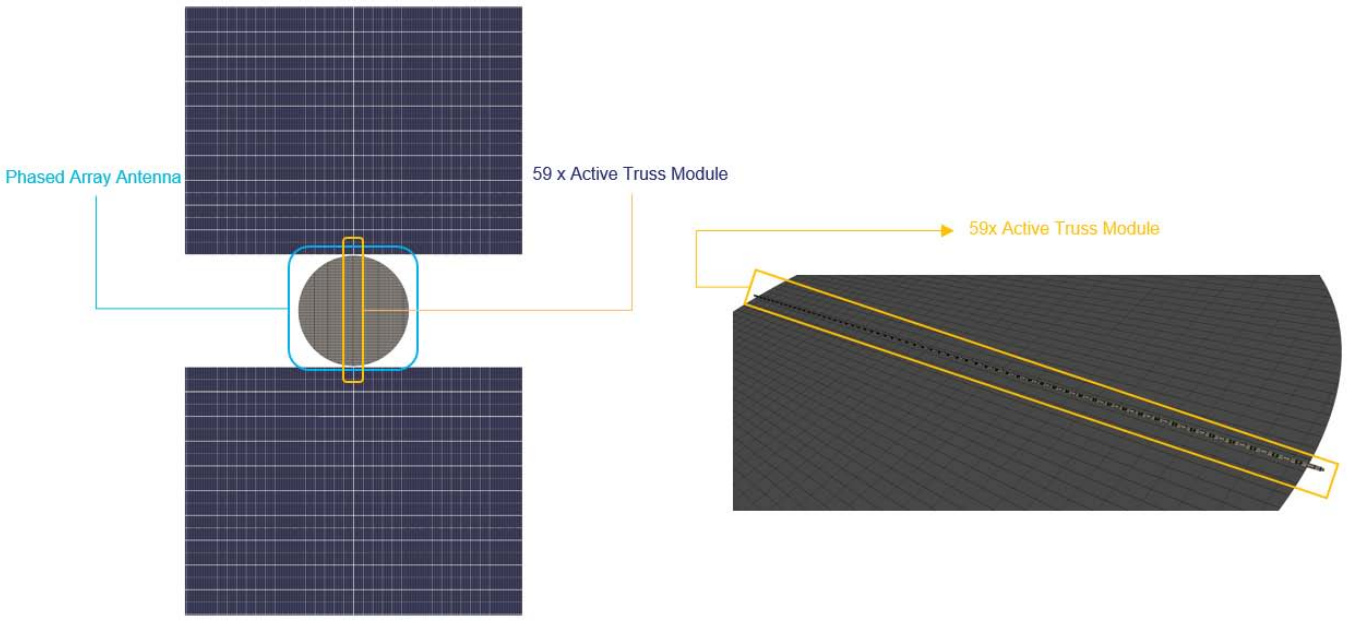

Figure 4-14 Phased Array Antenna Structure

4.2.2 Full Wings & Phased Array Antenna Rotation Strategy

Due to the size of the solar arrays system, the body axes are considered fixed w.r.t. the two solar array full wings. In this reference frame, the antenna rotates along the x-axis to follow the Earth's relative movement.

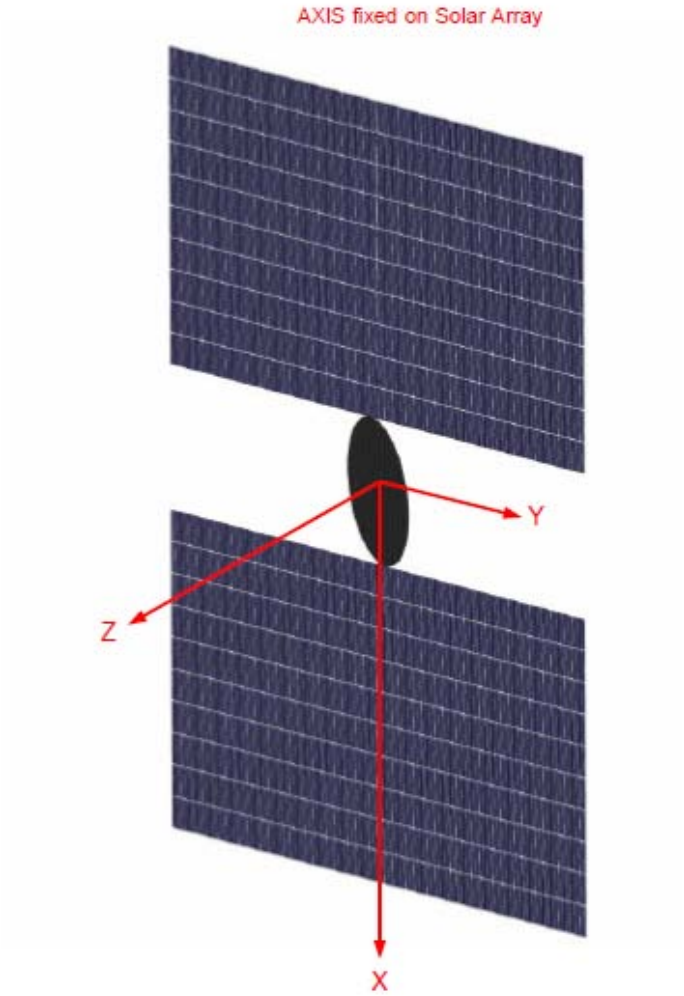

Figure 4-15 Satellite axis reference frame

In terms of attitude, the antenna shall be nadir pointing, while the solar array z-axis shall be parallel to the Sun vector as much as possible. This means that the antenna shall be nadir pointing for the whole duration of the mission, thus the body plane y-z is considered to be on the same plane of the equator. The rotation of the Phased antenna structure (0.75km diameter, 250tons mass) is one of the main technological challenges of this project. Although the speed is very limited (360°/24h, i.e. 15°/h), there is no space heritage for similar bulky solutions. The use of thrusters coupled with a free joint is excluded (for fuel consumption reasons) so only motorized rotary joints can be baselined.

The closest TRL9 mechanism is the Solar Alpha Rotary Joint (SARJ), a single-axis pointing mechanism used to orient the solar power generating arrays relative to the sun for the International Space Station (ISS). The ISS has a backbone or set of trusses that house several ISS systems. These trusses are joined to a set of pressurized modules that house the crewmembers living and working aboard the ISS. The figure below shows the ISS after assembly mission 17A by the Space Shuttle. The pressurized modules are located along the center of the truss structure, extending forward and aft. The power generating solar arrays are located on the port and starboard sides of the truss structure outboard of the SARJs. The location of each Solar Alpha Rotary Joint (SARJ) is indicated in Figure below (outdated w.r.t. current ISS configuration, but applicable w.r.t. the heritage discussion).

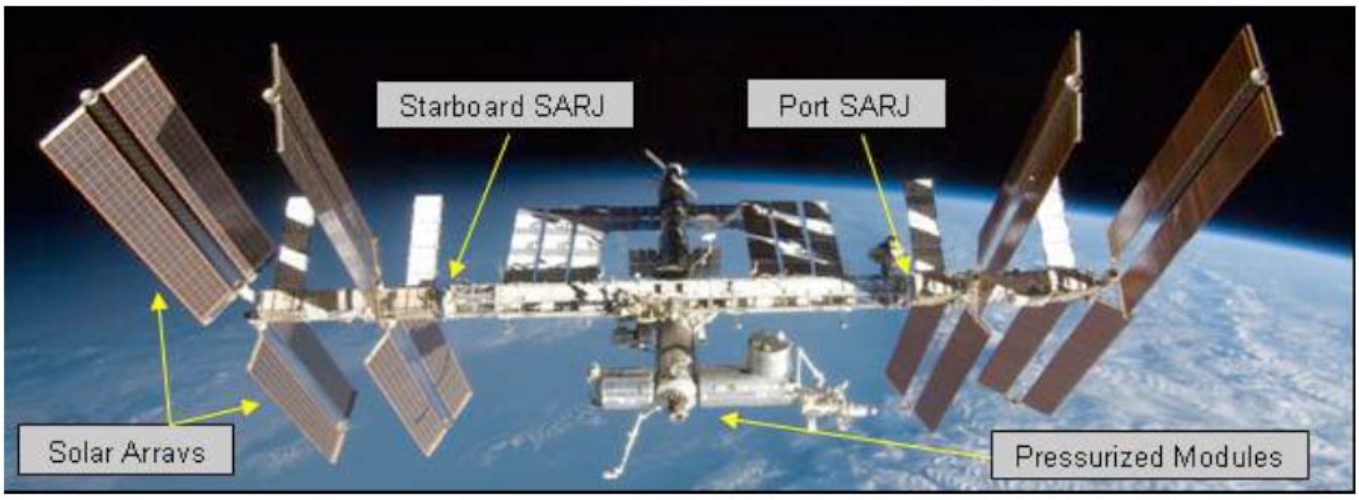

Figure 4-16 ISS after assembly mission 17A

The SARJ completes one full rotation per orbit of the ISS, approximately every 90 minutes. The figure below shows a drawing of the SARJ with the major components labeled. The SARJ is capable of transferring 60 kW of electrical power, spare low power (300 W), and data channels across the rotary joint. The total weight of the SARJ is 1161 kg. Two SARJ mechanisms are installed onboard the ISS - Port (activated December 2006) and Starboard (activated June 2007). The SARJ serves as the structural joint between the ISS inboard and outboard truss elements via twelve Trundle Bearing Assemblies (TBA). The trundle bearings straddle between an inboard and outboard triangular cross-section race rings. The race rings are approximately 3.2 meters in diameter.

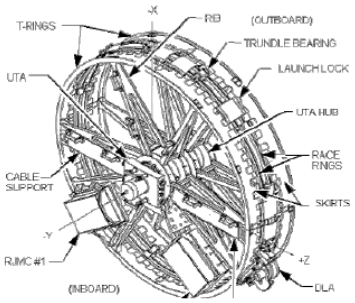

Figure 4-17 SARJ drawing

Considering to readapt such heritage, the concept proposed for the SPS is to equip the Phased Array Antenna truss modules (59x) with a motorized rotary joint, that can be disengaged in case of failure (to avoid single failures on the pointing function). The motorized rotary joint is preliminary specified as follows:

- 500 kg mass
- 100 W power consumption (rotating @ 15°/h)

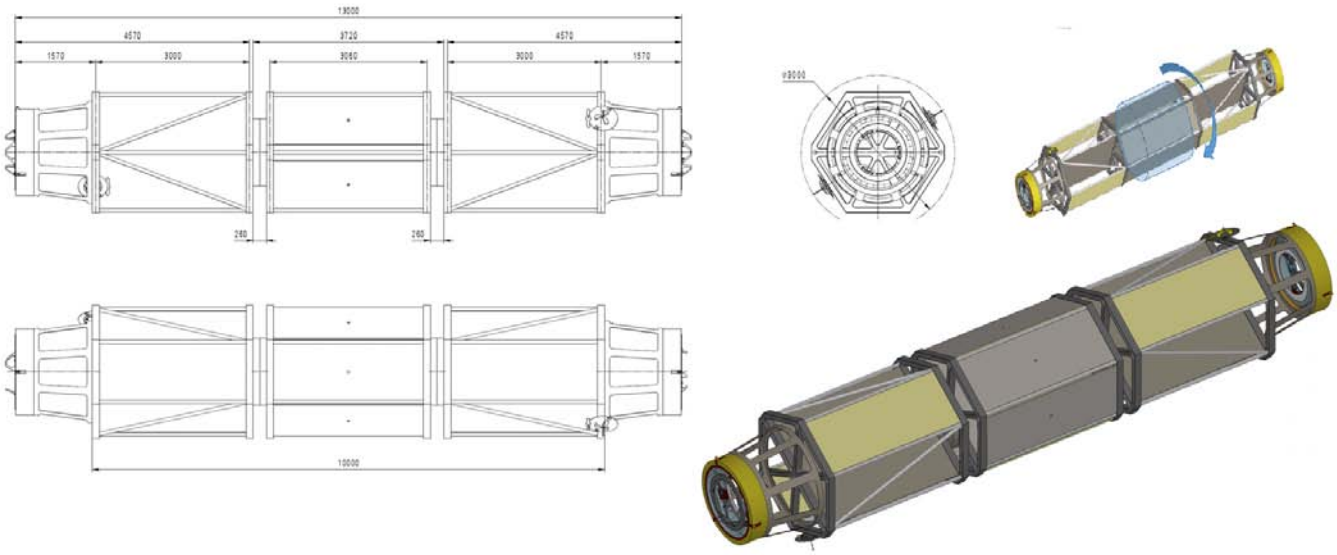

Figure 4-18 Active Truss Module

At the time of writing of this TNO this solution is derived from similar bulky TRL9 solution, but TAS-I advises to open a Technological Development Activity aiming to refine the current conceptual figures.

4.2.3 Structure

The structure is preliminary designed based on individual modules some of them acting as nodes, a more accurate sizing is demanded to the next program phases although a preliminary assessment has been performed hereafter based on the needed inertia of the structural framework to provide the minimum stiffness required by the AOCS.

Starting from [RD20], the significant control–structure interaction problem, which is a major concern for a very large Abacus platform (3.2 km x 3.2 km) where lowest structural mode frequency of 0.002 Hz is mentioned.

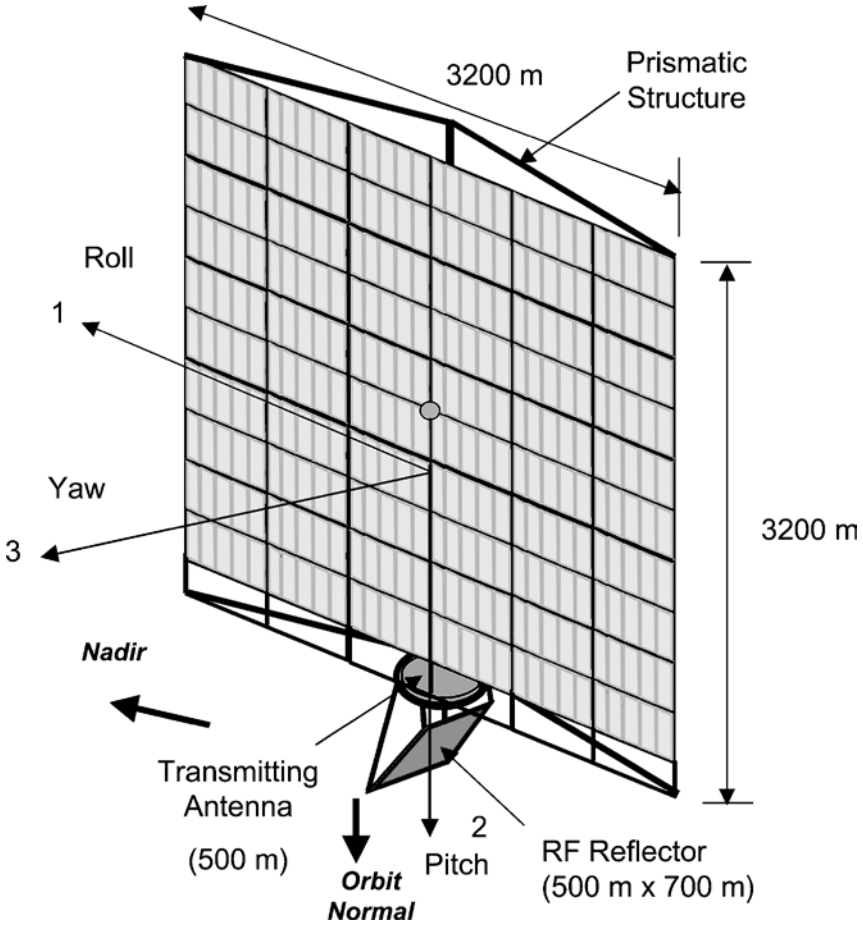

Figure 4-19 Baseline 1.2-GW Abacus satellite configuration

On the other hand the very same ISS (see RD[21]), after the first 6 modes which are associated to rigid body motion, the 7th natural frequency mode is the first significant one is in the range of 0.1 Hz and basically relevant to solar arrays:

Table 6.2-1 Mode of Vibration and Natural Frequency of ISS

Modes	Body 1 Frequency (Hz)	Body 2 Frequency (Hz)
1	1.63e-5	2.16e-5
2	9.16e-6	1.80e-5
3	1.95e-6	9.62e-6
4	2.33e-6	1.05e-5
5	9.95e-6	2.06e-5
6	1.53e-5	2.88e-5
7	0.0932	0.115
8	0.0955	0.116
9	0.0965	0.170
10	0.0969	0.172
11	0.0982	0.662
12	0.101	0.662
13	0.102	0.796
14	0.106	0.796
15	0.106	0.931

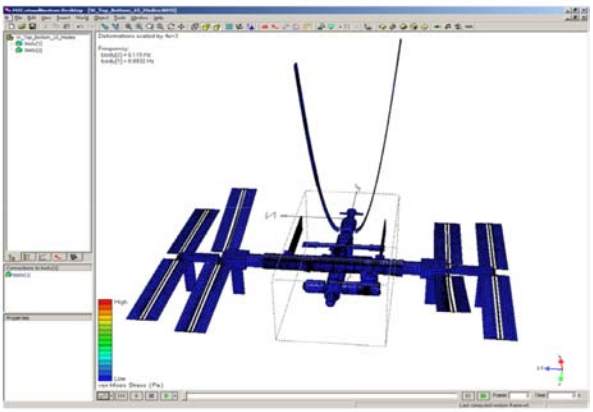

Figure 6.2-17 7th Mode of Vibration of ISS

Figure 4-20 ISS 6 Rigid Body Frequencies & 7th First Mode - RD[21]

A global stiffness requirement in terms of first frequency for the current SPS solution, has been established based also on AOCS considerations to **0.005 Hz**.

The SPS components first frequencies leading to the inertia needs for its individual skeleton structure given by the solar array booms, the central and lateral trusses are here evaluated based on the use of RD[22] formulae.

108 FORMULAS FOR NATURAL FREQUENCY AND MODE SHAPE

Table 8-1. Single-Span Beams.

Notation: x = distance along span of beam; m = mass per unit length of beam;
E = modulus of elasticity;
I = area moment of inertia of beam about neutral axis (Table 5-1); L = span of beam;
see Table 3-1 for consistent sets of units

Natural Frequency (hertz): $f_i = \frac{\lambda_i^2}{2\pi L^2}\left(\frac{EI}{m}\right)^{1/2}$; i=1,2,3...

Description[a]	λ_i; i=1,2,3...	Mode Shape, $Y_i\left(\frac{x}{L}\right)$	σ_i; i=1,2,3...
1. Free-Free 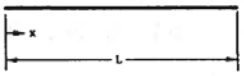	4.73004074 7.85320462 10.9956078 14.1371655 17.2787597 $(2i+1)\frac{\pi}{2}$; i>5	$\cosh\frac{\lambda_i x}{L} + \cos\frac{\lambda_i x}{L} - \sigma_i\left(\sinh\frac{\lambda_i x}{L} + \sin\frac{\lambda_i x}{L}\right)$	0.982502215 1.000777312 0.999966450 1.000001450 0.999999937 ≈1.0 for i>5 See Ref. 8-2
2. Free-Sliding 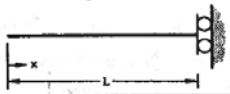	2.36502037 5.49780392 8.63937983 11.78097245 14.92256510 $(4i-1)\frac{\pi}{4}$; i>5	$\cosh\frac{\lambda_i x}{L} + \cos\frac{\lambda_i x}{L} - \sigma_i\left(\sinh\frac{\lambda_i x}{L} + \sin\frac{\lambda_i x}{L}\right)$	0.982502207 0.999966450 0.999999933 0.999999993 0.999999993 1.0; i>5
3. Clamped-Free 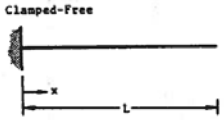	1.87510407 4.69409113 7.85475744 10.99554073 14.13716839 $(2i-1)\frac{\pi}{2}$; i>5	$\cosh\frac{\lambda_i x}{L} - \cos\frac{\lambda_i x}{L} - \sigma_i\left(\sinh\frac{\lambda_i x}{L} - \sin\frac{\lambda_i x}{L}\right)$	0.734095514 1.018467319 0.999224497 1.000033553 0.999998550 ≈1.0; i>5 See Ref. 8-2
4. Free-Pinned 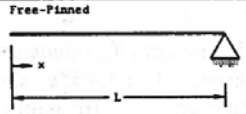	3.92660231 7.06858275 10.21017612 13.35176878 16.49336143 $(4i+1)\frac{\pi}{4}$; i>5	$\cosh\frac{\lambda_i x}{L} + \cos\frac{\lambda_i x}{L} - \sigma_i\left(\sinh\frac{\lambda_i x}{L} + \sin\frac{\lambda_i x}{L}\right)$	1.000777304 1.000001445 1.000000000 1.000000000 1.000000000 1.0; i>5

Table 4-2 Used Formulae from Blevins RD[22]

The followed approach for stiffness hand calculation in terms of first natural frequency, is based on 3 STEPS, starting from the individual Solar Array, then to 2 Adjacent Half Wings and finally to the entire SPS (Full Wings & Antenna).

STEP1 - Roll-Out or Extendable Flexible Solar Arrays

The first frequency of the Roll-Out or Extendable Flexible Solar Arrays has been preliminary evaluated considering the following dimensions of 80 m x 10 m:

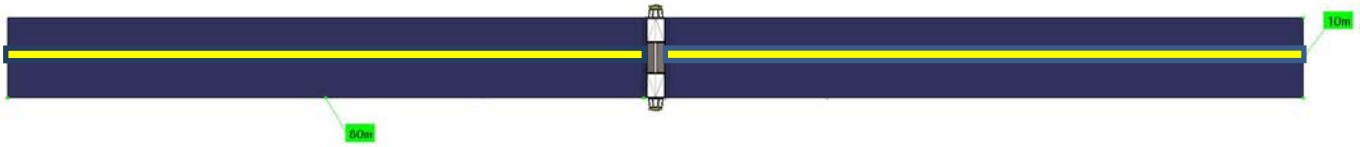

Figure 4-21 Roll-Out or Extendable Flexible Solar Arrays with Central Booms

Due to the 80 m length a coilable boom needs to be thin in order to be “coilable” and limit the drum size, to have a big diameter for sufficient inertia in addition to a high elastic modulus for the required stiffness in terms of first frequency value.

Figure 4-22 Telescoping structure – Credit Northrop Grumman/ASTRO

A rigid central telescopic boom with interior deployment device on the other hand allows more flexibility in terms of use of UHM (Ultra High Modulus) fibers, thickness and size of the section to achieve higher inertia and stiffness properties and is therefore considered more effective: rigid telescopic deployable booms up to 34 m length have been already manufactured and tested as reported in RD[23] and in **Figure 4-23**.

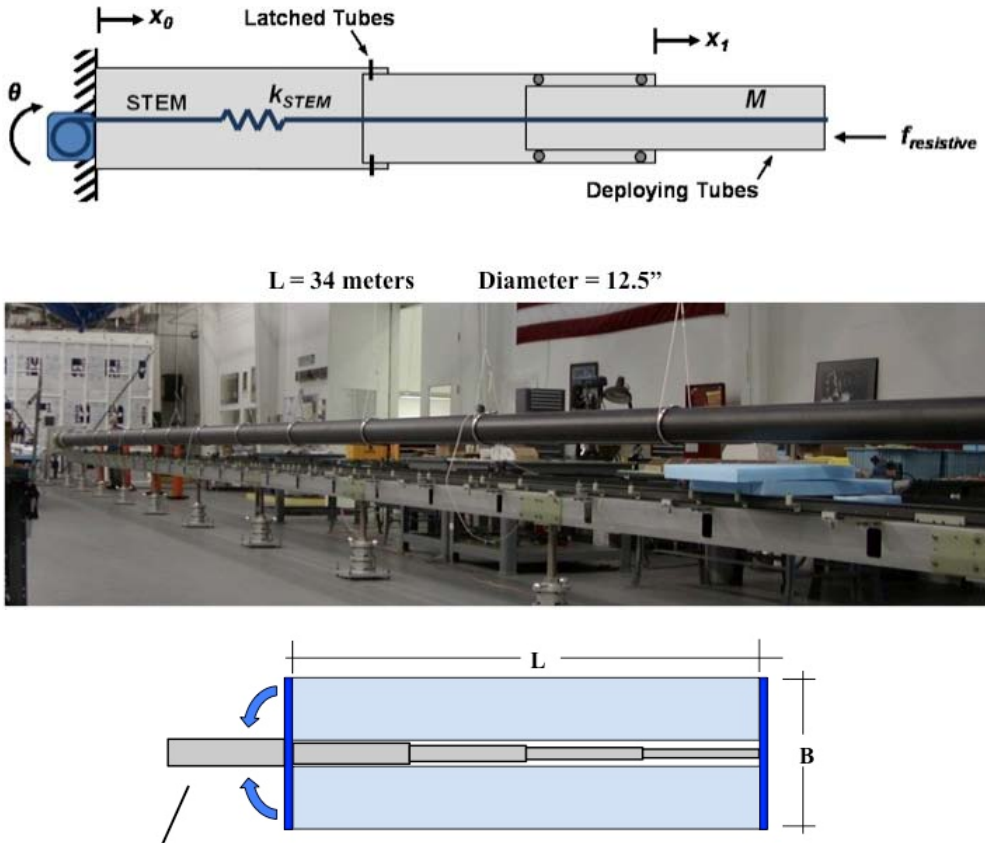

Figure 4-23 Telescoping structure – Credit Northrop Grumman/ASTRO

$$fi = \frac{\lambda i^2}{2 * \pi * L^2} * \sqrt{\frac{E * I}{m}} \quad with\ i = 1,2,3 \ldots.$$

The calculation is performed based on RD[22] formula considering case 3. In Blevins' table considering a clamped-free beam for the first frequency evaluation and assuming in the formula:

- E = 325000 MPa (based on CFRP high elastic modules material e.g. M55J/M18 with a 0 degs lay-up)
- λi = 1.875 (for the first natural frequency in free-clamped condition)
- L = 80 m (span of each Solar Array boom)

- m = 3 kg/m (mass x unit length of the flexible part 0.15 kg/m2 plus the 80 m boom with the inertia and section properties reported in **Table 4-3**)

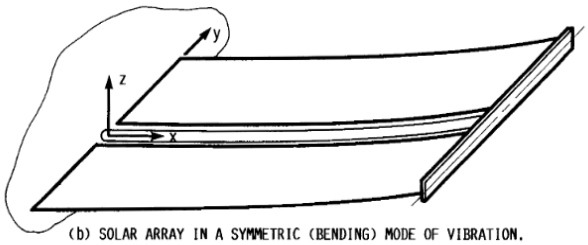

Figure 4-24 First Frequency Flexure Mode Shape (Boom driven)

The iterative calculation, considering a cantilever (clamped-free) solution, led to the following evaluation having as a preliminary target, a first frequency in the 0.15 Hz range for the single SPS Solar Array which is in any case higher than the one of the current ISS Solar Arrays having considerably lower dimensions.

A frequency of 0.186 Hz has been obtained with a CFRP boom of 0.3 m radius and a wall thickness of 0.5 mm.

SOLAR ARRAY - CLAMPED FREE BOOM								
Boom Radius Ext [m]	Boom Radius Int [m]	Boom Inertia [m4]	Boom Section Area [m2]	E [Pa]	rho [kg/m3]	Mass x unit length [kg/m]	Lambda i	fn [Hz]
0.3	0.2995	4.23E-05	9.42E-04	3.25E+11	1600	3.01	1.87	0.186
Thickness [mm]	Mass Boom [kg]	Mass of Flexible Part Solar Array [kg]						
0.5	121	120						

Table 4-3 Solar Array First Frequency

A structural mass of the single Solar Array of 241 kg which considering 388 Solar Arrays for 2 Adjacent Half Wings leads to 93328 kg as reported in the next picture.

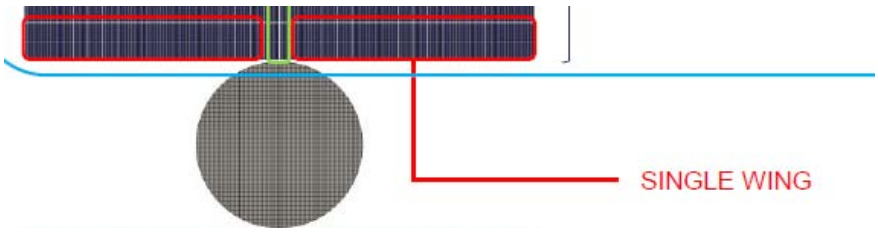

Figure 4-25 2 Adjacent Half Wings

STEP2 - 2 Adjacent Half Wings

The first frequency of 2 Adjacent Half Wings has been preliminary evaluated considering the extension of 2500 m and the Roll-out Modules assembly, indicated by the yellow area, as a free-free beam to which its own mass and the masses of the 388 Solar Arrays (flexible parts & booms) are considered in the mass per unit length calculation:

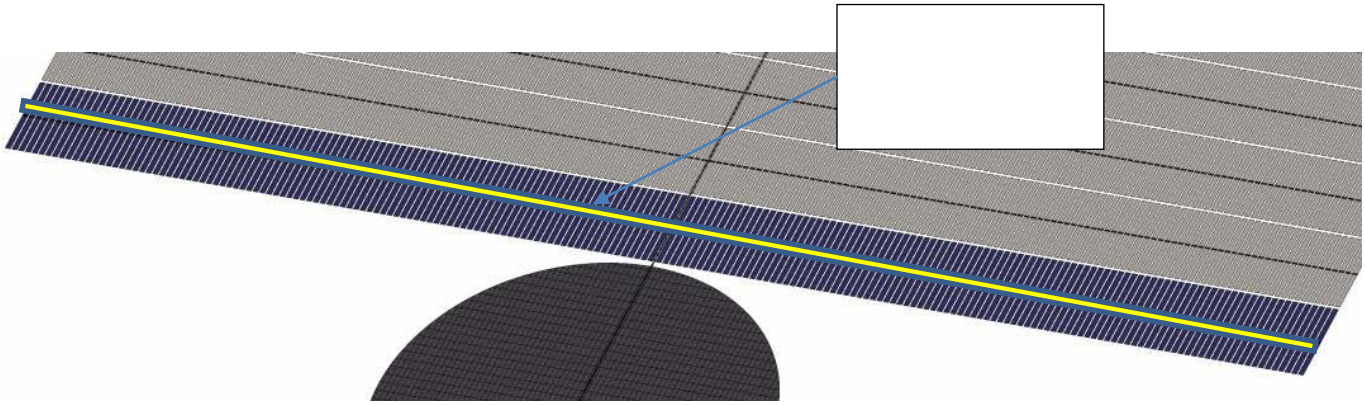

Figure 4-26 2 Adjacent Half Wings with Roll-out Modules

The Roll-out Modules sequence (depicted in yellow) acting as a beam with the 2 Adjacent Half Wings of Solar Arrays as distributed masses, is considered to have a first bending frequency in free-free conditions leading to the following mode shape:

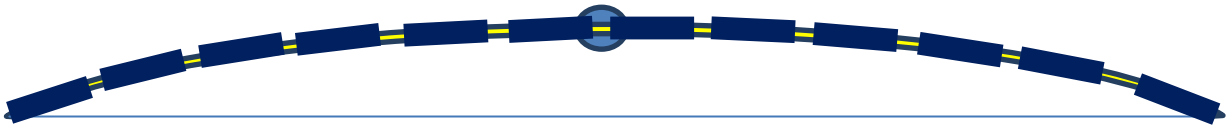

Figure 4-27 2 Adjacent Half Wings with Roll-out Modules Deformed Mode Shape (1 st Frequency)

The calculation is performed based on RD[22] formula considering case 1. and the following values:

- E = 325000 MPa (based on CFRP high elastic modules material e.g. M55J/M18 with a 0 degs unidirectional lay-up)
- λi = 4.73 (for the first natural frequency in free-free condition)
- L = 2500 m (span of the 2 Adjacent Half Wings with Roll-out Modules)

- m = 97.57 kg/m (mass x unit length given by the 388 Solar Arrays with Booms of 2 Adjacent Half Wings (93328 kg) and the mass of the 194 Roll-out Modules over a length of 2500 m (150595 kg) having the inertia and section properties reported in **Table 4-4**)

The iterative calculation, considering a free-free solution for the 194 Roll-out Modules of 2 Adjacent Half Wings, led to the following evaluation of a first frequency of 0.007 Hz.

The frequency of 0.007 Hz has been obtained with a CFRP equivalent circular module of 1.5 m radius and a wall thickness of 4 mm. This means that, in order to achieve this frequency, the single Roll-out Module shall have inertia properties in line with this equivalent module.

2 ADJACENT WING - FREE FREE ROLL-OUT MODULE SEQUENCE									
Module Radius Ext [m]	Module Radius Int [m]	Module Inertia [m4]	Module Section Area [m2]	E [Pa]	rho [kg/m3]	Mass x unit length [kg/m]	Lambda i	fn [Hz]	L [m]
1.5	1.496	4.22E-02	3.76E-02	3.25E+11	1600	97.57	4.73	0.007	2500
Thickness [mm]	Mass of 2 Adjacent Wings Modules (194) [kg]	Mass of Flexible Solar Arrays per 2 Adjacent Wings [kg]							
4	150595	93328							

Table 4-4 2 Adjacent Half Wings – Roll-out Module Properties & First Frequency

A total structural mass of 243924 kg is so obtained for the 2 Adjacent Half Wings of **Figure 4-26**.

STEP3 - Entire SPS (2 Full Wings & Antenna)

The first frequency of the entire SPS has been preliminary evaluated considering the extension of 4130 m and the Central Truss Modules assembly, indicated by the yellow area, acting as a free-free beam to which its own mass and the masses of the 20 Solar Arrays Wings with the relevant Truss Modules are considered in the mass per unit length calculation:

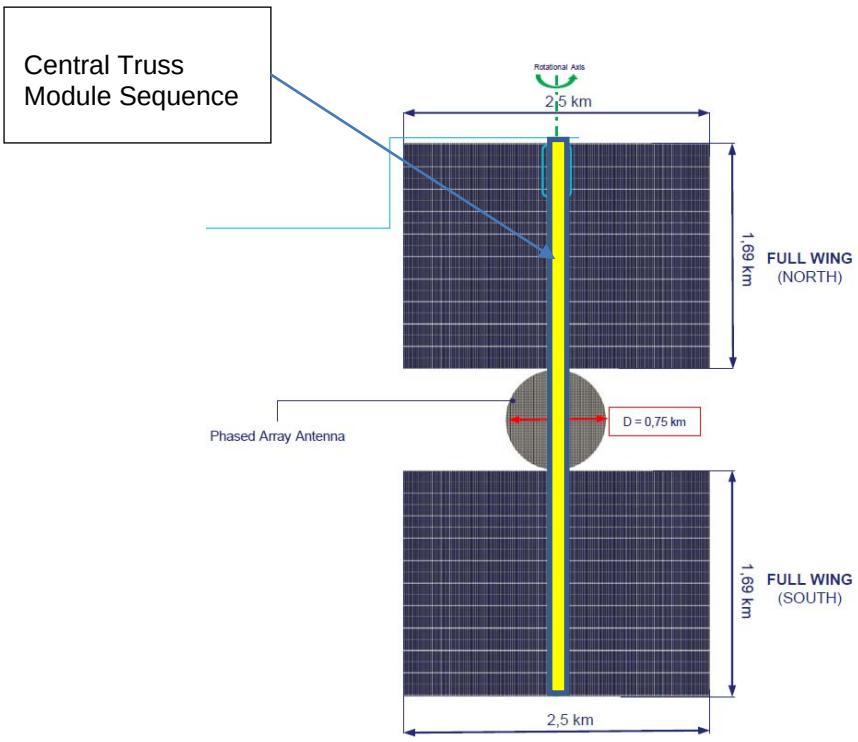

Figure 4-28 Full Wings with Central Truss Modules

The Central Truss Modules sequence (depicted in yellow) of the 2 Full Wings and Antenna is considered to have a free-free first bending frequency leading to the following mode shape:

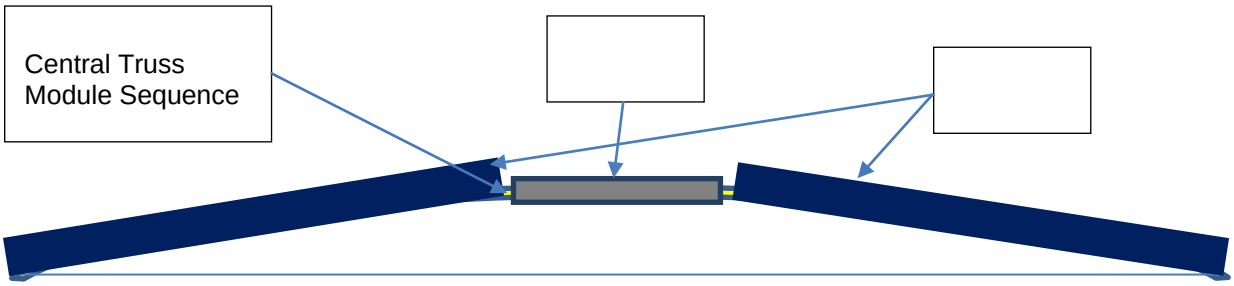

Figure 4-29 Full Wings (North & South) & Antenna with Central Truss Modules Deformed Mode Shape (1 st Frequency)

The calculation is performed based on RD[22] formula considering case 1. and the following values:

- E = 325000 MPa (based on CFRP high elastic modules material e.g. M55J/M18 with a 0 degs unidirectional lay-up)
- λi = 4.73 (for the first natural frequency in free-free condition)
- L = 4130 m (span of the 2 Full Wings with Active Truss Modules)
- m = 1357.27 kg/m (mass x unit length given by the 2 complete Full Wings and Antenna (4879061 kg) and the mass of the Central Truss Modules over a length of 4130 m (726458 kg) having the inertia and section properties reported in **Table 4-5**)

The iterative calculation, considering a free-free solution for the entire SPS, led to the following evaluation and by the Central Truss Module assembly of a first frequency of 0.005 Hz.

The frequency of 0.005 Hz has been obtained with a CFRP equivalent circular module of 7 m radius and a wall thickness of 2.5 mm. This means that, in order to achieve this final frequency, the single Module of the Central Truss shall have inertia properties in line with this equivalent module.

SBSP - 2 FULL WINGS - FREE FREE									
Module Radius Ext [m]	Module Radius Int [m]	Module Inertia [m4]	Module Section Area [m2]	E [Pa]	rho [kg/m3]	Mass x unit length [kg/m]	Lambda i	fn [Hz]	L [m]
7	6.9975	2.69E+00	1.10E-01	3.25E+11	1600	1357.27	4.73	0.005	4130
Thickness [mm]	Mass of Central Truss [kg]	Mass of Wings [kg]							
2.5	726458	4879061							

Table 4-5 SPS Central Truss Properties & First Frequency

A total basic structural mass of 5605519 kg is so obtained for the SPS structure under the assumptions used for the calculations of **Figure 4-28**.

4.2.4 AOCS

The analysis of the expected disturbances is used to select the type of actuators to be used and to estimate the required torque and force levels.

Based on this analysis, an architecture for the actuators is proposed.

4.2.4.1 Disturbance Analysis

The disturbance acting on the S/C have been estimated based on the following assumptions:

- Rotational axis (x) perpendicular to orbit plane
- Z axis pointed toward the Sun
- Diagonal inertia matrix with the following values:
  - I_{xx} = 2.78e12 kgm^2
  - I_{yy} = 9.19e12 kgm^2
  - I_{zz} = 11.96e12 kgm^2

4.2.4.1.1 Gravity gradient

Under the analysis assumptions, the gravity gradient torque is a periodic torque around the X axis with periodicity twice the orbital period and peak depending on the difference between the inertias I_{yy} and I_{zz}.

The following figure shows the behavior during an orbit of the gravity gradient torque and of the accumulated angular momentum.

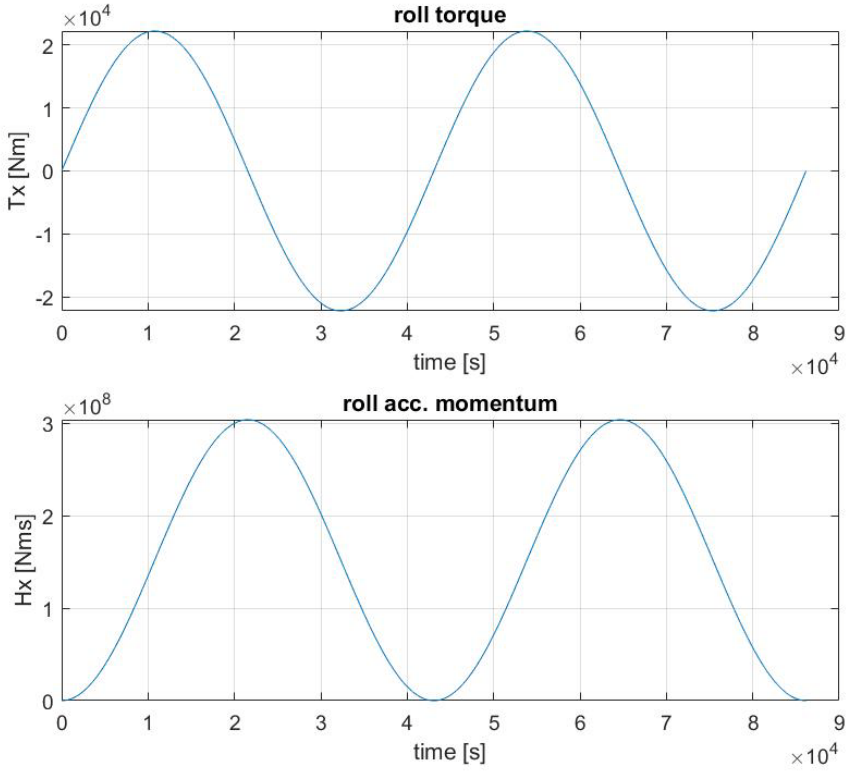

Figure 4-30 Gravity gradient torque and accumulated momentum

The peak torque is approximately 22000 Nm, while the peak accumulated angular momentum is 300e6 Nms.

Regarding the estimation of the torques around Y and Z axis, associated to pointing errors and non-diagonal inertia matrix, we will assume here a maximum value of 10% of the torque around X axis.

If this disturbance has to be controlled by means of angular momentum exchange devices, such as control momentum gyros (CMGs), this would require:

- 85 CMGs to produce the peak torque
- 64000 CMGs to store the angular momentum

This estimation is based on the properties of the CMGs used on the ISS, with the following characteristics:

- torque: 258 Nm
- momentum capacity: 4760 Nms
- mass: 272 kg

Since the mass of 64000 CMGs is approximately 17400 tons, this makes clearly unfeasible the options of using this type of devices to control the gravity gradient torque, even considering future and more performing units, with a much larger and more favorable ratio between mass and momentum storage capacity.

4.2.4.1.2 Solar pressure force and torque

The analysis of the force produced by the solar pressure is shown in section 4.1.2.

The maximum solar pressure force is approximately 57 N, parallel to the Z axis.

A preliminary estimation of the solar pressure torque is made considering a shift of 10 m along each axis between the center of mass and the center of pressure, resulting in a torque of approximately 600 Nm around X and Y.

4.2.4.2 Actuator sizing and proposed accommodation

Based on the analysis of the previous paragraphs, the required forces and torques to be produced by the control system are:

- Torque X: 22000 Nm (gravity gradient) + 600 Nm (solar pressure) + 600 Nm (other, added as a margin) = 23200 Nm
- Torque Y: 2200 Nm (gravity gradient) + 600 Nm (solar pressure) + 600 Nm (other, added as a margin) = 3400 Nm
- Torque Z: 2200 Nm (gravity gradient) + 600 Nm (other, added as a margin) = 2800 Nm
- Force X = 20 N (in both directions), for station-keeping maneuvers
- Force Y = 6 N (in both directions), for station-keeping maneuvers
- Force Z = 60 N for solar pressure removal + 6 N in opposite direction
- Force along beaming vector = 7 N for antenna photon pressure removal

The force along X has been computed in order to implement the station-keeping maneuvers described in section 4.1.2 (i.e. 90-days continuous firings around the equinoxes for north-south corrections). For the force along Y (east-west corrections) and along Z opposite to solar pressure (other corrections), a value of 10% of the solar pressure has been assumed.

It is proposed a simplified and fully decoupled architecture, i.e. the accommodation of the thrusters is selected in order to have a set that produces a pure torque around X, a second set that produces a pure Y torque and so on, for a total of six independent sets.

In order to minimize structural stress, a distributed mounting is preferred.

The thrusters are supposed to be mounted close to the border of the wings, in order to maximize the arm (maximum 1250 m available for X torque, 375+1690 available for Y and Z torque).

The accommodation concept is shown in the following figure.

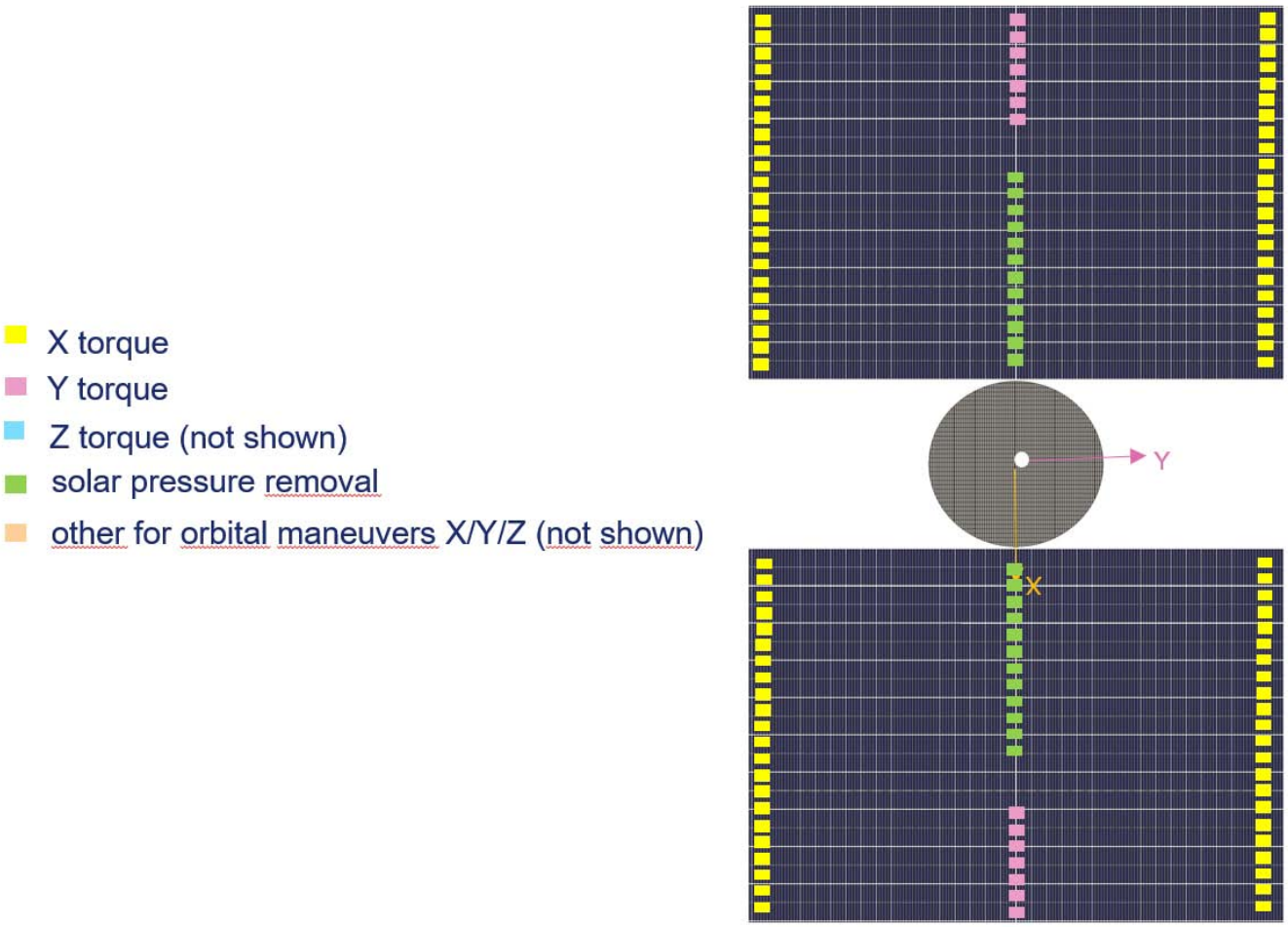

Figure 4-31 RCS accommodation

The number of thrusters depends on the thrust level of the selected thruster.

In order to maximize the possibility of a distributed accommodation, we consider Hall thrusters with a force level of 0.1 N. If the force level increases, the number of actuators will decrease approximately in a proportional way.

- Torque X. Required force = 23200/1250 ≈ 19 N → 190 thrusters for negative torque, 190 thrusters for positive torque. They can be divided in 8 groups, 4 firing along +Z, 4 firing along –Z
- Torque Y. Required force = 3400/(375+1690) ≈ 1.65 N → 17 thrusters for negative torque, 17 thrusters for positive torque
- Torque Z. Required force = 2800/(375+1690) ≈ 1.4 N → 14 thrusters for negative torque, 14 thrusters for positive torque
- Force X: 20 N along +X, 20 N along –X → total of 400 thrusters
- Force Y: 6 N along +Y, 6 N along –Y → total of 120 thrusters
- Force Z: 60 N along +Z, 6 N along –Z → total of 660 thrusters

- Force along beaming vector: 7 N along +beaming vector → total of 70 thrusters

The total number of thrusters is therefore 1692.

4.2.4.3 Yearly propellant consumption

Finally, we propose here an estimation of the amount of propellant needed during one year of operations.

The estimation is based on the following assumptions:

- Total mass: 6600 tons
- Solar pressure 60 N
- Force for disturbance removal: 20 N

The assumption for the force needed for disturbance removal is associated with the peak value of the gravity gradient torque, therefore this estimation can be considered very conservative.

The following figure shows the propellant consumption as a function of the specific impulse of the thrusters. Two components are considered: station-keeping maneuvers and disturbance control (assuming a continuous removal of solar pressure, gravity gradient and other disturbances).

The propellant associated to station-keeping maneuvers assumes a yearly ΔV of 50 m/s and is computed from the Tsiolkovsky rocket equation.

With a specific impulse of 5000 s, considered as baseline, the consumption is approximately 63 tons/year. Considering that the typical Hall thrusters propellant is Xenon, the required amount poses a challenge in terms of scale-up global production, as in 2015 the global production was in the order of 53 tons. Many alternative propellants are available that can overcome the Xenon shortage, but a dedicated study shall be conducted to compare the efficiencies and availability of such materials.

A sensitivity analysis is proposed in Figure 4-32 to show the required propellant amount based on the thruster's specific impulse, which can be a key element to choose alternative propellants or thruster types. The analysis shows how high Isp are extremely valuable to save propellant but even with an Isp of 1000 s a total of 4 launches per year are sufficient to refuel the AOCS subsystem, an amount that does not compromise the mission in terms of overall costs.

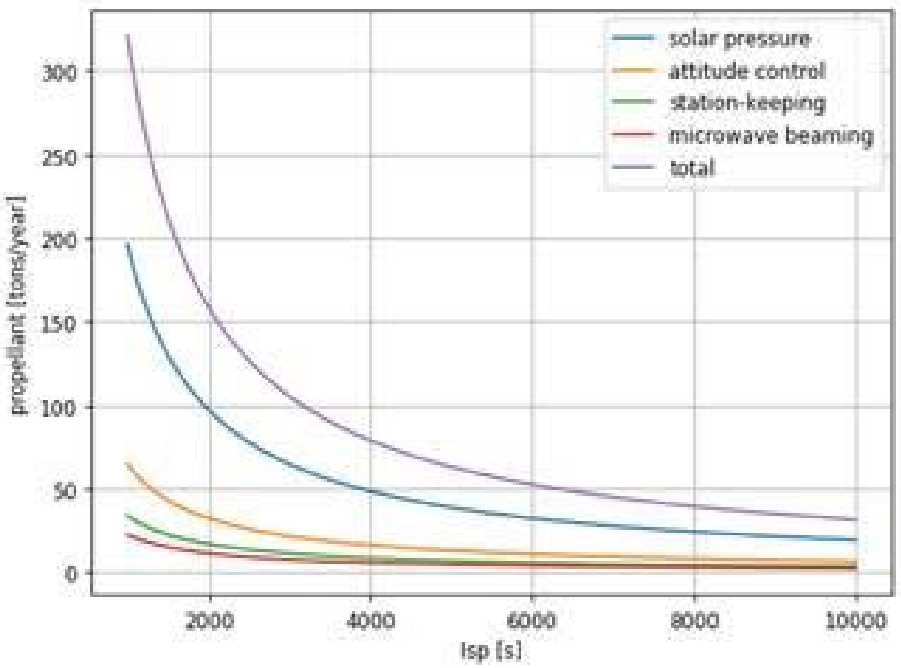

Figure 4-32 Yearly propellant consumption

4.2.4.4 Control concept

One of the major concerns in the design of the AOCS is the potential control–structure interaction, due to the expected low frequency of the structure.

The simplest way of dealing with this concern is to design a controller with sufficiently low bandwidth, such that the interaction with the structure frequencies is avoided by design. As shown in the paragraph that describes the structure, in our case the lowest structural frequency is 0.005 Hz. This value allows the design of a simple control law with a bandwidth in the order of $5 \cdot 10^{-5} \div 10^{-4}$ Hz, that is sufficiently apart from the structural frequency, but is expected to ensure a sufficiently prompt removal of the disturbances.

The AOCS is in charge of pointing the solar panels toward the Sun, while the pointing of the transmitting antenna toward the Earth is performed by the motorized rotary joints as described in the paragraph about the Antenna rotation strategy.

A pointing accuracy requirement of 0.5 deg (angle between Sun direction and Z axis) is assumed. It can be preliminary expected that a simplified control law, such as a classical PID controller, can be sufficient to ensure this level of accuracy. Independent control laws for each axis can be implemented, including a feedforward term to describe the expected disturbances, in particular the gravity gradient torque.

It has been shown ([RD20]) that a low-bandwidth attitude control system of this type, with a bandwidth in the order of 1e-5 Hz, is able (for a 3.2 km x 3.2 km planar SPS with a structural frequency of 0.002 Hz and equipped with ion thrusters) to provide a pointing accuracy in the order of 0.1 deg, in the presence of large, but slowly varying, external disturbances and dynamic modeling uncertainties.

Although the proposed control concept should avoid excitation of the structural modes, further investigations regarding the interactions between structure and control, requiring models more sophisticated than those available in this phase of the study, are expected to be needed to ensure the robustness of the AOCS design and to identify possible side effects, such as antenna pointing errors and effects associated to structural deformations (e.g. errors on sensor measurements).

For instance, control forces and torques can be affected, through the control algorithms, by signals induced in the sensor measurements by the structural vibrations. Another significant effect of the structural deformation that can be expected is that on the direction of the forces of the thrusters, with consequent generation of spurious disturbance forces and torques around the other axes, and degradation of the pointing performances. Another minor effect of the deformation could be the generation of solar radiation forces also in directions perpendicular to the nominal Sun direction. It has been shown ([RD32]) that the aforementioned effects can have a negative impact on the control performances (with respect to the performances obtained considering the system as a rigid body) leading to the need for a more complex control scheme, e.g. a coordinated orbit–attitude–vibration control.

Another issue associated with structural vibrations is the placement of sensors. While the possibility to select the location of the actuators is limited by the need to mount the thrusters as far as possible from the center of gravity in order to reduce the propellant consumption, there are more degrees of freedom for the placement of the attitude sensors. Using distributed attitude sensors (obtaining the attitude information by average processing of multiple sensors) is a way to minimize the influence of the structural flexibility on the attitude motion. It has been shown ([RD33]) that it is possible to find optimal locations that reduce the control–structure interaction, employing at the same time a reduced number of sensors (the advantage of using more than 20 sensors for a 3.2 km x 3.2 km plane SPS is minimal).

It must also be pointed out that the control is based on a prolonged and nearly continuous usage of electric propulsion. For instance, the thrusters used for removal of the sun pressure are assumed to be continuously active throughout the operating life of system. This represents a technological challenge for the actuation system, since a sufficiently long lifetime of the thrusters must be ensured.

Another point associated with the thrusters is the improvement of the specific impulse, since this has a direct impact on propellant consumption and refueling needs.

4.2.5 EPS

The Electrical Power Subsystem (EPS) is one of the most critical subsystems in the challenge of collecting and transmitting a huge amount of power from space to Earth, intended as the Space-based solar power system (SBSP) mission goal. The power demand and mission requirements are important driving factors in selecting the most suitable power electronics as well as the ultra-high voltage wires to be installed.

The EPS includes the Solar Array as primary energy source during sunlight, whereas the use of rechargeable batteries is restricted for eclipse periods, when no power generation from the SA is available. Furthermore, for the regulation, control, and distribution of power, the EPS architecture is equipped with a set of power management, distribution and switching units.

The EPS high level block diagram is reported below (for simplicity only few Single Wings are represented, as the others are identical). It is a purely functional and highly simplified architecture giving a rough overview of typical EPS technical contents.

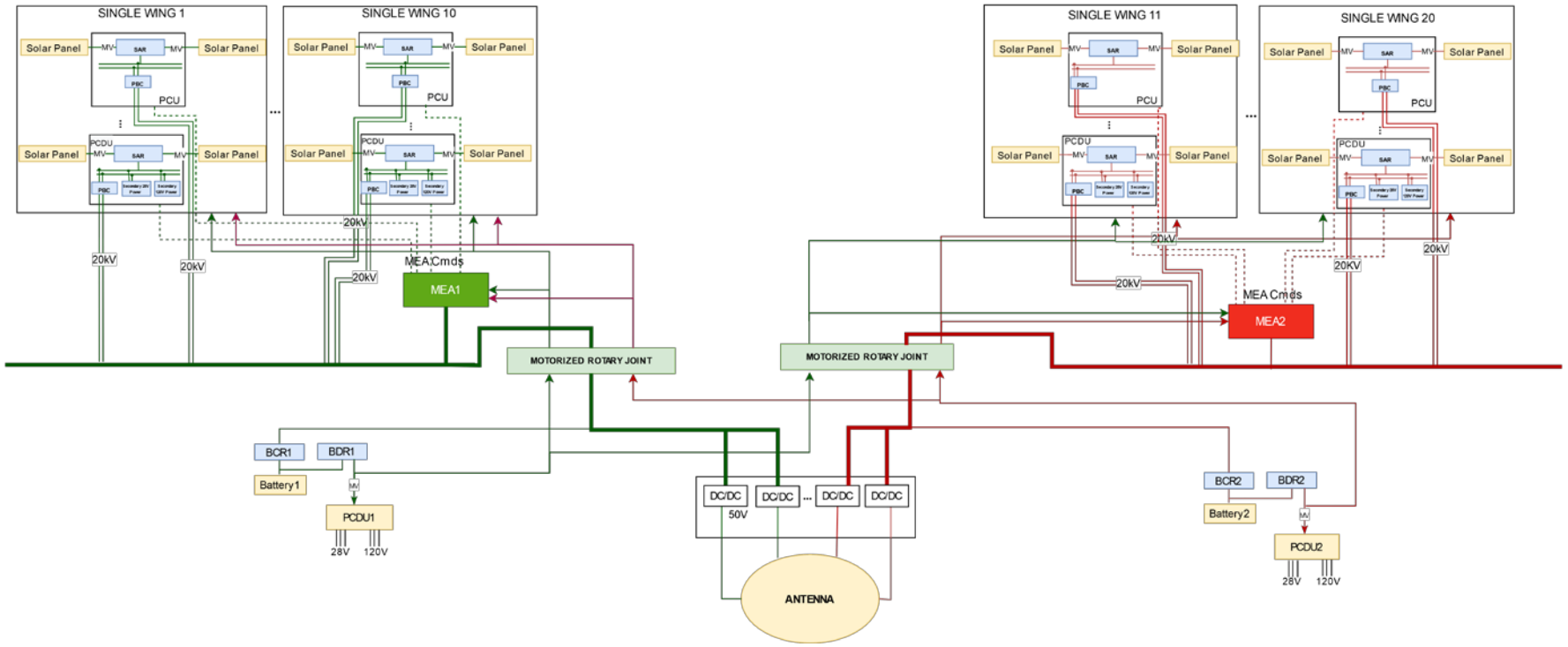

Figure 4-33 EPS block scheme

The SPS EPS shall be able to handle a maximum power capability of 2GW, used for:

- Transferring power to the antenna, for EM power beam transmission toward the Ground Power Station on Earth;
- Satisfying the SPS internal power consumption needs over the sunlight;
- Batteries recharging, needed to supply power for service devices during eclipse periods. At this moment, among the highest capacity qualified cells commercially available there are the 18650MJ1 ABSL cells (252 Wh/kg) which represent a promising candidate for optimizing the power-to-mass ratio and so maximizing the cost and mass saving. No electric thrusters are supposed to be active in eclipse, and thermal control is supposed passive, thus, only the power consumption related to control electronics and TT&C units is intended to be satisfied by batteries. By assuming a power demand of about 500W in eclipse, the battery mass should be negligible (in the order of tens of kg).

The proposed EPS architecture is focused on two independent power domain (green and red in Figure 4-33). In nominal operating scenario (no failure) the total system power is intended to be equally distributed between each power domain. Each domain is managed independently in order to face with a possible double failure scenario that would lead to lose an entire power domain.

The huge amount of power involved and the considerable distances make necessary working at voltage ranges (around 20kV) greater than those commonly used in space. Thus, the power coming from Solar panels is transmitted along the structure by means of ultra-high voltage cables, to decrease electric current, reducing the huge power transmission losses that otherwise there would be to cover the long distances involved. The driving factor for the voltage range assumption is due to the still acceptable power transmission efficiency, i.e about 0.98, computing by considering the worst case of the longest distance from the antenna.

High power electric cables represent a big challenge in space; at this moment there are no space grade high-power technology satisfying the needed voltage requirement, thus, cables used in both military and industrial high voltage applications are considered.

From the datasheets, a good compromise for mass saving and power losses reduction would be the 20kV cables AWG 16, each carrying 6.5A and 130kW. A less voltage value, instead, would lead to a considerable increase of the number of cables for the same section (and thus, at the same current capability), and, consequently, of the mass of the entire system.

The power regulation from the SA is intended at each roll-out module level, by means of a single PCU (Power Conditioning Unit) responsible of controlling the electrical power available from the Solar Array, at medium voltage range (about 400/500 V), via Sequential Switching Shunt regulators (S3R) which regulate the power from the roll-out module to the n buses connected together in the Main bus at central truss level. In some cases, PCDUs (Power Conditioning & Distribution Unit) are necessary for conditioning the SA power to the different voltage levels (120V and 28V) according to the platform equipment.

The power regulation at roll-out module level is assumed to be managed by a Main Error Amplifier (MEA) function based on two different domains, i.e Shunt domain and “Eclipse” one. In the first one, from each roll-out module it is extrapolated as long as sufficient power for power load request (from 0% to 100% of the maximum power capability), in the other no power generation is available.

To increase the voltage range from SA 400-500V up to 20kV, dedicated high power conversion electronics (“PBC” - Primary Bus Converter in the EPS schematic) are necessary so that the power transmission efficiency would increase as well. At this moment, among the best performant space qualified units, it has been developed power electronics for 1,85 kV and able to deliver up to 5kW with a mass of about 47kg. In the overall system about 368 tons are assumed for power conversion electronics.

However, new advanced materials and innovative components are expected to be developed for the high-power electric system in space, abling to satisfy the power and voltage requirements.

Dedicated Battery Control Electronics are also necessary for managing the battery charge and discharge (BCR/BDR) in accordance to the required methodology by regulating the Main Bus power to the battery. In this case the BCE regulates the battery charging through the BCR based on the following three-domain regulation scheme, while the BDR is a simple converter and always provide the required power to the system electronics (computer, RF, etc.):

- *Sunlit domain*: when the power available on the Main bus exceeds the power load consumption and the battery charge demand (the battery will be charged based on constant current/constant voltage (CC/CV) profile)
- *BDR domain*: when the power on the Main bus is not sufficient to satisfy the power requested by the load and for battery charging (the battery will be charged at variable current, smaller than the previous case)
- *Battery domain*: when the power available on the Main bus is not sufficient to satisfy the load demand, the batteries shall provide automatically the missing solar array power

Furthermore, a second stage of power conversion is at truss module level, before being transmitted to the antenna for the microwave generation.

4.2.6 Phased Array Antenna

We propose in this chapter to define the antenna of the WPT with a technical solution based on coherent phase array. It is a large planar phase array of hundreds of meters in diameter (750m in our case). It is made up of rigid sub-panels of few meters in side. Each sub-panel is made up of hundreds of bricks of few centimetres in side. Each brick includes few radiating elements (RE).

The sub-panels shall be rigid and preferably launched in one piece. Each sub-panel contains a local power distribution network to feed the EPC of the RF power generators. It will also be able to transmit electric current to its neighbours. For reasons of symmetry, it has roughly a square shape. It is equipped with assembly locks and hinges and electrical connectors to allow assembly in orbit.

The radiating element (RE) is the basic element of the antenna; it ensures the emission of RF power. In planar array it is slim and is sometimes called patch. Several RE constitute the aerial of a brick. The brick is equipped with a RF power generator, a phase and amplitude control device (for electronically steering) and supporting and ancillary electronics.

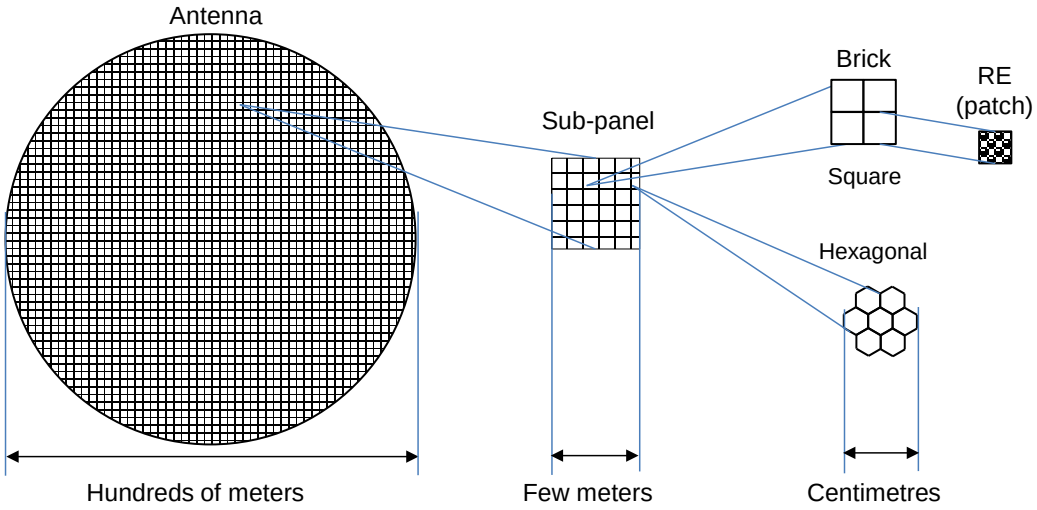

Figure 4-34 WPT antenna mechanical architecture

4.2.6.1 Radiating element (RE) definition

The RE are arranged in a lattice whose shape and spacing are constrained by the rejection requirement of the grating lobes and the scanning loss. There are typically two lattice patterns: the square lattice where the RE are equally spaced in the two directions and the equilateral triangle lattice (hexagonal). Equilateral triangle based lattice requires hexagonal RE. Hexagonal lattice requires less radiating elements than the square lattice for the same area.

There is a third configuration: an isosceles triangle based lattice, close to the hexagonal one, which is composed by rows of square radiating elements with half a step shift from one row to the next. We will consider the two first configurations: square and hexagonal.

The spacing is constrained by two conditions: to minimize the scanning loss and to control the grating lobes, so that they are out of the earth. The following figure is used to assess the RE

spacing.

θ_{earth} is the angle at which the earth is seen from GEO: $\sin(\theta_{earth}) = R_{earth}/R_{GEO}$, R_{earth} is the earth radius (6378km), R_{GEO} is the radius of the GEO (42164km).

θ_{beam} is the half beamwidth of the power beam ($1.22\lambda/Dtx$), Dtx is the antenna diameter.

θ_{scan} is the scanning range. This corresponds here to the uncertainty of the mechanical pointing of the antenna

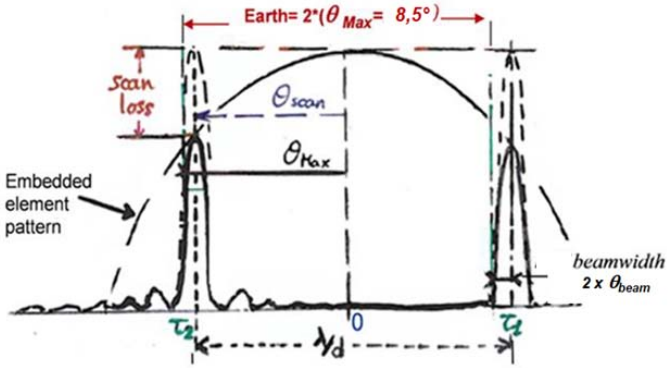

Figure 4-35 Grating lobe configuration

The condition to have grating lobes without a significant radiating power on earth is:

$d/\lambda < 1/(\tau1 + \tau2)$, where d is the RE spacing, $\tau1 = \sin(\theta_{earth} + \theta_{beam})$ and $\tau2 = \sin(\theta_{scan})$.

The RE gain is given by $G = 10.\log(\eta.4\pi.S / \lambda^2)$, η is the aperture efficiency (0.9) and S is the radiating surface.

The scanning loss at the edge of the scanning range is given by:

$$L = 3/(\frac{2}{\sqrt{3}} \times \frac{50.8}{\theta_{scan}.d})^2$$

In the frame of Solaris WPT antenna, θ_{scan} corresponds to the uncertainty of the mechanical pointing of the antenna. This uncertainty should be in the order of 1 to 2 deg. accordingly the scanning loss it is completely negligible.

4.2.6.2 Brick definition

A brick is the assembly of several RE. The arrangement of the RE must respect the lattice pattern (rectangular, triangular) and the maximum spacing ($d/\lambda < 1/(\tau1 + \tau2)$. Note also that RE with a side exceeding 3λ is very difficult to design with a good aperture efficiency.

The brick includes the aerial (patches), a polarizer (we assume circular polarization), a distribution network which feeds the patches, a RF generator and a phase setting device.

We give two examples of brick designs.

Square lattice

In the square lattice with a 6λ spacing, the brick could have a square surface of 6λ on each side.

Achieving a flat radiating surface of 6λ on a side with good aperture efficiency requires using smaller patch, for example: a sub-array of 4 patches of 3λ side.

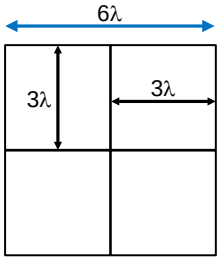

Sub-array 2x2

Example : sub-array made of horns

Hexagonal lattice

In the hexagonal lattice, the brick has a hexagonal area included in a rectangle.

To achieve a flat radiating surface of 6λ on a side with good aperture efficiency, it is necessary to use a sub-array of smaller radiating elements: here a sub-array of 7 patches.

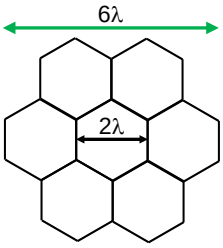

Sub-array 7

Example

4.2.6.3 Sub-panels definition

The sub-panel is a rigid infrastructure which houses the bricks. In the two cases of lattice, the sub-panel is roughly a square. The side of the panel will measure a few meters so that it can be launched in one piece and fit into the launcher fairing.

Radiofrequency wise, the sub-panel is a complete and autonomous phased array that is able to emit a continuous wave (CW) in a given direction. It includes a set of bricks, one or several synchronised frequency generators associated with a distribution network, possibly a beam forming network and control electronics. It includes also an electrical power distribution network to feed the RF generator within the brick.

There are at least two possible RF architectures:

- a centralized architecture where all the phase control devices (phase shifters) are centralized in a beam forming network fed by a frequency oscillator and providing CW to each brick. The beam forming network is controlled by electronics responsible for defining the required phases of all phase shifters to form and point the beam. Each brick shall include in its back: a RF power generator with its EPC and an input for the external oscillator.
- a distributed architecture where each brick has its own phase and amplitude control device. The brick has a local oscillator or it receives a CW from a centralizer oscillator. The required phase of its phase shifter is provided the control electronics at sub-panel level. Each brick shall include in its back: a RF power generator with its EPC, a phase shifter with its controller and a local oscillator or an input for an external oscillator.

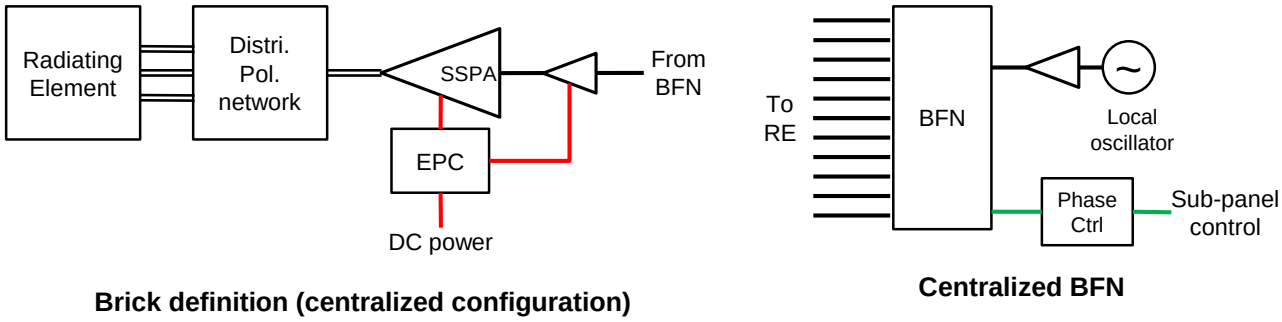

Brick definition (centralized configuration) **Centralized BFN**

Figure 4-36 Centralized architecture

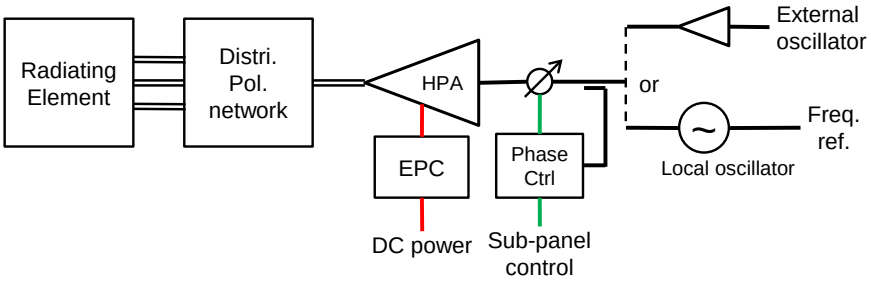

Figure 4-37 Brick definition (distributed configuration)

4.2.6.4 Consideration on brick failure

The antenna includes several hundreds of thousands of bricks. Each brick participates in the creation of the illumination law and it contributes to the transmission of RF power in proportion to the nominal power of its RF power generator (HPA).

Let's consider the most probable failure, the stopping of power transmission by a brick. In the event of a brick failure of this type, there are two impacts:

- a first impact is at the illumination law. The surface of the broken brick no longer participates in illumination and it becomes an obscured or non-radiating surface of the antenna. The aperture efficiency (η_{aper}) is therefore reduced accordingly (ratio between the surface of the brick and the radiating area of the antenna);
- a second impact is at the amount of power that is no more transmitted by the broken brick. Thus the power of the RF generator is no longer transmitted and it reduces the total power transmitted by the antenna in the corresponding ratio.

We therefore see that the breakdown of a brick has a double penalty. For example, a failure rate of 2% of the bricks reduces the overall efficiency of the WTP by 0.96 (0.98x0.98).

Note that it seems inappropriate (too costly) to add redundancies to reduce the failure rate.

4.2.6.5 Consideration on beam pointing

The pointing of the power beam is a very challenging topic.

To point the beam towards the GPS, it is a matter of defining and programming the phase shifts between the hundreds of thousands of radiating elements with a precision better than ten's de-

grees.

The definition and programming of the phase and amplitude shifts in the RF transmitters of the radiating elements must be done in real time to follow the evolution of the geometry of the system. Indeed, the geometry of the system constantly evolves following deformations of the antenna, dynamic inaccuracies in the mechanical pointing of the antenna, movements in the orbit, etc.

The calculation of each phase shift of each radiating element (or brick) can be done in open loop or closed loop.

In open loop it is necessary to locate very precisely the phase centre of each radiating element (in absolute or in relative to a local phase reference to the antenna), to precisely locate the centre of the Ground Power Station (GPS), then to carry out the calculations of the phase shifts and program the transmitters accordingly.

In a closed loop, it is possible to use the technique of retrodirectivity. A retrodirective antenna transmits the signal in the opposite direction to that of reception of a beacon signal emitted from the centre of the target, here the centre of the GPS. For this, each radiating element measures the received phase ($e^{j\varphi}$) of the beacon, calculates the conjugate ($e^{-j\varphi}$) of this phase and programs the transmitter with this phase. This is called conjugate matching beam-forming. Retrodirectivity can be achieved entirely passively with the use of a Van Atta array.

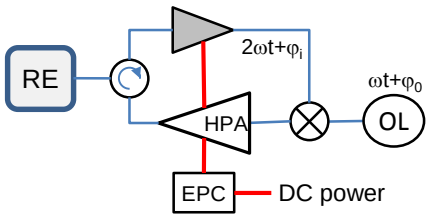

Figure 4-38 Retrodirective radiating element

An active retrodirectional configuration requires a beacon at twice the frequency of the transmitters and the distribution of a local oscillator at the transmission frequency (see on the left). The difficulty is to isolate the receiver from the high power of the transmitter and the distribution of the local oscillator to hundreds of thousands of radiating element with the same phase (as a phase reference).

The precision of calculation and material realization of phase shifts and also the precision of the power level setting of the transmitter have an impact on:

- beam pointing accuracy: This point can be critical if the beam does not point very precisely to the centre of the GPS. We are looking here for pointing accuracy of the order of a hundred meters on ground (1.6E-4 deg.).
- beam shape: When the actual illumination law deviates from the ideal uniform illumination law of the aperture, the shape of the main beam flattens and the level of the secondary lobes increases (loss of power).

Beam pointing accuracy: According to [RD26], the RMS Beam Pointing Error due to the RMS phase error of the phase shifters is very negligible in case of very substantial number of phased shifters are involved for electronic beam steering. This is intuitively explained by the fact that the contribution of the error of each phase shifter to the total error is divided by the number of phase shifters, which in our case is hundreds of thousands.

Beam pattern: The impact of inaccuracies in the phase and amplitude (power level) setting of the radiating elements of a phase array antenna could be very important on the radiating pattern. In the telecommunication and radar antennas, the degradation of the gain (the ability to

focus energy in the main lobe) due to amplitude and phase uncertainties can reach 5% to 15% loss. Without adequate simulation means, it is difficult to estimate the losses for phase arrays with hundreds of thousands of radiating elements.

4.2.6.6 Consideration on power handling

Two contradictory paths are possible in the design of the very large antenna of GEO WPT.

- The first consists of having the bricks with the largest possible surface to minimize their number and therefore the number of amplifiers, phase shifters, local oscillator distribution subscribers, etc... But this leads to extreme power levels for amplifiers.
- The second consists of having the smallest brick to minimize the amplifier power level. Of course this leads to maximizing the number of amplifiers, phase shifters, local oscillator distribution subscribers, etc...

Let's take our example: a WPT antenna of 750 m in diameter, an RF power to transmit of 1.63 GW and operating at 5.8GHz (see next table)..

Spacing	Brick type	Number	HPA power (W)
3,2 λ	Square 1RE	16 035 958	100
9,6 λ	Square 3x3RE	1 781 773	915
16 λ	Hexagonal 19RE	806 820	2020

Table 4-6 HPA power vs. number of bricks

4.2.6.7 Beacon link budget for retrodirective pointing

The next table gives the link budget of the beacon to be received by each brick to be able to perform conjugate matching beam forming (retrodirective).

The received power of the beacon depends on the brick size and RE spacing & lattice. The example is given with the hexagonal mesh with 7RE brick and 3.2λ spacing.

Frequency	11,60	GHz	
GPS antenna diameter	32	m	
GPS antenna gain	69,6	dB	
Half power Beamwidth	0,11	deg.	GEO arc of 70 km
GPS transmit power	2000	W	
GPS EIRP	100,1	dBW	
Distance	37323	km	
Free Space Loss	-205,2	dB	
Atmospheric loss	-0,54	dB	Europe average at 98% availability
Brick type	Hexa 7RE		
RE spacing	3,2	$\lambda_{/d}$	
Brick Gain	28,5	dB	
Received power (brick ouput)	-47,1	dBm	0,03 mV
Reception gain	30,0	dB	
Achieved input level	-17,14	dBm	0,98 mV

Table 4-7 Beacon link budget

The GPS requires an antenna of 32 meter in diameter and a power amplifier of 25 kW. The operating frequency is twice the frequency of the WPT.

4.2.6.8 Phased Array Antenna Definition

Let's take our case of a WPT operating at 5.8 GHz, which WPT antenna has a diameter of 750 meters and emitting 1.6GW.

4.2.6.9 RE design

First let find the RE spacing. In our case:

- θ_{beam} is 4.8 millidegres (84 µrad)
- θ_{scan} is 2 deg. which corresponds to an mechanical pointing uncertainty of +/- 1 deg.

The resulting maximum spacing is ~5.4λ and so ~28cm (wavelength at 5.8GHz is 5.2cm).

In order to have a good aperture efficient for the RE, we will limit the RE spacing to less than 3.2λ. Larger spacing will lead to lower aperture efficiency.

WPT antenna diameter (Dtx)	750	m	5,8 GHz
Half Beam Width	0,0046	deg.	1,22 λ / Dtx
Scanning range	2	deg.	mechanical pointing inaccuracy
Required RE spacing	5,4	λ/d	

Table 4-8 Antenna characteristics

For a 750 m diameter the total number of RE can reach tens of millions of RE depending on spacing (see next figure).

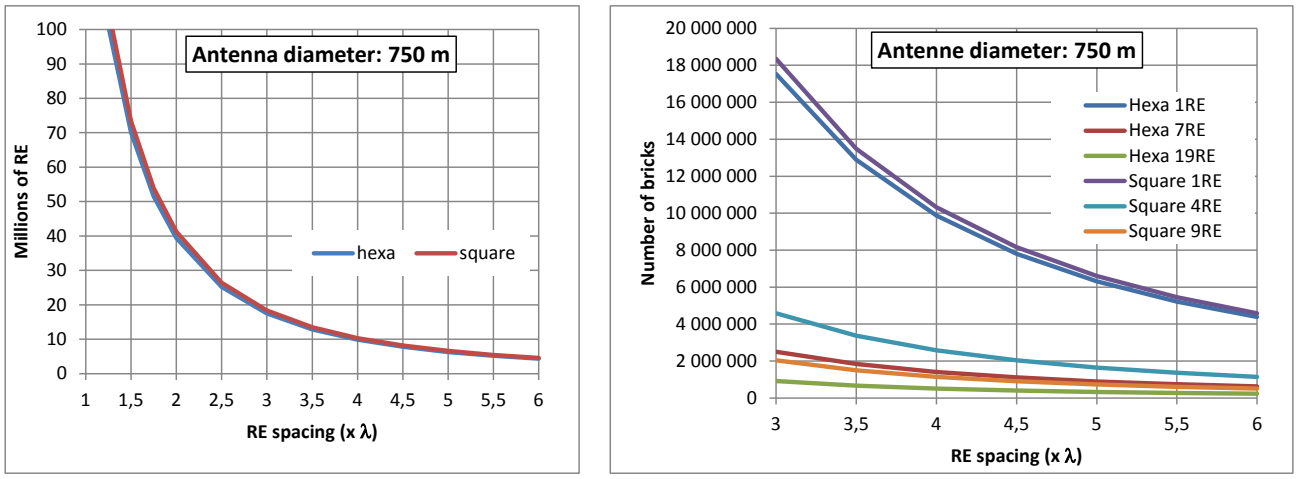

Figure 4-39 Number of RE and brick vs. spacing

4.2.6.10 Brick design

We consider six types of lattice, three square lattices and three hexagonal or triangular lattices (see next figure).

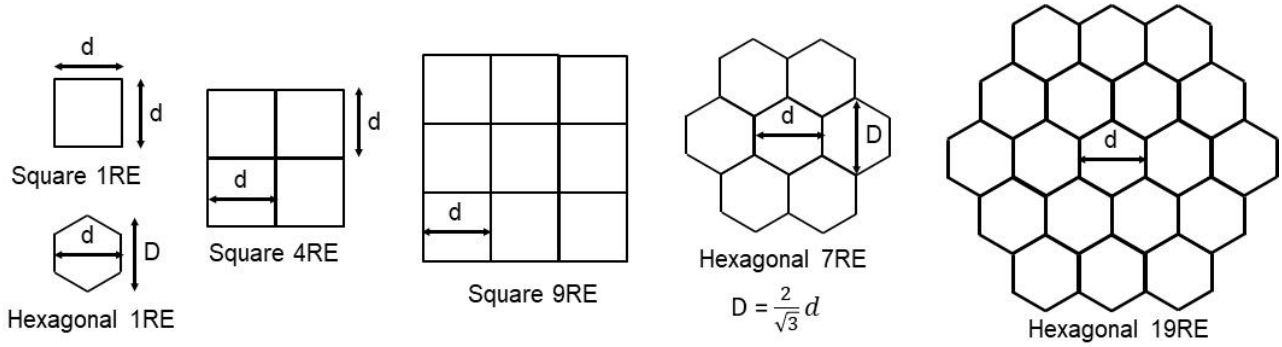

Figure 4-40 Brick designs

For the sake of our example, we select two RE spacings, 3.2λ which corresponds to a RE whose main beam covers the earth (~16 deg) and 5.4λ which corresponds to the largest spacing without grating lobes on the earth. We consider two lattices: a square lattice with 4 RE and a triangular lattice with 7 RE.

We choose a sub-panel side of about 8 meters which could allow a launch in one piece which will avoid deployment in orbit before assembly.

Spacing	3,2λ		5,4λ	
Lattice	Squa 4RE	Hexa 7RE	Squa 4RE	Hexa 7RE
Number of RE	16 121 245	15 411 067	5 660 364	5 414 977
Number of brick	4 030 311	2 201 581	1 415 091	773 568
Sub-panel size (m x m)	8,3 x 8,3	8,5 x 8,1	8,4 x 8,4	8,4 x 8,1
Number of sub-panel	6415	7578	6309	7759

Table 4-9 Example of antenna design (RE, brick, panel)

Consequently, in our case of an antenna of 750 meter in diameter, the total number of RE ranges from 16 million for 3.2 spacing to 5 and a half millions for the 5.2 spacing.

With a choice of sub-panel side about 8 meter (what would be compatible with a one-piece launch), the number of sub-panel to launch, assemble and wire is around 7000.

In the case of the SBSP Pre-Phase A, we recommend taking the conservative solution which maximizes aperture efficiency and eases thermal management: a spacing of 3.2λ and bricks of 4 X 4 RE (see orange column in above table).

4.2.7 TCS

4.2.7.1 Introduction of thermal design

In the context of this Pre-Phase A study of Space Based Solar Power, the thermal aspects are critical to understand if the material and equipment can withstand the harsh scenario and be operative during the mission. The SBSP project is particularly challenging from the thermal point of view, due both to the huge dimension of elements which constitute it, and hence the heat power received, and also to the modularity of the system. These constraints practically prevent the implementation of typical active thermal control solutions for high-dissipation equipment, such as cooling loops and external radiators, to manage the heat power received from the Sun and generated by avionics. As a consequence, the thermal design can only be based on fully passive thermal control solutions. The design proposed in the earlier phases of this study, in line with the outcome of the literature review, capitalizes the spacecraft substantial size, exploiting the large inactive surfaces of the modules that can act as radiators, and is based on a careful selection of coating materials and paints in order to optimize the thermo-optical properties on the active surfaces.

The thermal design of the spacecraft bus, including avionic units and propulsion system, will be addressed when the detailed design of these elements is defined. In particular, thrusters are supposed to have dedicated thermal control systems which allow the compliance of thermal requirements at element level (not assembly element). Nevertheless, the low maturity level of the design of these elements is acceptable at the current stage, and it is not critical from the thermal point of view. Indeed, the contribution to the overall thermal budget of the spacecraft bus is negligible, compared to those given by the antenna and the solar panels, and do not significantly affect the radiating exchange of the larger modules.

In this section, a thermal analysis will be described, performed with ESATAN software, on a simplified model; the aim of this analysis is to evaluate heat power received and rejected by the S/C and compute the temperature achieved during the mission.

This first analysis is focused only on the main, large elements (antenna and solar panels). As anticipated, avionics and thrusters are considered negligible for the purpose of the analysis and are currently omitted from the thermal model. Nevertheless, they can be addressed in future phases, once their design will be consolidated, and the results of the analysis will drive the decision about the most suitable techniques to be implemented for the thermal control.

The results reported in the next paragraphs will consider only the “equinoxes scenario” where the Sun is on the nodes in his apparent path around the Earth. In facts, this scenario has been found to represent for the solar panels and the antenna both the worst hot case, as in this position the Sun is normal to all S/C surfaces (and so the heat fluxes from the Star is maximum) and the worst cold case, as the S/C experiences the longest eclipse period during which temperature drops considerably.

4.2.7.2 Assumptions and Thermal Model

This section presents all assumptions made to carry out the analysis. Considering the current low maturity of the configuration, the implementation of a detailed model of the SPS is neither practicable nor significant in this phase. Nevertheless, in parallel to analytical calculations, a

preliminary simple ESATAN model has been created to support the verification of the feasibility of a passive thermal management of the antenna and the solar arrays. The model is constituted only by three elements: two rectangular wings and one circular antenna. Structures supporting and connecting the modules constituting the antenna and the solar arrays are not modelled, because their temperature requirement are not driving and their contribution to the thermal network can be considered negligible in such a large and modular system characterized by high dissipation and solar input. The shape and the size of elements are quite the same as the real ones defined in this document except for the full wing. As the model simplifies the full wing as a continuous rectangle, while it is formed by several solar panels not united with each other (not a continuous), the sides of full wings are made so that the total area of the rectangle is the same as assumed above. All elements have been considered shells, as the thickness has been assumed to be negligible considering the other dimensions. As already mentioned, avionics, thrusters and relevant propulsion system are not included in the thermal model. Their dissipation is in any case negligible with respect to the other dissipations (e.g. solar panels).

Assumptions made about the materials and thermo-optical properties of solar panels and antenna are listed in Table 4-10. Also in this case, all values are assumed based on available information and heritage. Perovskite thermal properties have been taken from specific papers while thermo-optical properties have been assumed based on common solar panels (values are not too dissimilar). The antenna has been assumed to be in aluminum as bulk material, assuming a rigid supporting structure. Two cases were considered for the analysis: in the first case, we conservatively assumed no specific surface coating on the active side with mediocre optical properties (to account for possible constraints and from impacts from the detailed geometry not known at present), while in the second case we assumed a dedicated paint with low alpha/epsilon ration on the active side, which is probably more realistic.

The rear side of the antenna is assumed to have a radiator-like coating (specifically, the properties of the new First-Flex interferential coating have been used), in order to lower the amount of power received from the Sun and reject the power dissipation, so to remain in the operative temperature range.

Concerning solar panels, with the optical properties of the front side imposed by solar cells and a quite small thermal capacitance per unit area, it will be shown that the critical point is minimum temperature during eclipse, when both the Sun flux and, consequently, the dissipation drop to zero. So, the rear side of the panels shall be characterized by very low emittance: this design driver has been reflected in the assumptions of the thermal model

SOLAR PANEL		ANTENNA	
Parameter	**Assumption**	**Parameter**	**Assumption**
Solar Panels front side Emittance	**0.84** (typical value for solar panels)	**Antenna front side Emittance**	**0.5** (no coating case) or **0.81** (coating case)
Solar Panels front side Absorption	**0.75** (typical values for solar panels)	**Antenna front side Absorption**	**0.5** (no coating case) or **0.2** (coating case)
Solar Panels rear side Emittance	**0.1**	**Antenna rear side Emittance**	**0.81** (First-Flex)
Solar Panels rear side Absorption	**0.5** (First-Flex)	**Antenna rear side Absorption**	**0.1** (First-Flex)
Density **Specific Heat** **Thermal Conductivity of Perovskite**	**Rho=3190 kg/m3** **Cp= about 500 J/(kg*K)** **K= 0.19 (W/(m*K)**	**Density** **Specific Heat** **Thermal Conductivity Antenna of Aluminum (aluminum only for reference)**	**Rho=2700 kg/m3** **Cp= about 870 J/(kg*K)** **K= 237 (W/(m*K)**
Solar Panels Thickness	**1E-3m (1mm)**	**Antenna Thickness**	**1E-2 m (1cm)**

Table 4-10 Assumptions made on thermal model

Concerning the requirements, as said before, in this pre-phase-A of project, constraints and temperature limits can not be defined in a precise and consolidated way. For this reason, the requirements listed in Table 4-11 shall be considered preliminary reference temperature ranges, based on the current maturity of the overall design and related available information and on literature values when solid heritage is missing on the candidate materials/components. They are, however, suitable enough for this first assessment on the mission, in terms of thermal management, and to indicate the critical areas where design/technological efforts shall be done. Of course, the considered temperatures depend strongly on the specific design (of both the solar panels and the antenna) and they could evolve in future.

	MAXIMUM TEMPERATURE	MINIMUM TEMPERATURE
SOLAR PANELS	+150°C	-140°C
ANTENNA	70°C	-50°C

Table 4-11 Reference requirements

4.2.7.3 Thermal Analysis: Solar Panels

In the following section, the front side of solar panels is defined as the one exposed directly to the Sun, while the rear side is the one never exposed. Figure 4-41 and Figure 4-42 show the heat fluxes (solar, IR and albedo) received by the front and rear sides of solar panels.

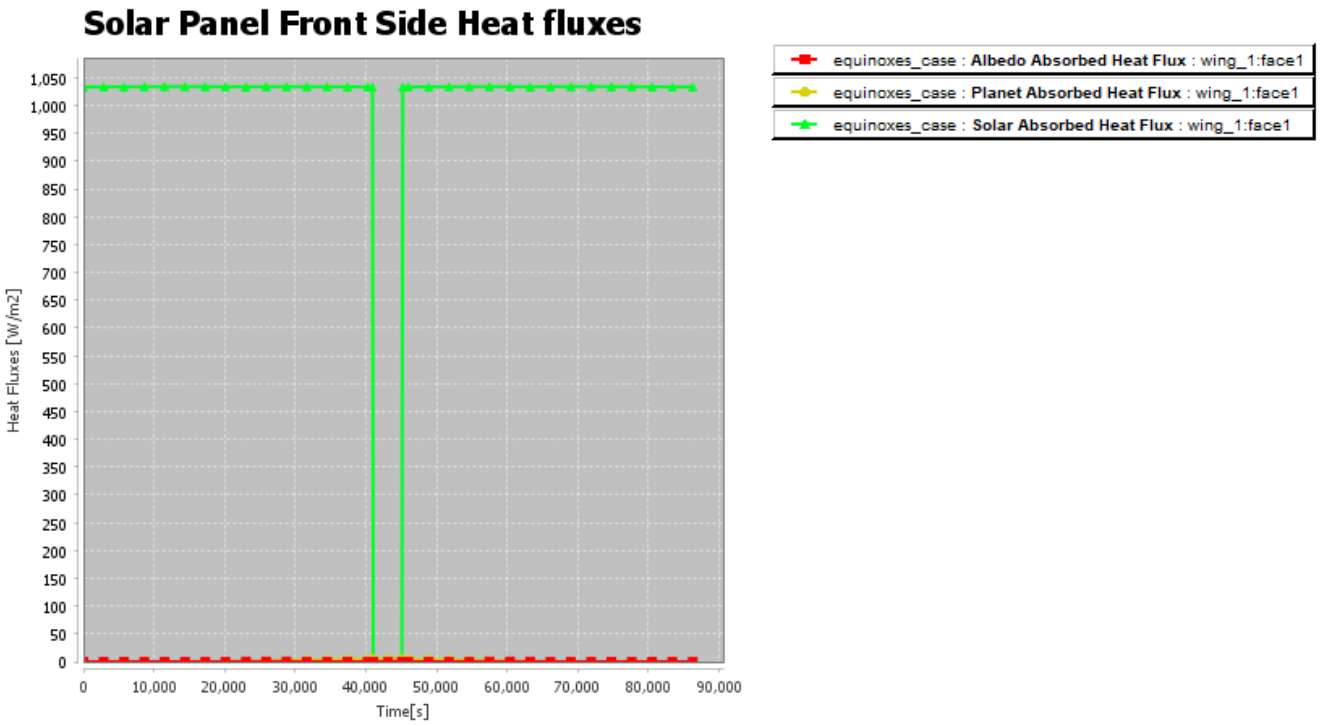

Figure 4-41 Heat Flow received by front side of Solar Panels

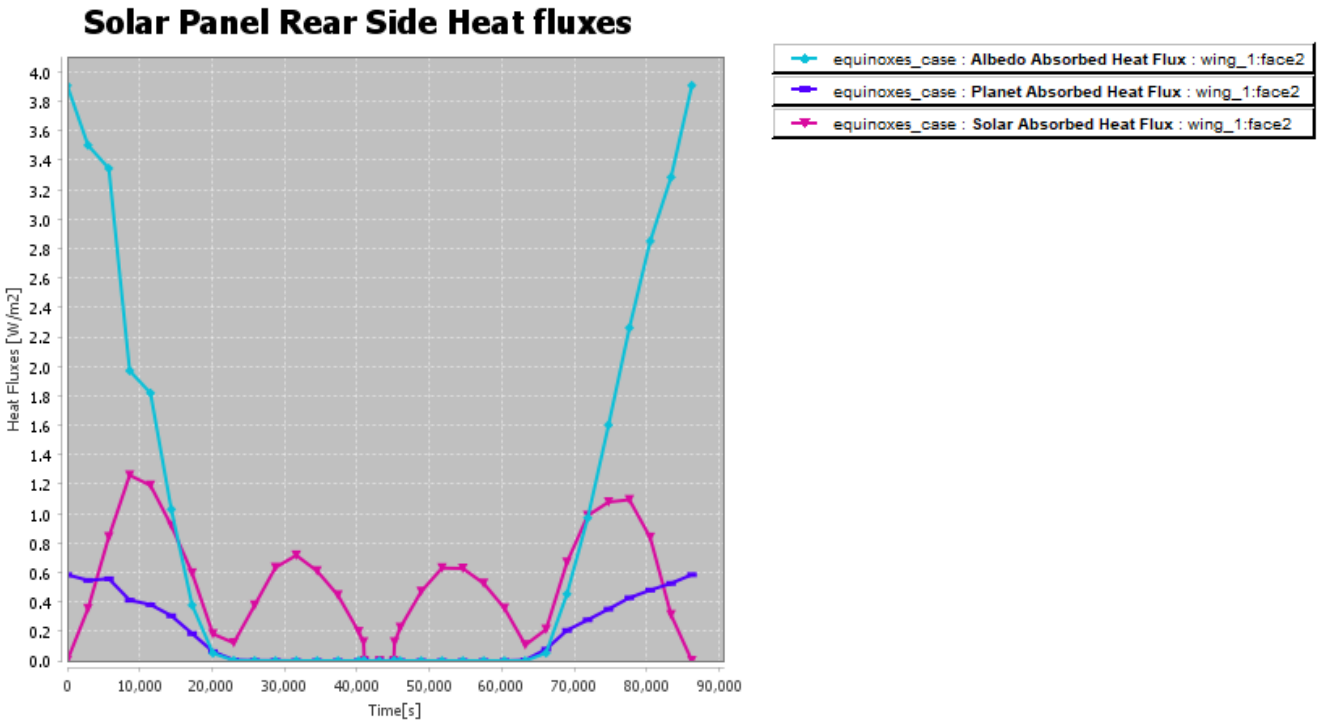

Figure 4-42 Heat Flow received by rear side of Solar Panels

As shown in Figure 4-41, the most relevant contribute to the heat flow received by the solar panels is the solar one (about 1000/1025 W/m2); this value is constant because the solar panels always point the Sun and receive the same amount of power around the whole orbit. The contributions of IR planet radiation and albedo are negligible due to the distance of spacecraft from the Earth in a GEO orbit (about 36000 km).It is possible also to see the eclipse period (between 40000 and 45000 s) where solar flux drops to zero. Figure 4-42 shows the heat flow received by the rear side of solar panels. The main contributors, in this case, are the IR planet radiation and the albedo (as the side does not see directly the Sun); the maximum value occurs when the Sun is " behind" the spacecraft and so the back side of solar panels is directly exposed to the Earth. The heat flow values are, anyway, very low (maximum 4 W/m2) due to the distance from the Earth, and negligible compared to the Sun power received by the front side. In conclusion, the most relevant contributor to the whole solar panels is the solar power received by the front side and it is about constant along the orbit, whereas the back side of the panels can reject the power received about constantly (mostly exposed to deep space). During eclipse, the amount of heat power received is negligible. The result of this heat balance is shown in Figure 4-43, reporting the temperature of solar panels.

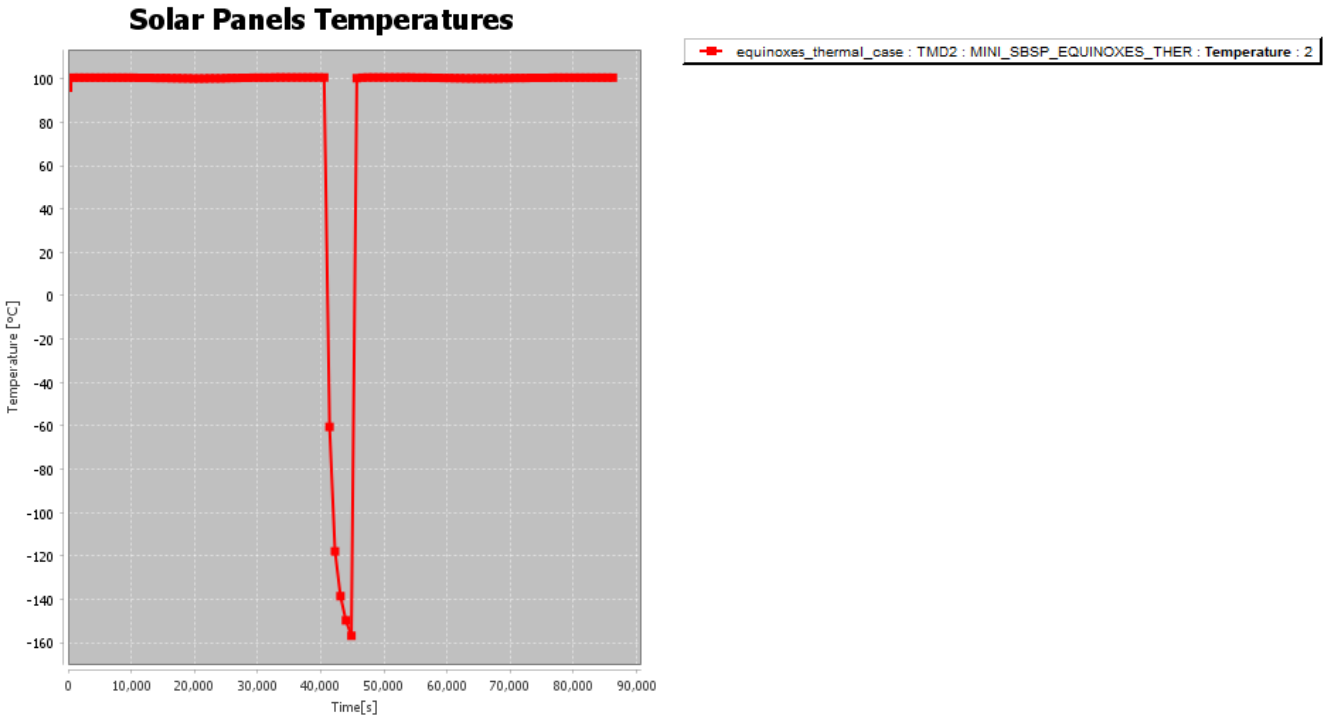

Figure 4-43 Temperatures of Solar Panels

The temperature is constant along the orbit, at about 100 °C, except in the eclipse period where it drops noticeably (down to -156°C, slightly exceeding the reference requirement of Table 4-11). This behavior can be explained by the fact that the solar panels have very small thermal capacity, due to the small mass. Indeed, the information about the minimum temperature requirements of the solar panels materials and components currently available is not consolidated. Either the hardware can accommodate the calculated temperatures or design solutions to increase the thermal capacitance of the deployable substrate shall be put in place, to limit the temperature drop in eclipse.

4.2.7.4 Thermal Analysis: Antenna

The thermal analysis of the antenna involved two cases. The first analysis considers a worst case where coating is not implemented on the front side of the antenna, and so the thermo-optical properties are not optimal (intermediate alpha and epsilon values). The second analysis assumes it is allowed to implement proper surface finish, to get radiator-like properties on the antenna, namely standard white paint.

4.2.7.4.1 Case 1: No coating on Front side of Antenna

In this first analysis we assumed the front side of antenna has no coating, this means that the thermo-optical values used are:

- α=0.5
- ε=0.5

These values are not optimal, but are evaluated to assess the impact of optical properties in

case of future constraints from the supplier of the antenna.

The rear side of the antenna receives only the Sun power radiation, as the front side always point to Earth. As shown in Figure 4-44, the highest value of power received by Sun occurs when the Sun hits perpendicularly the back of the spacecraft (heat power per area is about 135 W/m2).

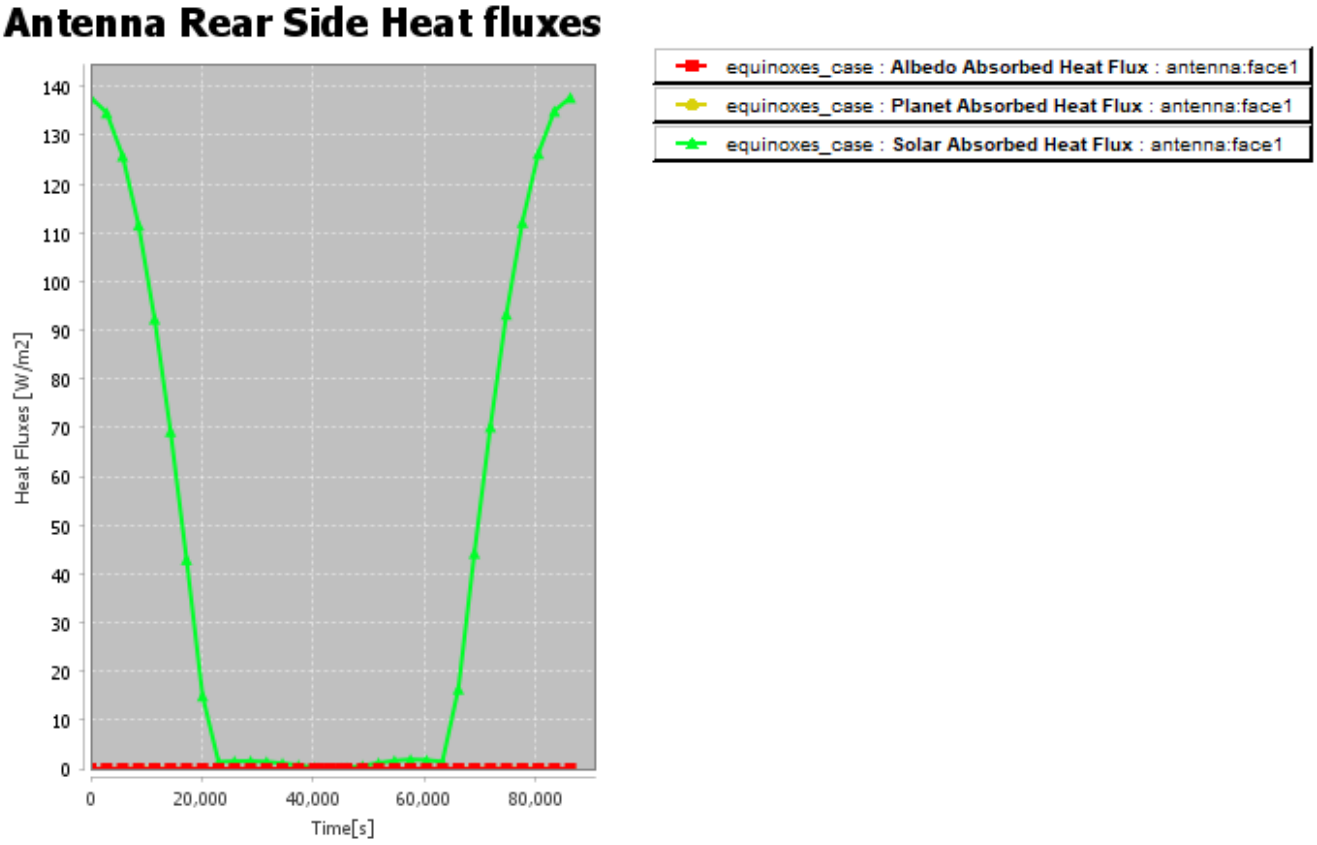

Figure 4-44 Heat power per area surface received by rear side of antenna

The front side of antenna receives always the planet IR and albedo radiation and also the Sun power which represents, also in this case, the most relevant contribute. In particular, the highest values of solar power received occurs when the Sun is “in front” of the antenna (opposite side to the respect of the Earth); also in this case it can be seen the eclipse period during which the solar flux in the front side drops to zero. The lowest value, occurs when the Sun is back to the antenna. Figure 4-45 shows the various contributors to the total flux. It can be seen that the highest flux is about 650/700 W/m2.

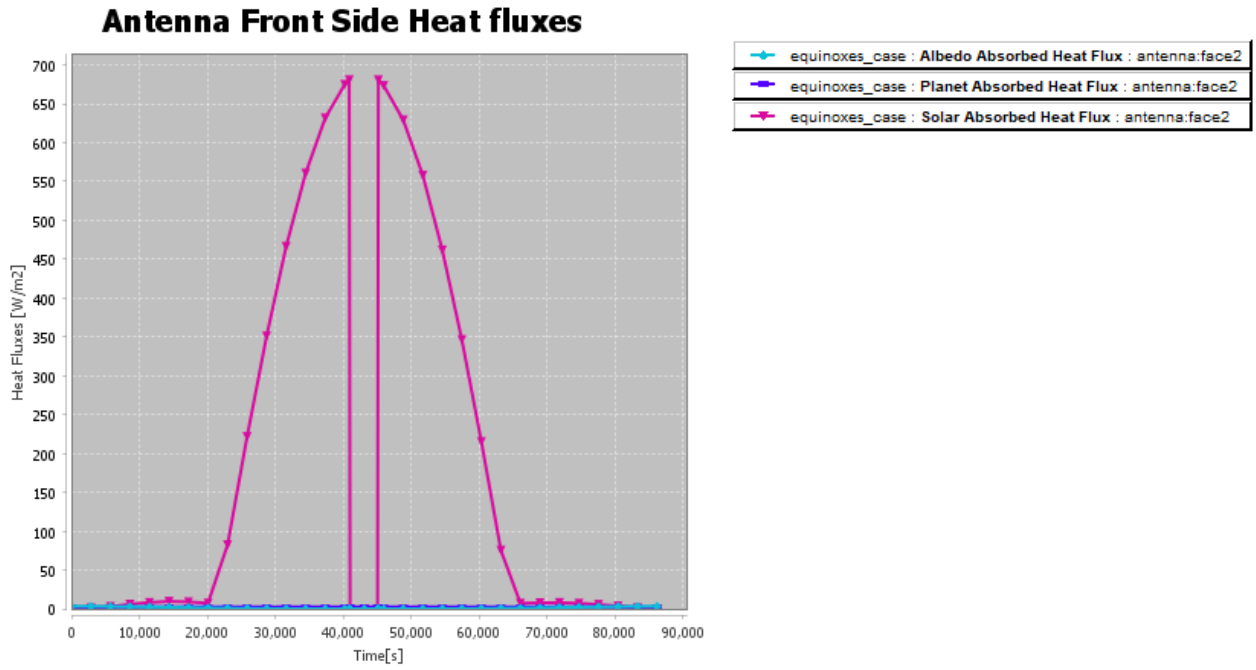

Figure 4-45 Heat fluxes received by antenna front side (no coating)

The temperatures are reported below in Figure 4-46. Temperature has a maximum when the Sun gets in front of the S/C followed by a minimum when the satellites enters into the eclipse. Like the solar panels, the quick drop of temperature can be explained by the low heat capacity of antenna. It must be also remarked that during eclipse antenna does not dissipate heat power (it does not send power to Earth) and so the 430 MW of power is not considered during this period. The highest temperature is about 112°C while the lowest is about -7°C (during eclipse).

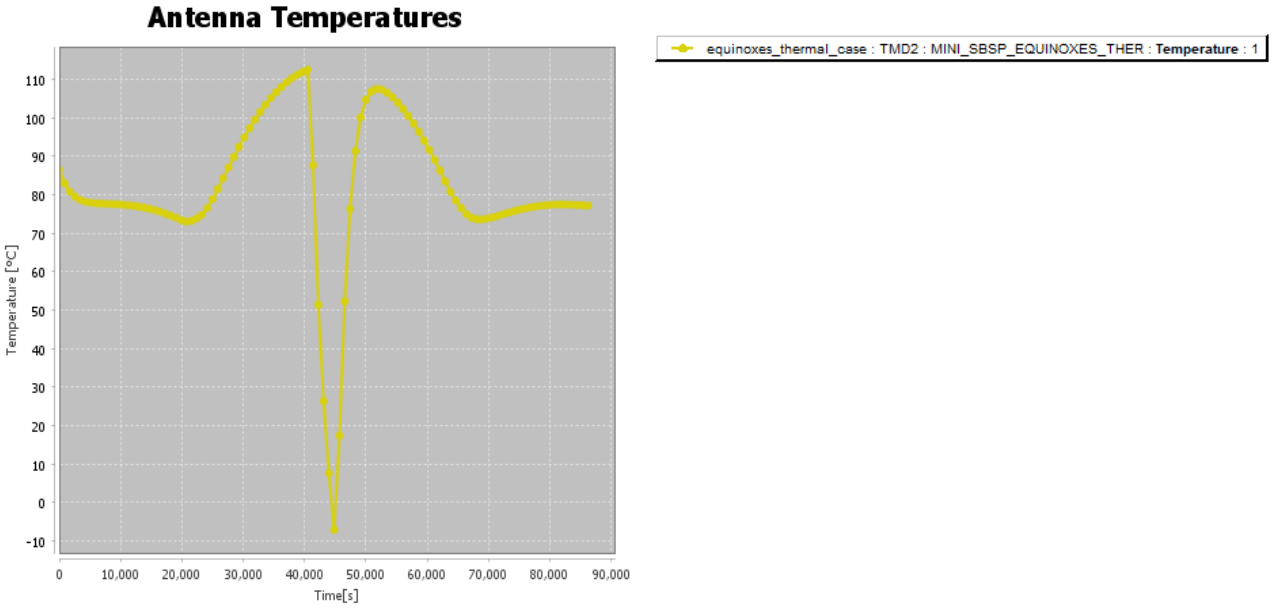

Figure 4-46 Temperatures of Antenna (no coating case)

The temperatures found are likely out of the operational temperature range of antenna, although further assessment shall be performed in future to define more precise requirements. What is more, it is expected in the future new material and technologies will be investigated to withstand these harsh temperatures. To lower the maximum temperature on antenna it is possible to consider coating on the front side of this.

4.2.7.4.2 Case 2: White Paint on Front side of Antenna

The second case assumed to cover the front side of antenna with white paint to lower the power received when the Sun is in front to S/C and increase the power rejected by the surface; the reference values come from TAS-I heritage. Thermo-optical values are:

- α=0.2
- ε=0.81

It is worth to highlight that the heat power received by rear side of antenna is the same received in the previous “no coating” case. Therefore, only the heat fluxes received by the active side of the antenna are reported in the following figure.

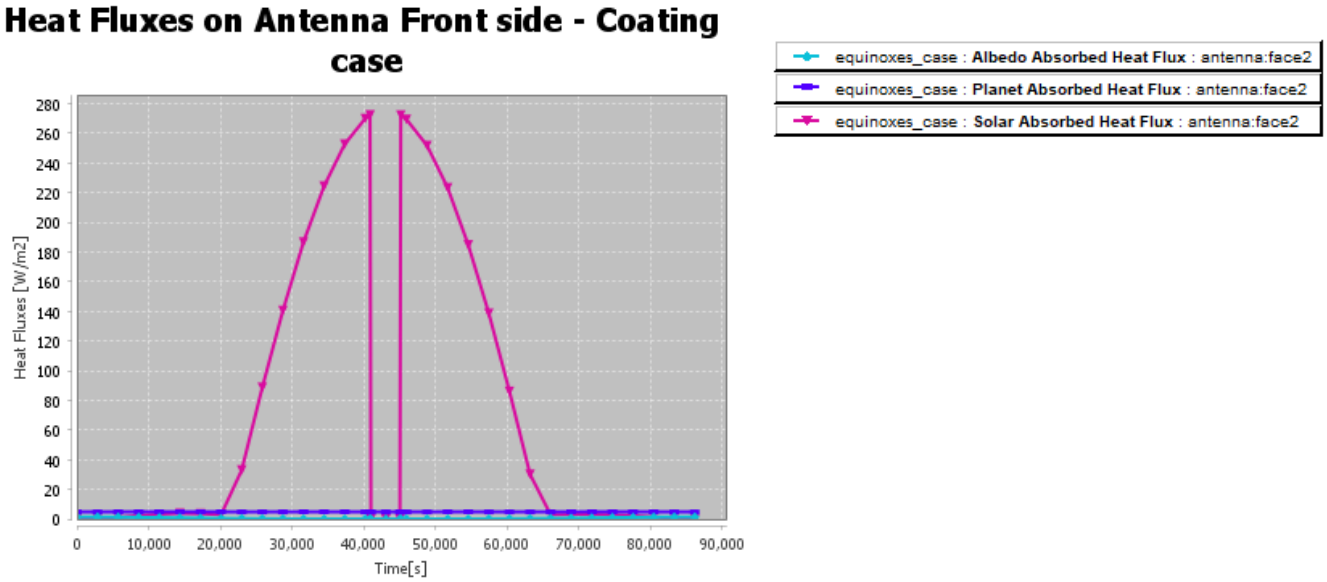

Figure 4-47 Heat fluxes received by antenna front side (coating case)

The effect of applying paint to the active side of the antenna appears to be beneficial, significantly attenuating the peaks of the heat fluxes. The maximum flux achieved in this case is 270 W/m2, against a value that reached 700 W/m2 when no coating was applied.

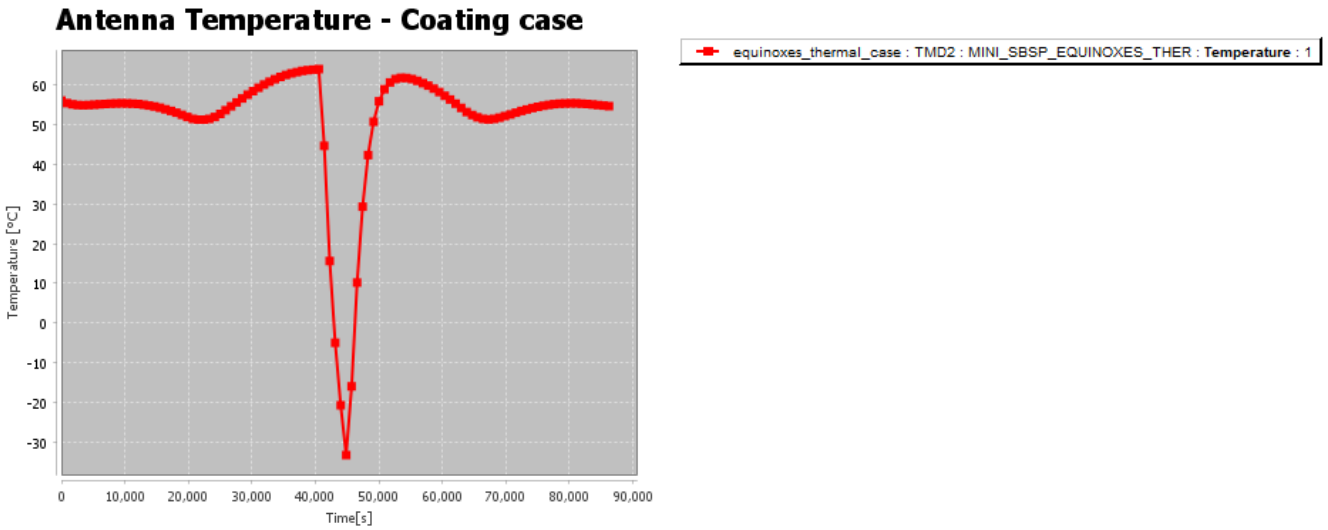

Figure 4-48 Temperatures of Antenna (coating case)

The temperature achieved by the antenna is reported in Figure 4-48. In this second case, as expected, the thermo-optical values modulates the temperature, which is significantly reduced with respect to the previous case. Both the maximum (64°C) and the minimum (-35°C) temperature remains within the reference requirements, with some margin helping to cover the uncertainty embedded in this preliminary model. This confirms the design indication.

4.2.7.5 Conclusions

The selection of the SPS architecture has been driven by the strong constraints of the mass budget and the transmission to Earth function, resulting in a very large and modular concept equipped with huge solar panel fields and flat phased array antenna. The outcomes of the literature review and of our preliminary assessment indicate that the thermal control of this kind of space system shall be achieved with the use of passive solutions, due to the complexity and the enormous mass and reliability penalties that would be associated to the application of an active control (e.g. fluid loops, dedicated radiators) to such a huge and modular system. The thermal analyses therefore assumed a fully passive thermal control, defined by the choice of the modules material, and in particular the thermo-optical characteristics of the solar panel and the phased array antenna.

The thermal analyses of SPS in GEO orbit show, as expected, that the temperatures of the modules are mainly affected by the power dissipation, the solar flux and the thermal capacitance of the system, being the planetary contribution negligible. On both the hot and cold sides, the most critical scenario occurs during the equinoxes when the Sun is perpendicular to the S/C surfaces (and so the heat fluxes are maximum) and the S/C experiences the longest eclipse periods. Due to the low thermal capacitance per unit area of both the antenna and, especially, the solar panels, temperature drops a lot, and quickly, while entering the eclipse periods. This represents a significant challenge for the thermal design.

Overall, the results on solar panels show compliance against the maximum temperature in all mission conditions, but are borderline on the cold side with respect to the typical operating range found in bibliography for this type of arrays. Indeed, various assumptions and conserva-

tivism are embedded in the model about the composition, mass and thermal properties of the cells and the deployable supporting structure, and the temperature requirements need consolidation as well. In conclusion, the outcomes of the analysis suggest that the project is feasible with passive thermal control means but will probably require dedicated technologies (e.g. materials able to withstand extreme temperatures) and/or some design solutions to limit a bit the temperature excursion (for instance increasing the thermal capacitance of the support).

Temperatures on the antenna are compliant to the reference requirements (although marginally, if uncertainty is considered), provided that radiator-like optical properties are assured to radiate the enormous power dissipation. Also concerning the antenna the project is considered feasible, in this case with technologies and design solutions that are already available (namely, use of the First-Flex coating on the rear side and white paint on the front one have been preliminarily assumed in the analysis).

In conclusion, the thermal analyses demonstrated that the proposed SPS concept can function within the expected parameters. No show-stoppers have been identified. Indeed, the analyses confirmed that a passive control solution is feasible and adequate as long as a meticulous selection of materials and coatings is included into the design.

In this sense, it will be necessary to select or develop materials and passive control solution allowing satisfaction of requirements without major impacts on mass and system complexity; in particular fine trimming of thermo-optical properties and increasing of thermal capacitance.

Concerning the path forward, although considerations about the thermal control definition of thrusters, avionics and other service functions of the spacecraft bus are premature at the current stage, this aspect shall obviously be investigated in the future phases of the study.

4.3 Ground Segment

4.3.1 Ground Power Station

The Ground Power Station dimensions depend on:

- Transmission frequency (the higher the frequency the lower will be the GPS area, if the antenna area is fixed)
- GPS latitude (the higher the latitude the longer will be the footprint of the power beam)
- On-board antenna area (the higher the antenna area the lower will be the GPS area, if the frequency is fixed)

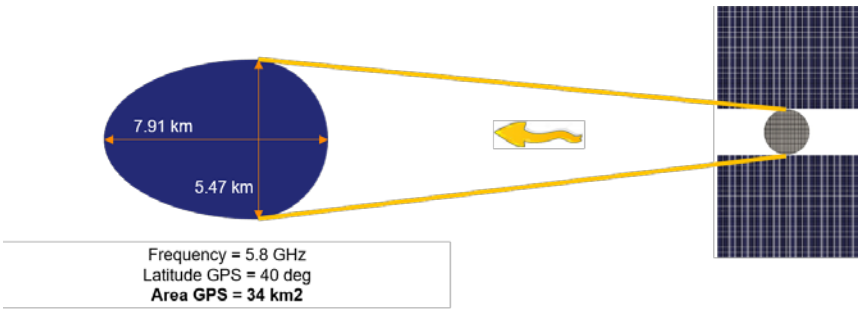

Figure 4-49 GPS footprint

Two options for the rectennas layout in the GPS:

1. Rectennas are laid flat on the ground and cover the entire surface of the elliptical footprint of the beam. More rectennas required (34 km²), simple accommodation (stretched net), no pointing constraint
2. Rectennas are put on inclined mesh panels. To avoid shadowing the panel lines are separated by some distance (1/sin(e)). Less rectennas required (23.8 km²), need panel infrastructure, requires fixed pointing

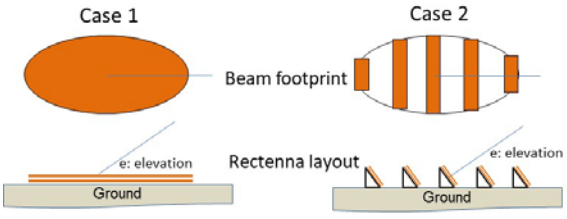

Figure 4-50 Rectennas layout

The selected option, based on inclined mesh panels, and the retrodirective beam pointing concept is shown below.

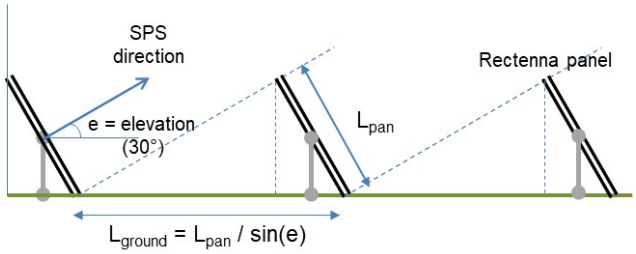

Figure 4-51 Inclined mesh panel

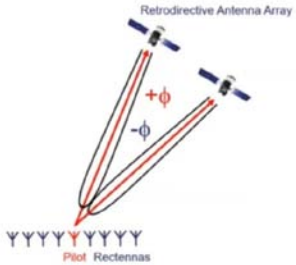

Figure 4-52 Retrodirective beam pointing concept (Credits: CWI)

The free area between the inclined mesh panels could be used for dual purpose, such as crop production.

4.3.2 Ground Stations & Control Centers

Ground stations are terrestrial facilities designed to receive and transmit signals to and from satellites in orbit. They form a crucial link in the communication chain between satellites and operators on the ground. The key aspects of ground stations are:

- Communication: receive downlink signals from SBSP S/C and transmit uplink signals to them;
- Tracking and Data Acquisition: track the position of SBSP S/C and collect data from them
- Control and Monitoring: control the operation (sending commands and software updates) and monitor SBSP S/C health & status;
- Orbit Determination and Navigation: help determine the precise position of SBSP S/C and contribute to navigation systems by providing accurate time signals;
- Data Processing: process the received data and distribute it to relevant Control Centers or user applications. They may also perform initial data analysis and quality checks.

Control Centers serve as central command hubs that manage and oversee the operation of satellites, space missions, or any complex systems. The key aspects of control centers are:

- Satellite Operations: control and operate SBSP S/C in space ensuring that the S/C is functioning as intended, perform necessary maneuvers, and execute mission objectives;
- Command and Control: send command to SBSP S/C for various purposes, such as reconfiguring payload settings or performing maintenance tasks;
- Mission Planning: develop mission plans and schedules that align with SBSP S/C objectives and scientific requirements. They analyze data collected from Ground Stations and collaborate with other teams to optimize mission success;
- Payload Management: in control centers operators manage SBSP S/C payload;
- Anomaly Investigation: control centers are responsible for investigating and troubleshooting any anomalies or unexpected behavior exhibited by SBSP S/C. They analyze telemetry data and work towards resolving issues;

- System Monitoring: monitor health & performance of SBSP S/C ensuring compliance with safety and operational constraints.

In summary Ground Stations provide the necessary infrastructure for SBSP S/C communication, while Control Centers manage and operate the S/C ensuring its smooth functioning and fulfillment of mission objectives.

4.3.3 Electrical Substation

4.3.3.1 Criteria for connection to the transmission grid: minimum design and equipment requirements

The system operator carries out specific studies to determine the access capacity of generation facilities. This assessment will be based on compliance with the technical criteria of safety, regularity, quality of supply and sustainability and efficiency established in the regulations in force.

The network access capacity for generation in a node or zone of the transmission network shall constitute the limit for granting the access permit to generation facilities connected to the transmission network in such node or zone.

The access capacity of a node or zone of the network for a type of generation (MGES or MPE) will be the minimum of the capacities resulting from the short-circuit power criteria (WSCR criteria), static behavior and dynamic behavior applicable to it.

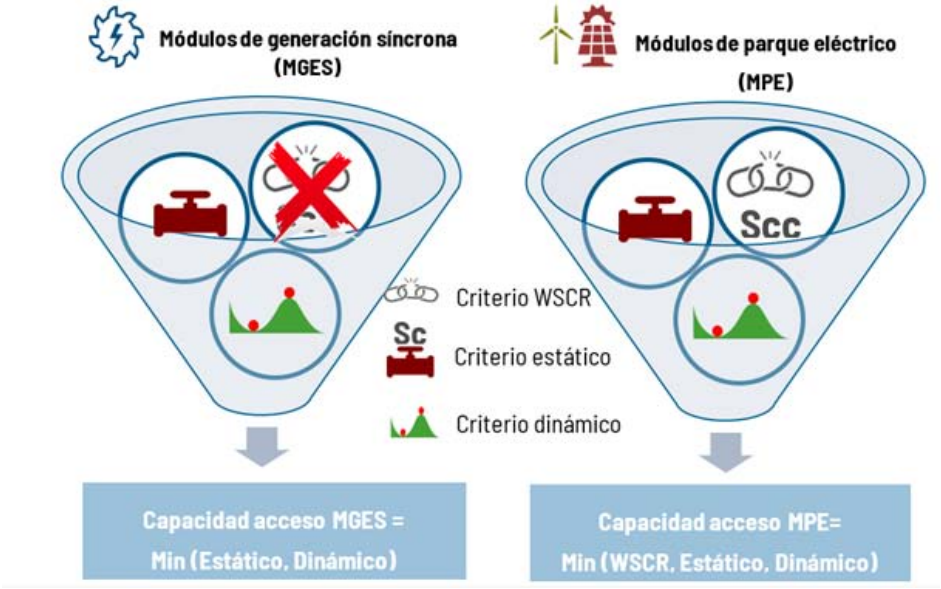

Figure 4-53 MGES/MPE

Any facility requesting connection to the transmission grid must comply with a series of requirements that guarantee that its operation will not interfere with the normal operation of the system and that it will behave as foreseen in both normal and exceptional situations. These requirements are defined in the current mandatory regulations.

Those included in the REE document "Facilities connected to the transmission grid: minimum design and equipment requirements" of June 2022, specify technical issues related to:

- Documentation to be provided in the connection processes: Project, report, budgets, etc.
- Energy exchange conditions: wave quality, perturbations, etc.
- Design and equipment requirements such as:
  - Short circuit power
  - Coordination of insulation and grounding network
  - Power equipment, (lines, transformers...)
  - Definition of boundaries.
  - Degree of criticity
  - Protection systems and comunications.
  - etc.
- Operating Conditions: Maintenance, maneuvers, etc..

The preferred configurations for application to the new ES are as follows:

- 400 kV one and a half breaker, evolutionary ring
- 220 kV breaker and a half, evolutionary ring, double busbar with coupling

The switch and a half will be required whenever 4 Inputs/Outputs at 400 kV or 5 I/O at 220 kV are required.

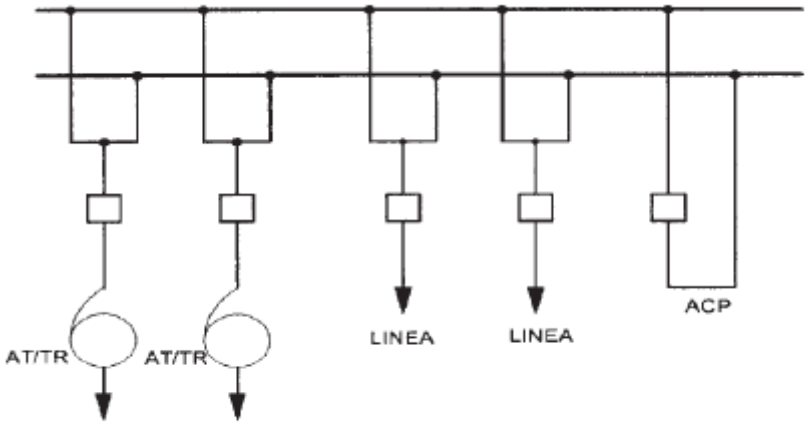

Figure 4-54 Double bar configuration with coupling

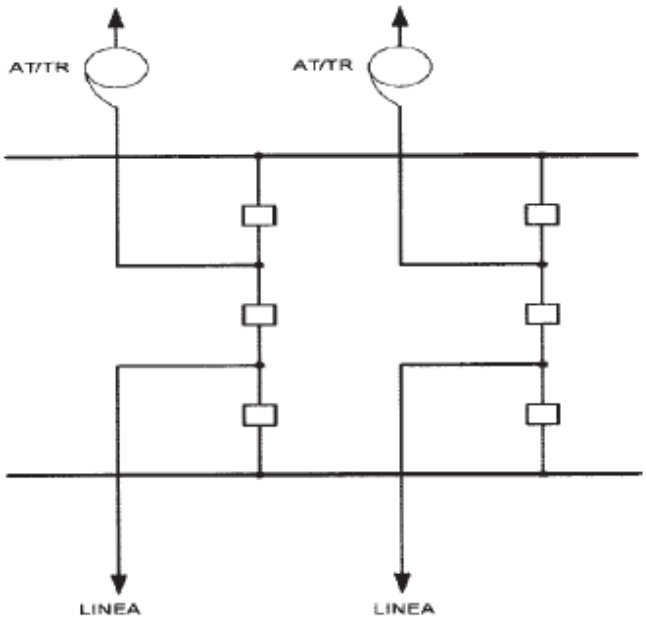

Configuración interruptor y medio

Figure 4-55 Configuration switch and a half

4.3.3.2 Limits of electromagnetic disturbances

The emission limits of the most significant characteristics of the voltage wave at the border points between the transmission grid with voltage levels greater than or equal to 220 kV and the generation or consumption facilities connected to the transmission grid are established:

- **Flicker:** The following flicker emission limits are established at each node of the transmission grid:
  - Perception of flicker short term <10 min (Pst) ≤ 0,8
  - Perception of flicker long term - 2 h (Plt) ≤ 0.6
- **Harmonics:** The following emission limits are established at the harmonic voltages of each node of the transmission system:

Not a multiple of 3		Multiple of 3			
Harmonic Order (n)	**Harmonic Voltage (%)**	**Harmonic Order (n)**	**Harmonic Stress (%)**	**Harmonic Order**	**Harmonic Voltage (%)**
5	1,8	3	1,8	2	1
7	1,8	9	0.9	4	0,7
11	1,3	15	0,3	6	0,3
13	1,3	21	0,2	8	0,3
17≤ n ≤ 49	$1{,}1 \cdot \frac{17}{n}$	21< n ≤ 45	0,2	10 ≤ n ≤ 50	$0{,}17 \cdot \frac{10}{n} + 0{,}14$
TOTAL HARMONIC DISTORTION RATE (THD) 3.00%					

- **Voltage unbalances:** emitters of this type shall not exceed the following limits of total voltage unbalance at each node of the transmission system:
    - short-term limit - μ < 0.7%
    - very short-term limit - μ < 1%

4.3.3.3 Costs and Costruction Timing

The costs and times described below refer only to the main HV substation: if other customers of the secondary distribution (MV or LV) shall be connected to the earth station, the costs and times of other HV/MV substations and further network branches shall be considered.

An indicative cost of the typical Transmission Station is 42 M€ and the total time for the design, development, component supplies and costruction is 36 months minimum.

The area required for the typical Station is approximately 30000 Sqm.

4.3.4 Electrical Storage System

This section defines the characteristics of the Electrical Energy Storage System (according to IEC 62933 series) based on energy intensive supercapacitors to be installed in a.c. systems with a declared fundamental frequency of 50 Hz.

4.3.4.1 EESS architecture

By according to IEC 62933 series, EESS must be designed in several subsystems with the following hierarchy:

a. primary subsystem;
    a. accumulation subsystem;

b. power conversion subsystem;

b. auxiliary subsystem;

c. control subsystem;

a. communication subsystem;

b. management subsystem;

c. protection subsystem.

By according to IEC 62933 series two different architectures may be required:

d. EES system architecture with one POC type (**Figure 4-56** EES system architecture with one POC type

e.);

f. EES system architecture with two POC types (**Figure 4-57** EES system architecture with two POC types).

EESS architecture with two POC types includes also the second one, that means that auxiliary subsystem can be configured to take the energy from the primary subsystem. This transition must be possible also during any EESS operating mode, without any impact to that operating mode. EES system architecture with two POC type is selected in this specification; in order to have the maximum level of reliability.

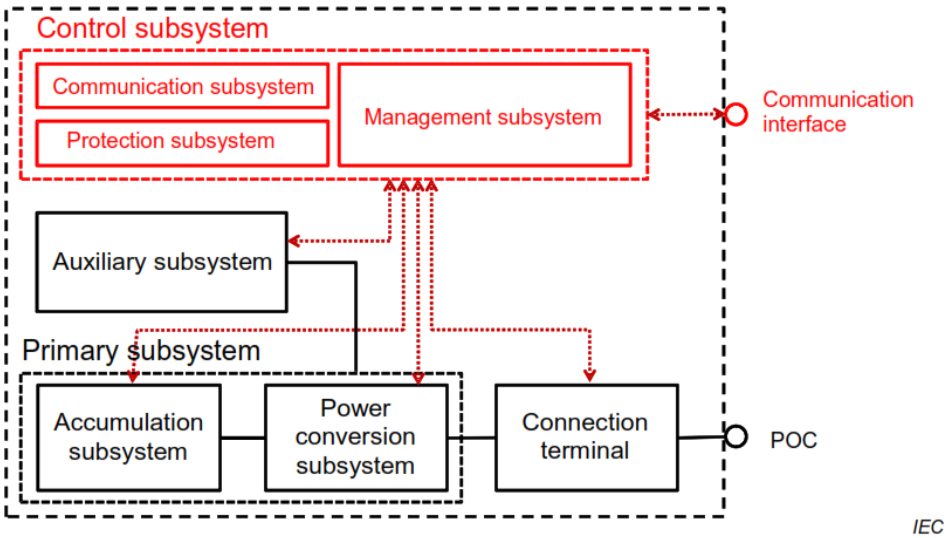

Figure 4-56 EES system architecture with one POC type

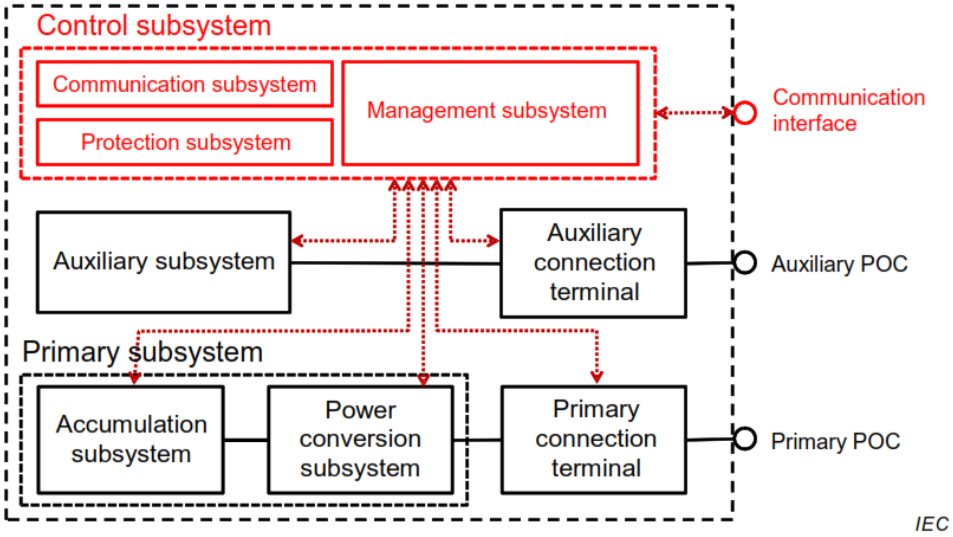

Figure 4-57 EES system architecture with two POC types

4.3.4.2 EESS modularity and reliability

By according to IEC 62933-1 an EESS module (or EESS unit) is a part of an EESS, which is itself, an EESS, so in according to the possible architectures; nevertheless the terminals, the auxiliary and the control subsystems may be absent in an EESS module, because they may be centralized at EESS level.

The EESS module is a specific EESS subsystem, in fact the EESS subsystem is a part of an EES system, which is itself, a system; a subsystem is normally at a lower indenture level than the system of which it is a part.

The EESS must be modular, following two possible modular approach:

a. full modular;

b. modularity for redundancy.

Any failure or lack of operation inside an EESS module must not impact the other modules.

In the full modular approach, all the EESS module must be an EESS able to work autonomously if needed. The EESS module must respect the architecture of the EESS; so they will share only the POCs.

In the modularity for redundancy, all the EESS module must share terminals, the auxiliary and the control subsystem; that are centralized at EESS level. Where present as a final stage of power conversion subsystem (immediately before the connection terminal) also transformers may be centralized.

Again, in order to stress the reliability the full modular approach is selected.

4.3.4.3 EESS on field

With the mentioned assumption, the EESS module may be included inside a 40ft standard container, by obtaining an on field installation based on:

- 1 single delivery substation (40ft container).
- Several 3 MVA / 3 MWh EESS modules (40ft containers).

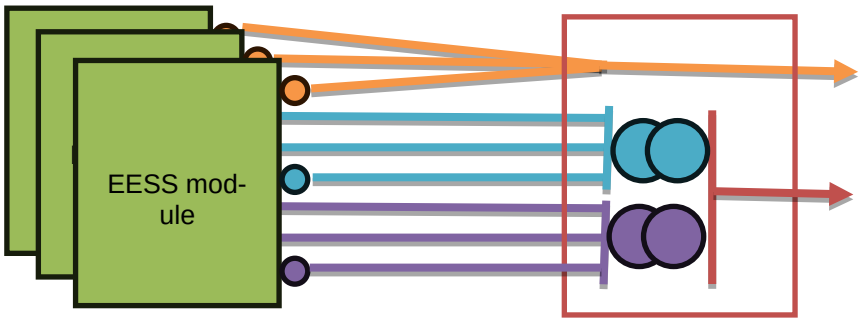

Figure 4-58 EES system installation

The delivery substation may be incorporated inside the electrical substation (refer to section 4.3.3). The delivery substation:

- Will receive cables from the primary connection terminals (400 V threephase in EU), for each of them will offer protection and switching arriving to a bus bar where a MV/LV transformer will adapt the voltage to the electrical substation requirements, then from the MV busbar a protected cable will be extended to the electrical substation.
- Will receive cables from the auxiliary connection terminals (400 V threephase in EU), for each of them will offer protection and switching arriving to a bus bar where a MV/LV transformer will adapt the voltage to the electrical substation requirements, then from the MV busbar aprotected cable will be extended to the electrical substation. The need to have a separated transformer is to improve reliability and to avoid to maintain the bigger transformer energized only to fed the auxiliary subsystems.
- Will receive cables from the communication interfaces connecting them to the external control link.

The final on site installation will be very similar to the traditional BESS installation with the exeption that the HVAC system are not required.

4.3.4.4 EESS module general requirements

Table 4-12 presents the EESS general requirements needed for the system identification; IEC 62933 series and the additional clarifications in this document are fundamental for its correct understanding.

Parameter	Requested values
Nominal frequency (f_N)	f_N = 50 Hz
Nominal voltage (V_N)	V_N = 400 V
Rated frequency and continuous operating frequency range (f_R)	f_R = 50 Hz ± 5 Hz
Rated voltage and continuous operating voltage range (V_R)	V_R = 400 V ± 60 V
Nominal energy capacity (E_{NC})	E_{NC} ≥ 3 MWh
Nominal powers (S_N, P_N, Q_N)	S_N ≥ 3 MVA circular power capability chart
Rated voltage of the auxiliary subsystem (V_{AN})	V_{AN} = 400 V ± 60 V
Rated apparent power of the auxiliary subsystem (S_{AN})	S_{AN} ≤ 20 kVA
Expected service life expressed in C_{pcd1} (T_{SLC})	T_{SLC} ≥ 100000
Expected service life expressed in years (T_{SLY})	T_{SLY} ≥ 10 years
Nominal charging time ($T_{NC} = E_{NC}/P_{CN}$)	$T_{NC} = E_{NC}/P_{CN}$ = 1 h
Nominal discharging time ($T_{ND} = E_{NC}/P_{DN}$)	$T_{ND} = E_{NC}/P_{DN}$ = 1 h
Primary subsystem roundtrip efficiency (η_{PT})	η_{PT} ≥ 0.85
Settling time (T_S)	T_S ≤ 300 ms T_S ≤ 3 s Depending to the operating mode
Specified tolerance limit ($\varepsilon=2\Delta y_S$)	ε ≤ 1% of Y_∞ ε ≤ 0.1% of f_∞ Depending to the operating mode
Self-discharge (E_{SD})	E_{SD} ≤ 15 kWh per day per MWh of E_{NC}
Energy consumption of the auxiliary subsystems (E_X)	E_X ≤ 50 kWh per day per MWh of E_{NC}
Energy stand-by consumption of the auxiliary subsystems (E_{XS})	E_{XS} ≤ 20 kWh per day per MWh of E_{NC}
Reliability	MTTF ≥ 1350h MTTR ≤ 150h
Ordinary maintenance per year (M_O)	M_O ≤ 0.01 FTE in one single intervention
Noise emission (DB_E)	DB_E ≤ 35 dBA

Table 4-12 EESS general requirements

4.3.4.5 EESS reference environmental conditions

The IEC 62933-2 series, provides applicable EESS operating conditions, moreover additional requirements are provided in this section.

Some EESS components have specific requirements that must be also respected.

Table 4-13 – EESS reference environmental conditions			
	Operating range	**On storage and transport range**	**Reference**
Temperature	-20 °C ÷ 50 °C	-40 °C ÷ 80 °C	
Humidity	0 % ÷ 95% RH, non condens-ing		
Atmospheric pressure	500 hPa ÷ 1100 hPa		
Altitude above sea level	0 m ÷ 2000 m		
Pollution degree	3		IEC 60664 series
Protection against dust, water and foreign bodies	IP65	IP20	IEC 60529
Shipping vibration		10 Hz to 11,8 Hz 11,9 Hz to 150 Hz Amplitude: 3,5 mm Acceleration: 2 g, 1 oc-tave/min Duration on each axis: 2 h Overall: 6 h	

Table 4-14 EESS reference environmental conditions

The operating ranges are applicable at the EESS perimeter, EESS subsystems and components are normally included in enclosures (e.g. containers, civil structures), so that ranges must be verified at the perimeters of such enclosures.

The on storage and transport ranges must be applied at each EESS component.

4.3.4.6 EESS module accumulation subsystem

The accumulation subsystem must be based on the energy intensive supercapacitor technologies; IEC 62391 series provides generic specifications, because of the earlier stage of energy intensive supercapacitor technologies, the adoption of LiIon based standards is possible to complement the overmentioned IEC 62391 series, in particular for planning, installation, operation and safety.

Components of the accumulation subsystem do not require heating or air conditioning to operate in the EESS reference environmental conditions (par. 0). Ventilation may be accepted.

Encapsulated Hybrid Graphene Solid State and Tantalum Capacitor are used in this design.

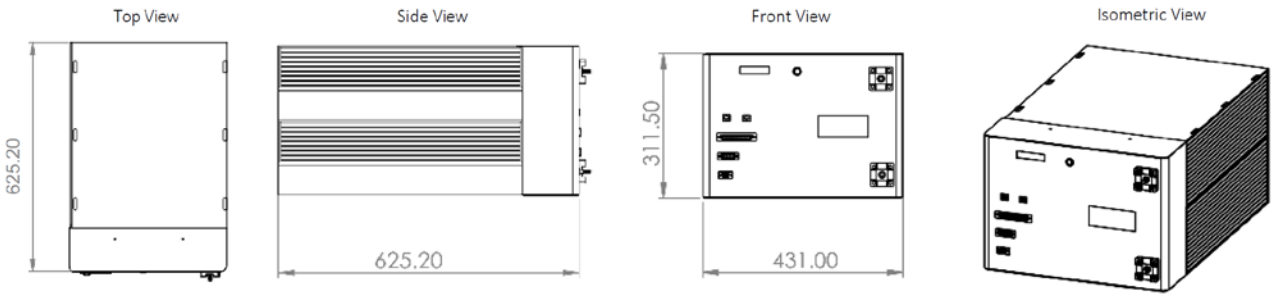

Figure 4-59 Encapsulated Hybrid Graphene Solid State and Tantalum Capacitor

- Cell Energy Density: 250Wh/kg
- Module Energy Density: 110Wh/kg
- Volumetric Density: 120Wh/Liter
- Weight: 90kg
- Upto 4MWh in a 40ft container
- Nominal voltage: 48VDC
- Voltage range: 43.2 V to 60.8V
- Capacity: 10kWh
- Compatible with all inverters
- Unlimited parallel connection
- Up to 1000VDC series connection
- Galvanic Isolation: 5000V
- Embedded Module Combiner

4.3.4.7 EESS module power conversion subsystem

The power converter subsystem must be made by bi-directional grid-connected power converters (GCPC) by according to IEC 62909 series.

IEC 62909-1 specifies general aspects of bi-directional grid-connected power converters, consisting of a grid-side inverter with two or more types of DC-port interfaces on the application side with system voltages not exceeding 1000 V a.c. or 1500 V d.c.

In this EESS case, GCPC must provide only one DC-port interface and the connected resource must be the accumulation subsystem. In case of multi storage technologies, the accumulation subsystem may be splitted in several subsystems and it is allowed to have one port for each storage technology.

So, the EESS GCPC consists of the following components:

a. a bidirectional DC/DC power converter connected to the accumulation subsystem;
b. a DC-connection interface which connects the DC/DC converter with the bi-directional inverter;
c. one bi-directional inverter connected to the primary POC;
d. Low level control to realize interaction or cooperation among bidirectional inverter, DC/DC converters and control subsystem;

Accumulation subsystem cannot be connected to DC-connection interface directly.

IEC 62909-2 introduces additional requirements for the GCPC in the EESS that must be respected as well by taking into accounts that in the IEC 62909-2 the GCPC in connected to a battery system that include a DC/DC converter, in this standard the GCPC include all the converters and it is connected to the accumulation subsystem, so all the requirements of the IEC 62909-2 must be applied also to the DC/DC converter.

The DC/AC converter must support both current source inverter (CSI) mode and voltage source inverter (VSI) mode.

4.3.4.8 EESS communication subsystem

The communication subsystem must contain an arrangement of hardware, software, and propagation media to allow the transfer of messages from one EESS component/subsystem to another one, including the data interface with external links.

The supplier must provide a control design that include control architecture, conceptual view and state machine of the EESS, based state machine for DER (IEC 61850 series), that approach both communication and management subsystems.

For the communication point of view, the control design must be approached like an industrial-process measurement, control and automation, in particular

a. Both IEC 61850 series and Modbus TCP (IEC 61158 series) must be adopted for the interoperability with external links (e. g. SCADA);
b. IEC 61918 specifies basic requirements for the installation of media for communication networks in EESS premises.

4.3.4.9 EESS management subsystem

The management subsystem of the EESS must provide the functionality needed for the safe, effective and efficient EES system operation, therefore it determines EESS functionalities.

The management subsystem must be multi stage starting from a EESS main controller (MC) that is the top level, the accumulation subsystem must have is own management system as a first level management (below the MC), the power conversion subsystem must have is own management system as a first level management (below the MC), the auxiliary subsystem must have is own management system as a first level management (below the MC), the primary connection terminal must have is own management system as a first level management (below the MC).

For the communication point of view, the control design must be approached like an industrial-process measurement, control and automation, in particular

a. IEC 61850-3 defines the general requirements, mainly regarding construction, design and environmental conditions for the controllers and IED inside the management sub-system;
b. the management subsystem must support all the commands, operating states, operating modes, operating procedures, warnings, alarms and any other event recalled in this standard, in the IEC 62933 series and in any other standard recalled in this standard;
c. IEC 62419 must be used for designation of different types of measuring instruments and of measuring instrument features;
d. the EMC requirements for measurement and control equipment must be approached trough IEC 61326 series in compliance with the EESS requirements;
e. IEC 61508 series specifies electrical/electronic/programmable electronic (E/E/PE) systems used to carry out safety functions;
f. IEC 62682 specify general principles and processes for the lifecycle management of alarm systems based on programmable electronic controller and computer-based human-machine interface (HMI) technology;
g. IEC 60546 series specifies controllers with analogue signals;
h. IEC 60770 series specifies transmitters with pneumatic or electric output signals;
i. IEC 61003 series specifies pneumatic and electric industrial-process instruments or control device using measured values that are continuous signals either a mechanical (position, force, etc.) or a standard electric signal;
j. IEC 61131 series specifies the programmable controllers;
k. IEC 61298 series specifies functional and performance characteristics of process measurement and control devices;
l. IEC TS 62098 provides background information for developing evaluation methods for microprocessor-based instruments;
m. IEC 61506 defines the requirements for the documentation of software in industrial process measurement and control systems.

The management subsystem devices must be based on solid state solutions (for example rotating hard disks are not admitted).

4.3.4.10 EESS remote Interface

The EESS must be able to respond to commands and exchange signals (warnings, measures, alarms etc.) with an external supervisory controller using a secure internet-based protocol (par. 4.3.4.8).

The EESS must remain functional in the absence or loss of communication from the remote controller, It must continue its current mode of operation for a set time period (variable setting, 15 minute default); on expiration of the time, the EESS will turn to stand-by mode.

During an interruption to communications, the EESS and remote controller will make repeated attempts to re-establish communications at a set time interval (variable setting, default of 5 minutes). When communications have been re-established, the EESS and remote controller must make any necessary updates to resume performance.

4.3.4.11 EESS local Human Machine Interface

A local Human Machine Interface (HMI) must be provided to permit local monitoring and control.

All settings must be viewable and settable, statuses viewable, operating parameters viewable, and logs configurable and viewable. Local password protection is required; different login accounts must be set up to allow for different types of operators (i.e. observer: read, operator: read/write).

Meaningful control buttons and indicating lights must be provided for monitor and control status and operations.

All control and alarm functions available remotely must also be available locally.

4.3.4.12 Protection subsystem

By according to IEC 62933-1, the protection subsystem is the EESS subsystem containing an arrangement of one or more protection equipment, and other devices intended to perform one or more specified protection functions. The protection subsystem includes one or more protection equipment, instrument transformer(s), transducers, wiring, tripping circuit(s), auxiliary supply(ies). Depending upon the principle(s) of the protection subsystem, it may include one end or all ends of the protected section and, possibly, automatic reclosing equipment.

Breakers must be used as actuators.

The supplier must design and develop a protection subsystem, with a protection scheme able to assure in a coordinated way the following attribute:

a. selectivity (whether to trip or not);
b. sensitivity (whether a fault can be detected);
c. speed (the trip time).

The protection subsystem is made by protection devices, a protection device may include one or more protection functions.

A protection scheme document must be provided by the supplier where all the devices, functions, settings and coordination plan are included; this document must be elaborated by using power system simulation.

With reference to the protection scheme, two setting scheme has to be developed, one for the operation in parallel with the grid and the other to be used with the EESS in islanding operation. In the elaboration of the protection scheme document the supplier must take into account all the possible internal and external fault or dangerous events; the protection subsystem must be designed and developed by according to this document.

With reference to protection subsystem selectivity, any protection devices must have is own protected section, two or more protection device cannot share some part of the same section for the same protection function (only backup are admitted), exceptions are possible if adequately motivated in the coordination plan.

With reference to protection subsystem sensitivity and speed, any protection devices must have is own setting plan, for any protection function, a coordination plan must be present.

Protection devices must by according to IEC 60255 series and IEC 60947 series (only for LV).

The transformer protection require at least the following IEEE C37.2 devices:

a. 23 Temperature Control Device;
b. 50 Instantaneous Overcurrent Relay;
c. 51 Ac Time Overcurrent Relay;
d. 59 Overvoltage Relay;
e. 64 Ground Protective Relay.

The GCPC protection require at least the following IEEE C37.2 devices:

f. 50 Instantaneous Overcurrent Relay;
g. 51 Ac Time Overcurrent Relay;
h. 59 Overvoltage Relay;
i. 64 Ground Protective Relay.

These are minimum requirements, the supplier must add any additional protection function or devices needed to reach the goal of the protection scheme document.

The auxiliary subsystem and control subsystem protection require at least the following IEEE C37.2 devices:

a. 27 Undervoltage Relay;
b. 50 Instantaneous Overcurrent Relay;
c. 51 Ac Time Overcurrent Relay;
d. 59 Overvoltage Relay;
e. 64 Ground Protective Relay;
f. 87 Differential Protective Relay.

The component fed in DC require also:

g. 72 DC Circuit Breaker;
h. 76 DC Overcurrent Relay;
i. 82 DC Reclosing Relay.

These are minimum requirements, the supplier must add any additional protection function or devices needed to reach the goal of the protection scheme document.

Because of the earlier stage of energy intensive supercapacitor technologies, the adoption of LiIon based standards is possible.

Grid interface protection must have at least a backup in case of failure.

The grid interface protection require at least the following IEEE C37.2 devices:

a. 27 Undervoltage Relay;
b. 50 Instantaneous Overcurrent Relay;

c. 51 Ac Time Overcurrent Relay;
d. 59 Overvoltage Relay;
e. 64 Ground Protective Relay;
f. 67 Ac Directional Overcurrent Relay;
g. 81 Frequency Relay;
h. 87 Differential Protective Relay.

4.3.4.13 Final consideration about dimensions and cost

For >10 MVA / 10 MWh installations the following parameters are valid:

- 700 k€/MWh full cost EESS;
- 60 m^2/MWh land consumption.

4.4 Launch segment

With the operational orbit selected, the amount of launches required to bring the SPS in orbit can be further analysed. First, an estimation of the amount of Orbital Tugs required to bring the SPS in orbit is presented. Secondly, an evaluation based on the amount of transportable mass due to volume constraints is performed. Then, analysis based on the available launchers of ArianeGroup and RFA are developed.

4.4.1 Required Tugs based on time constraints

Considering an SPS mass of 6600 [tons] and assuming a Tug mass of 60 [tons] and a transportable payload of 100 [tons] both by the launcher and the Tug, it is possible to evaluate the time required for the Tug LEO-GEO roundtrip and the amount of Tugs required to bring all the SPS modules in GEO in 2 years.

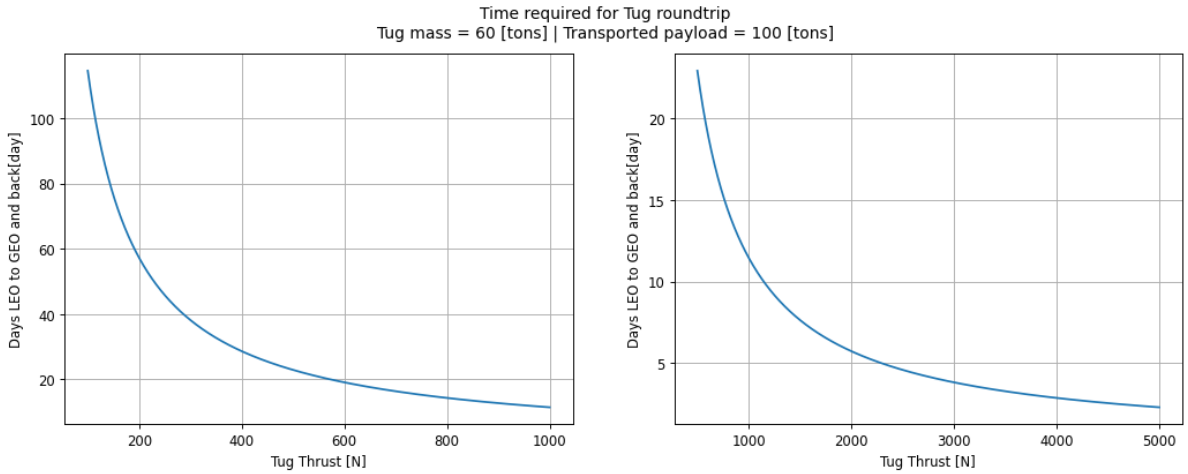

Figure 4-60 Time required for Tug roundtrip based on Tug thrust

Assuming a Tug thrust of 200 N, 60 days are required per roundtrip. This means that 6 Tugs need to work continuously to bring all the modules in GEO in 2 years.

4.4.2 Volume Constraints Analysis

Due to the limiting capacity of launchers' fairings in terms of volume, it is mandatory to assess the potential increment in term of launches due to this factor. For this evaluation, the Orbital Tug have a crucial role in determining the system's overall performances. All evaluation are done considering a 0 deg inclination, 500 km altitude parking LEO orbit and a 0 deg inclination operational GEO orbit, using finite burns with a Isp of 1000 s.

If no strategy is taken, considering an Orbital Tug with a mass of 60 tons that bring the amount of modules launched in a single launch in the operational orbit gives the following output:

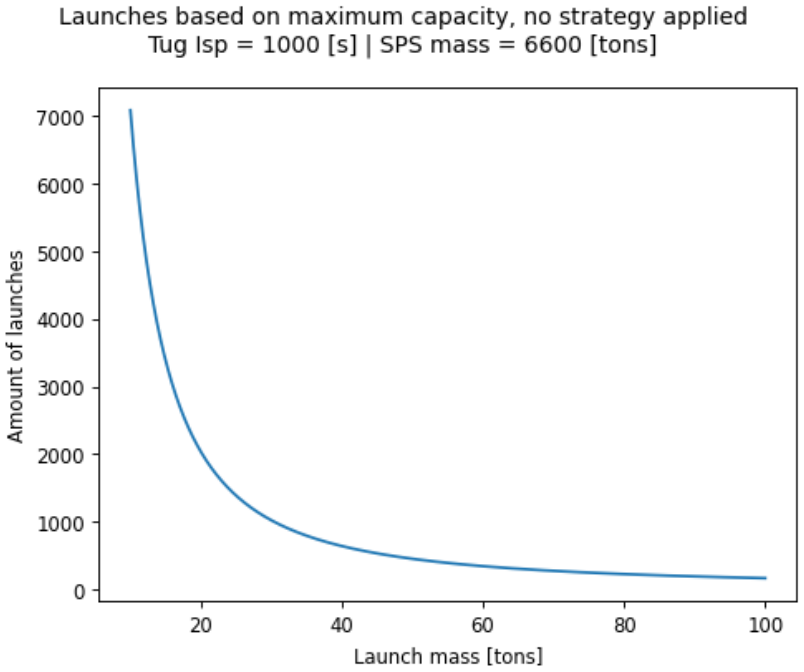

Figure 4-61 Launches based on maximum capacity without implementing strategies

The Figure 4-62 considers also the propellant launches with the volume constraints. A clearer plot can be done considering a full fairing when evaluating the propellant launches required:

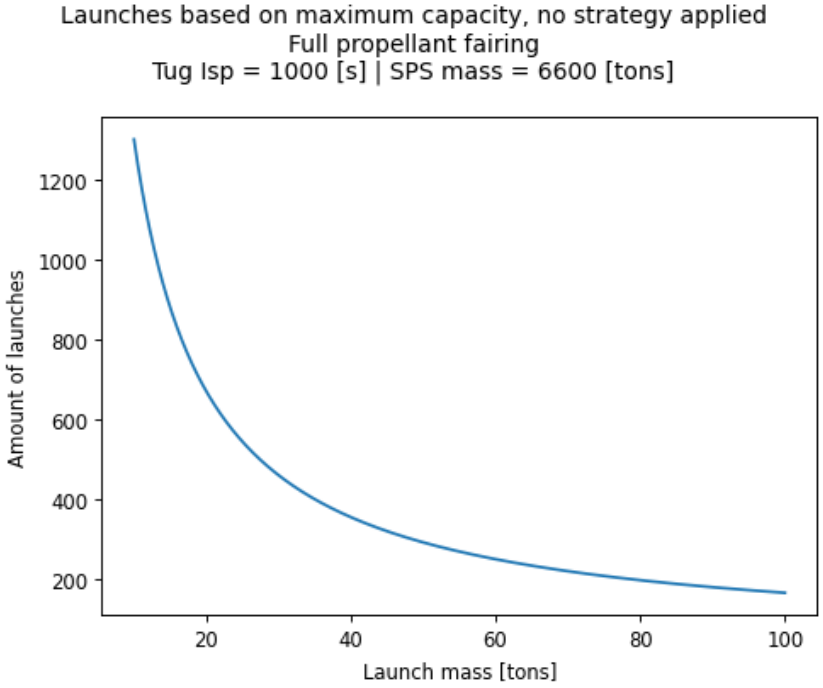

Figure 4-62 Launches based on maximum capacity with full propellant fairing

In order to prevent this escalation in terms of launches two possible strategies can be followed:

1. The Orbital Tug will have a mass of 60 tons and will carry for every trip 100 tons of structure. This means that the amount of modules launches will not coincide with the amount of Tug trips to GEO and back.
2. The Orbital Tug will have a mass equal to 60% of the launcher transportable mass. This means that the Tug is considered of proportional dimensions w.r.t. the fairing capacity.

The amount of launches required to bring the modules in orbit will change, while the amount required for the propellant will remain constant. The resultant amount of launches is shown in the Figure 4-63:

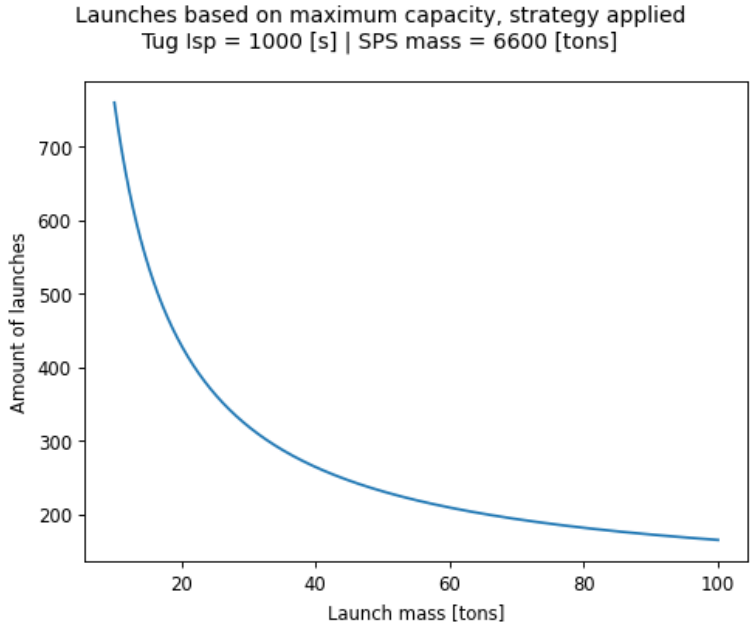

Figure 4-63 Launches based on maximum capacity with strategies implemented

Both strategies are feasible and will depend on the development of the Orbital Tug.

4.4.3 In-Orbit Assembly Highlights

The in-orbit manufacturing is a crucial technology allowing to fully exploit the launcher's fairing. With robotic systems capable of join components in the operational orbit it would be possible to maximize the amount of transported mass without modifying the modules design. By stacking the module's components in a tight configuration, the fairing can be fully exploited.

It would be possible to link each modules with no need of docking mechanisms. This means a a substantial decrease in LCOE. In fact, a single docking unit has been considered to cost around 3 M€. Considering the learning curve it adds up to more than 3 B€ which is the majority of the structure's cost.

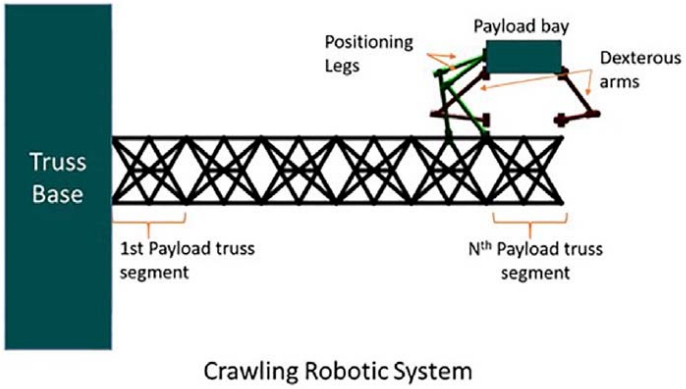

Figure 4-64 Robotic system example (Credits: U.S. Naval Research Laboratory)

In order to evaluate the amount of robotic systems required to perform the in-orbit assembly the following assumptions are taken:

- 4 robots to assembly 1 module in 4 hours
- 8 hours/day for robotic operations
- 100 modules arrive at the same time with the orbital tug and have to assembled in 11 days (before the next tug with other modules arrives)

With these assumptions, the required amount of robotic systems to build the SPS in 2 years is 24.

Space pallet meant to host assembly parts in space logistics, robotically actuated package fillers and fasteners and interfaces compatible with robots need to be studied.

4.4.4 Decommissioning launches evaluation

Based on the decommissioning strategy proposed in Section 2.4, it is possible to evaluate the required amount of launches of propellant required to bring all the disassembled SPS from GEO to Moon. Assuming a Tug mass of 60 [tons] and an SPS mass of 6600 [tons], a sensitivity analysis based on the Tug Isp is proposed below:

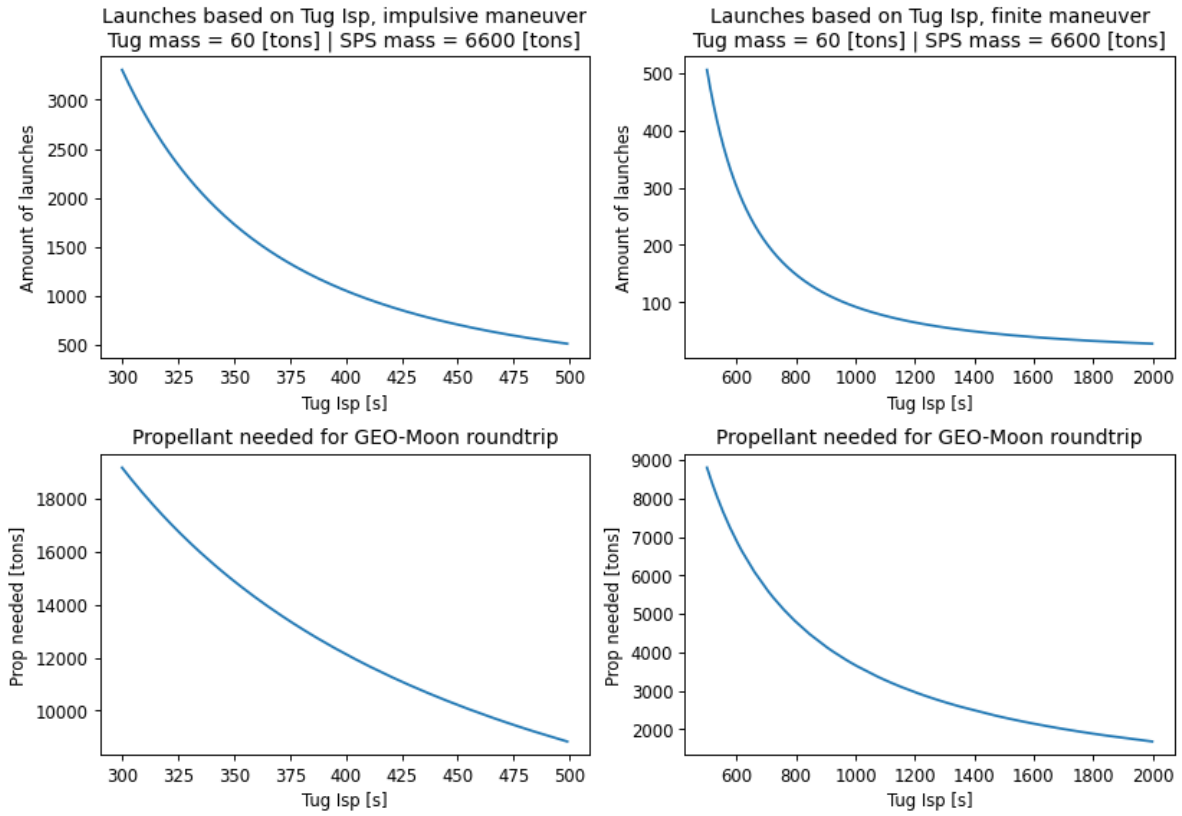

Figure 4-65 Propellant launches and mass required for decommissioning based on Tug Isp

The amount of launches is for both the propellant required for the GEO-Moon roundtrip and the one required to bring the fuel from LEO to GEO.

Similarly, a sensitivity analysis based on Tug mass is performed, considering both an Isp of 360 [s] and 1000 [s].

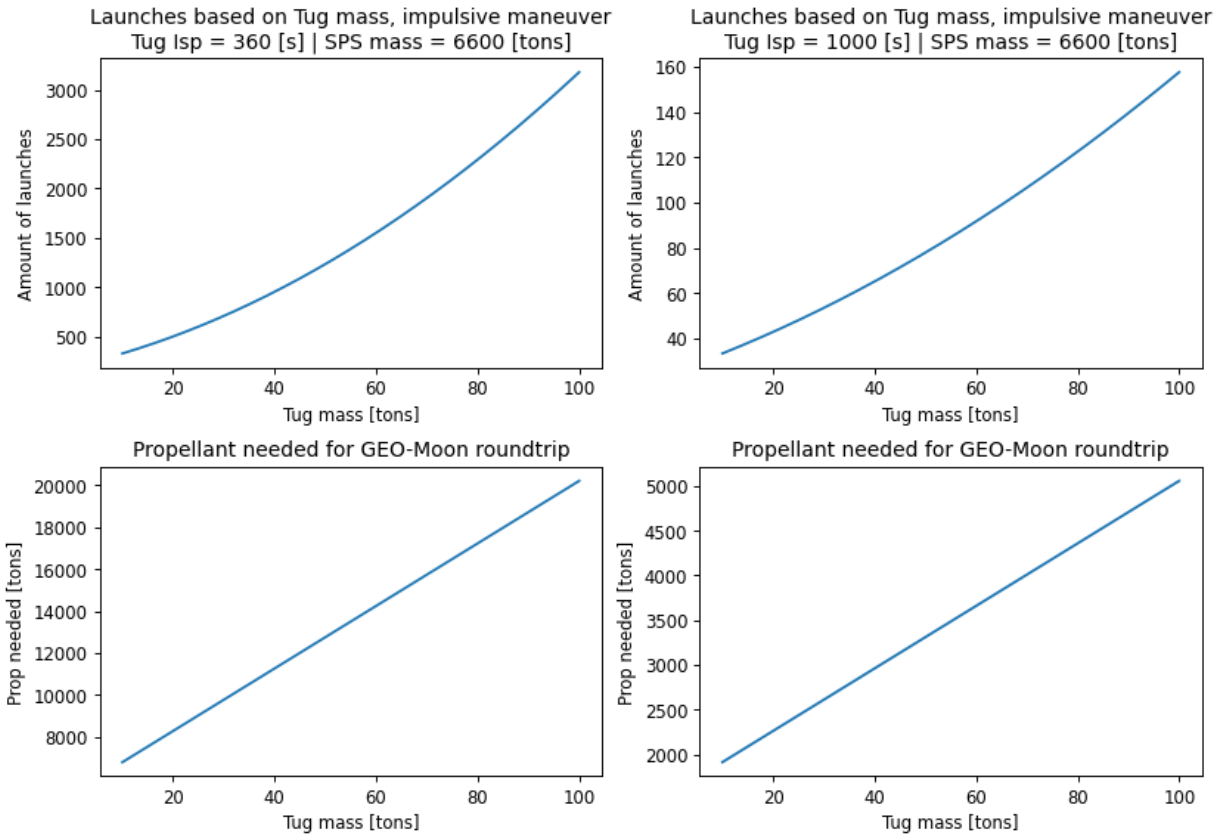

Figure 4-66 Propellant launches and mass required for decommissioning based on Tug mass

5 Functional Analysis & Physical Architecture

5.1 Functional Analysis

The functional analysis based on the logical layer has been developed to define functions for the physical architecture. The following three macro functions containing all the sub-functions of the system are considered:

- Generate and trasform solar energy into RF;
- Convert RF in Electrical power and distribute to end-users;
- Perform & Support Satellite functions (specific functions for the SPS).

The functional tree related to the first function "**Generate and trasform solar energy into RF**", shown in the picture below, describes the process of transformation of the solar energy in electrical power on board, the transformation in radiofrequency waves and the transmission on ground.

The green functions are the ones allocated to our system, the blue ones are performed by external actors outside our area of responsibility (ground control segment or end users). These functions are used to specify the external interfaces with the system.

The functional architecture has been developed during the physical architecture elaboration and is detailed in section 5.2.

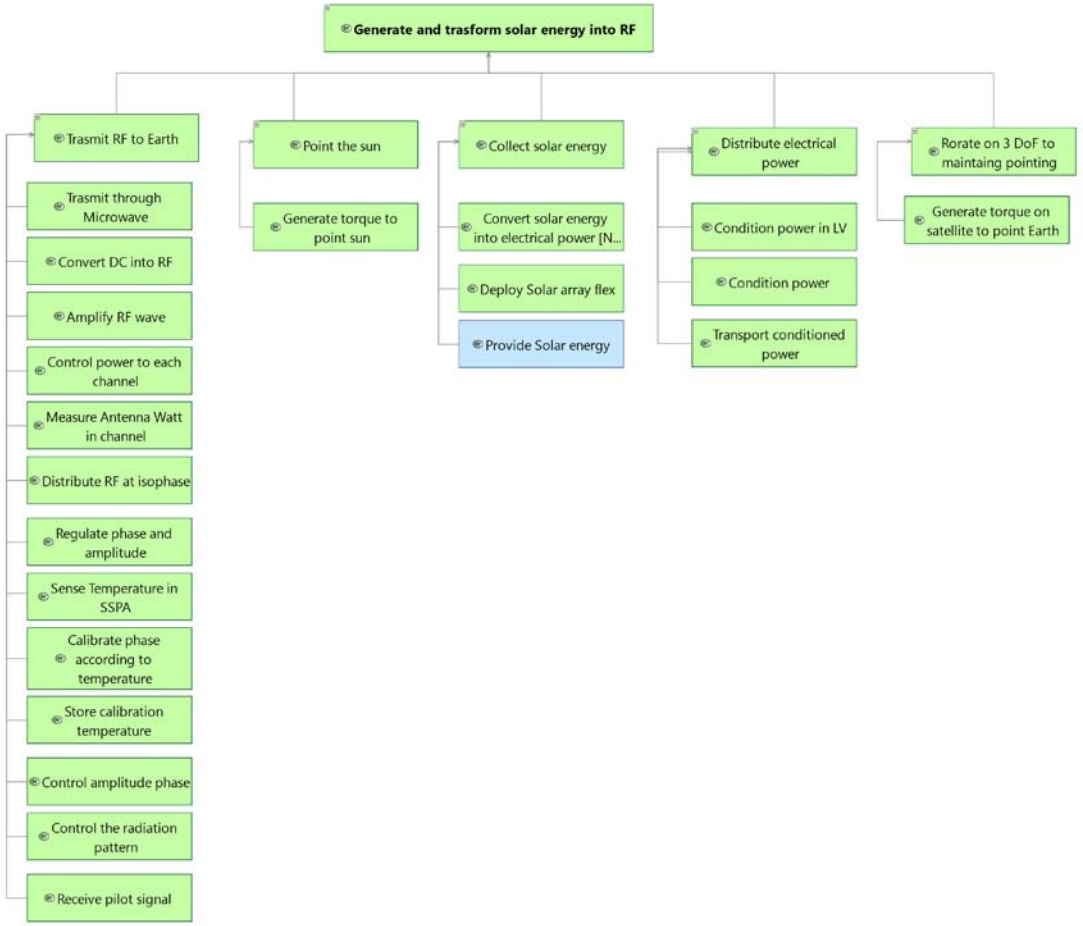

Figure 5-1 Functional tree (part 1/3)

The same organisation has been put in place for the conversion on ground in electrical power "**Convert RF in Electrical power and distribute to end-users"** with the distribution into the national grid or the provision to specific end user.

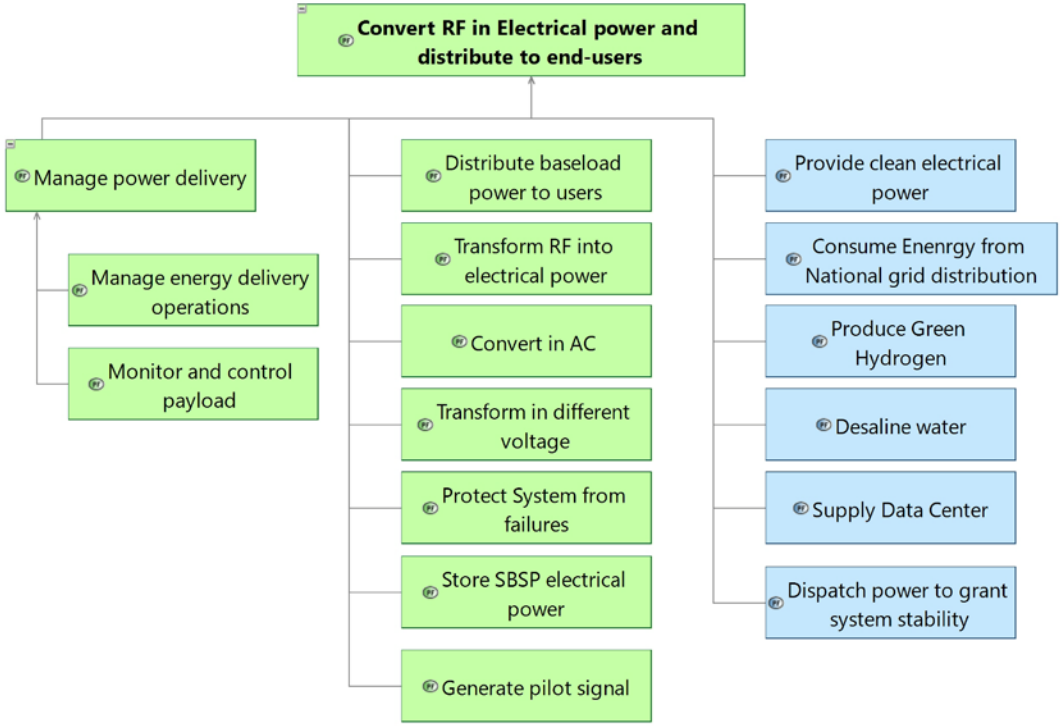

Figure 5-2 Functional tree (part 2/3)

These functions have been discussed and agreed with all the architects involved in the study.

The third branch is dedicated to the functions specific to the satellite which has an high level of complexity (especially in terms of maneuvers and station keeping to support the solar array and the phased array antenna).

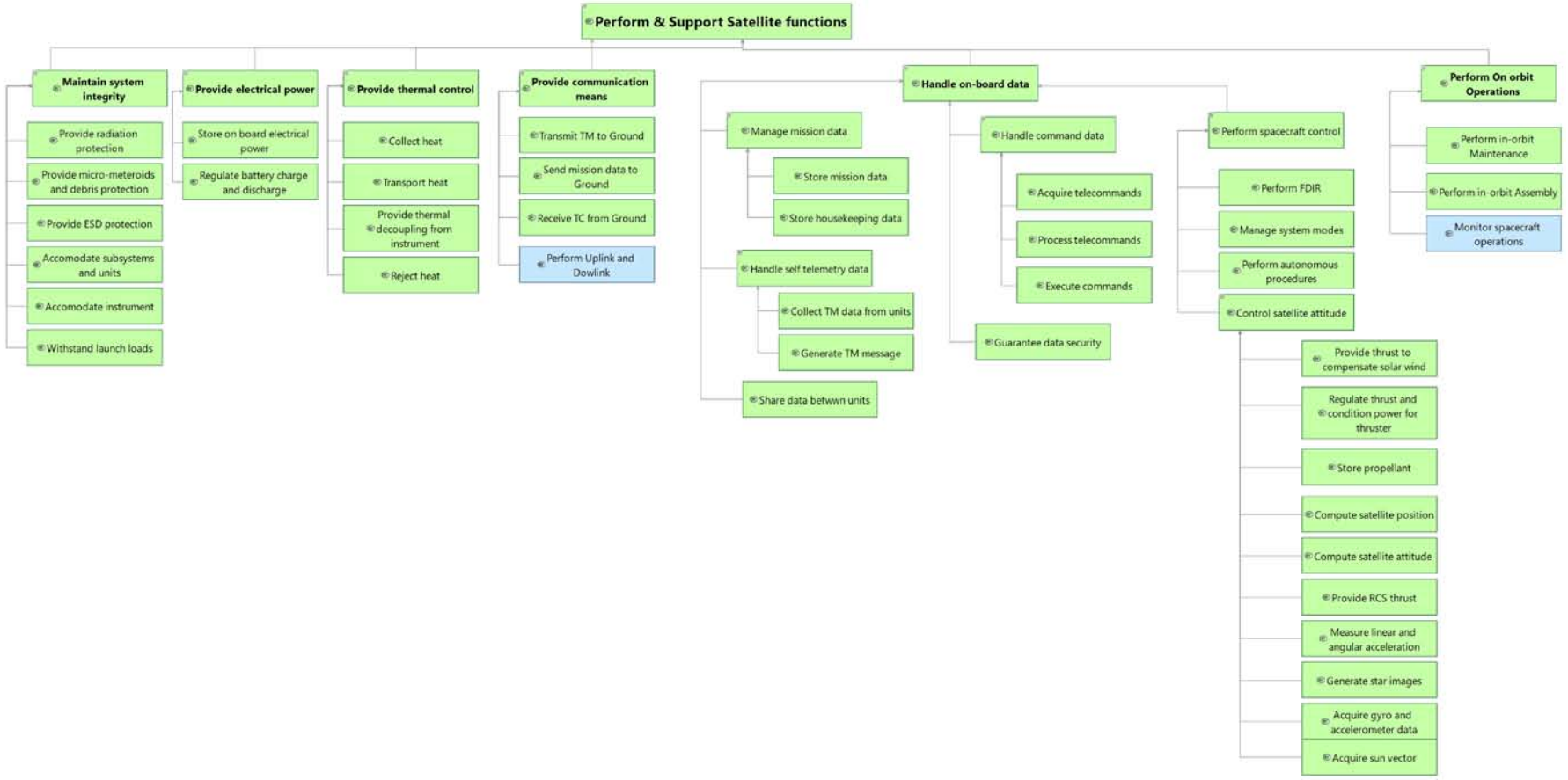

Figure 5-3 Functional tree (part 3/3)

5.2 Physical Architecture

The functional architecture has been developed following the evolution of the sub-system design. Once the sub-system design has been frozen by the specialists, the integration in the Capella model has been performed.

The physical architecture is the result of a functional analysis detailed at component level and the definition of interfaces among components. Thus, functions and functional exchanges (data exchanged among functions) are allocated to the physical components and physical interfaces. The result is a preliminary design of a SBSP systems with his building blocks, components and the associated functions.

The space segment is composed of three building blocks:

1. Full wing assembly: it includes the flexible solar arrays with the deployment mechanism, the hall effect thruster assembly and the PCU to condition the electrical power to the desired voltage;
2. The satellite Platform: it includes the typical equipment of a standard satellite such as on-board computer, Low gain antenna and battery. In addition, the central truss which includes the main power bus is described as well as the motorized rotary joints allowing the motion of the antenna to point the GPS on Earth;
3. The phased array antenna assembly: it includes dedicated PCUs to condition power, the RF generation and transmission assembly and the Antenna central Unit controlling the phase shifters.

The yellow block represents the hardware components (e.g. the OBC or the Low Gain Antenna) that are under satellite platform responsibility and that will be distributed (e.g. hosted on the roll-out module) according to the configuration evolution.

The blue blocks represent the behaviour of the component and allow the allocation of the functions in the components.

The functions are described with green blocks and are allocated to each yellow component of the architecture. As already mentioned before, the functions are organized in functional trees and represent the leaves of the branches, satisfying ARCADIA rules.

The most important added value of the Physical Architecture, reported Figure 5-6, is the definition of the interfaces:

- the green exchanges represent the functional exchanges, meaning the data exchange between the executions of two functions;
- the blue exchanges represent the kind of interfaces between two component (electrical, data, hydraulic, etc.);
- The coloured ones, detailed in Figure 5-4, correspond to a preliminary definition of physical interfaces, in this case high voltage (20 KV), low voltage (28V, 120V, 50V) and data interfaces.

The following legend has been developed to help the visual understanding of the model:

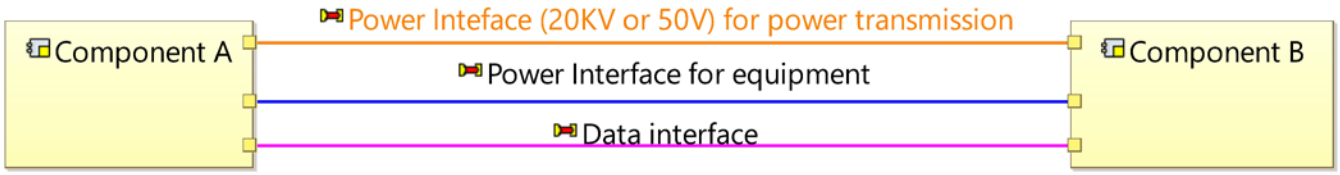

Figure 5-4 Interface legend

The interfaces, described with a specific Capella add-on called Property Values, allow the user to define properties of component or interfaces. In this case, the specification of the wiring has been chosen and applied to all the physical interfaces.

In the picture below the field with the properties applied to the wiring is shown.

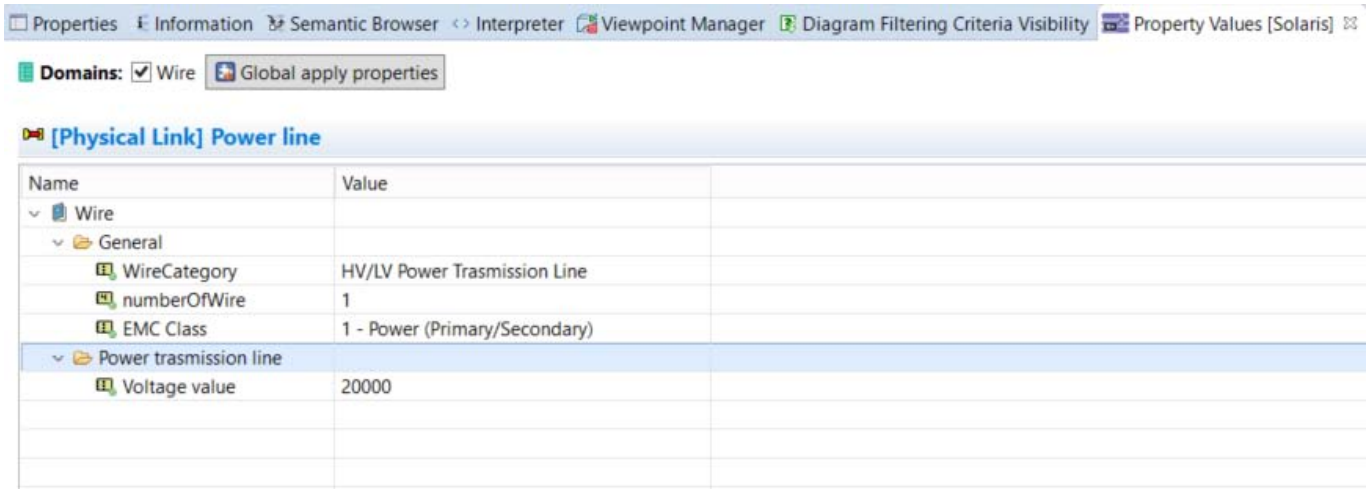

Figure 5-5 Property values field

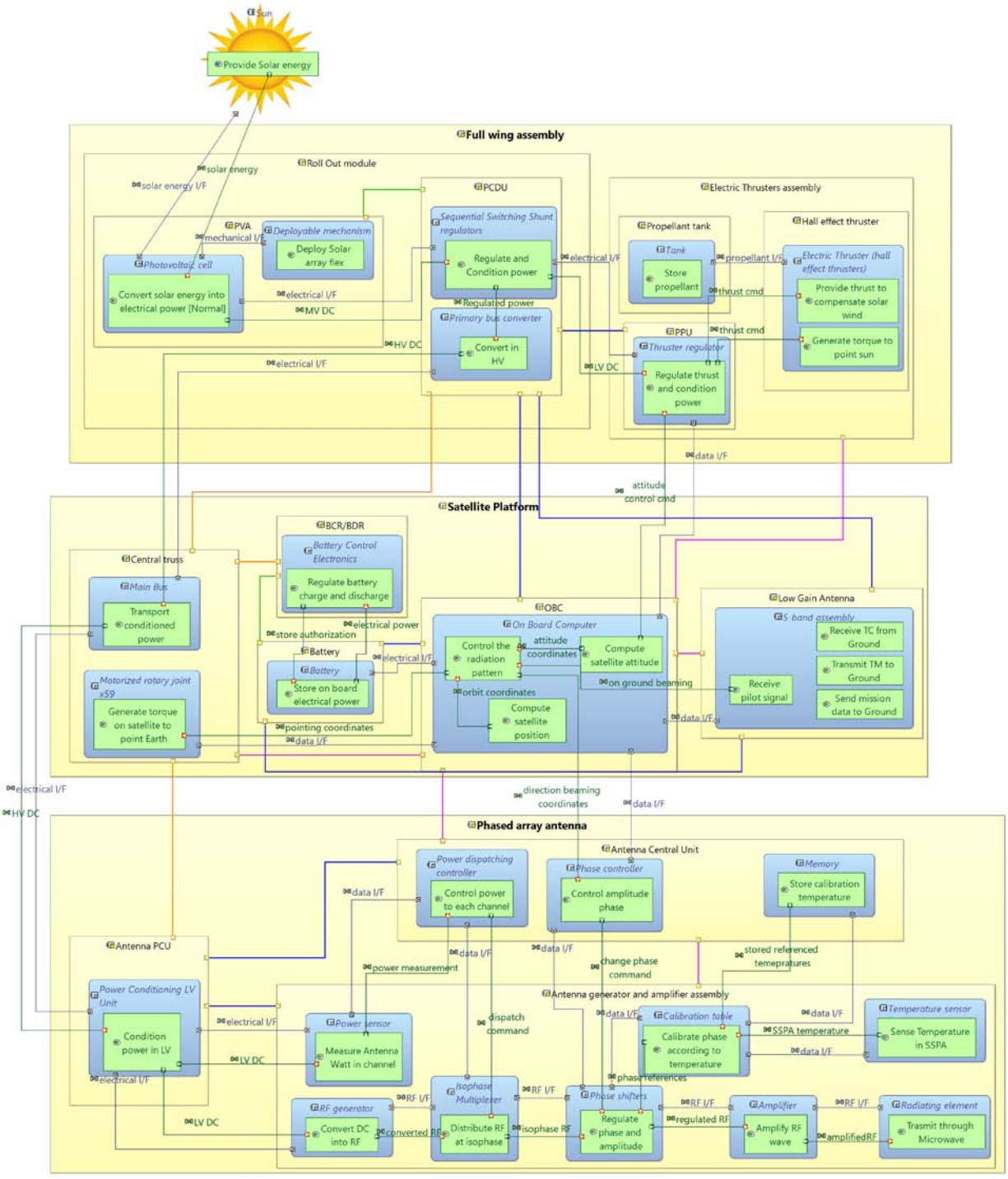

Figure 5-6 SBSP physical architecture

The on-ground architecture, shown in Figure 5-7, foresees the RF coming to ground through the beam emitted by the antenna, collected by the rectennas and transformed into electrical power before being distributed to the final users. The power is then regulated by an Electrical Substation that can be either dedicated to a specific end users (data center, desalination center,…) or to the national electric grid. If the specific end user is isolated without the connection on the public grid, it is an **off-grid configuration** otherwise (if there is a backup connection with the grid) is an **on grid configuration**.

Two functional chains (red and blue) describe the distribution to large scale end users into a national grid or the distribution to specific and high demanding end users.

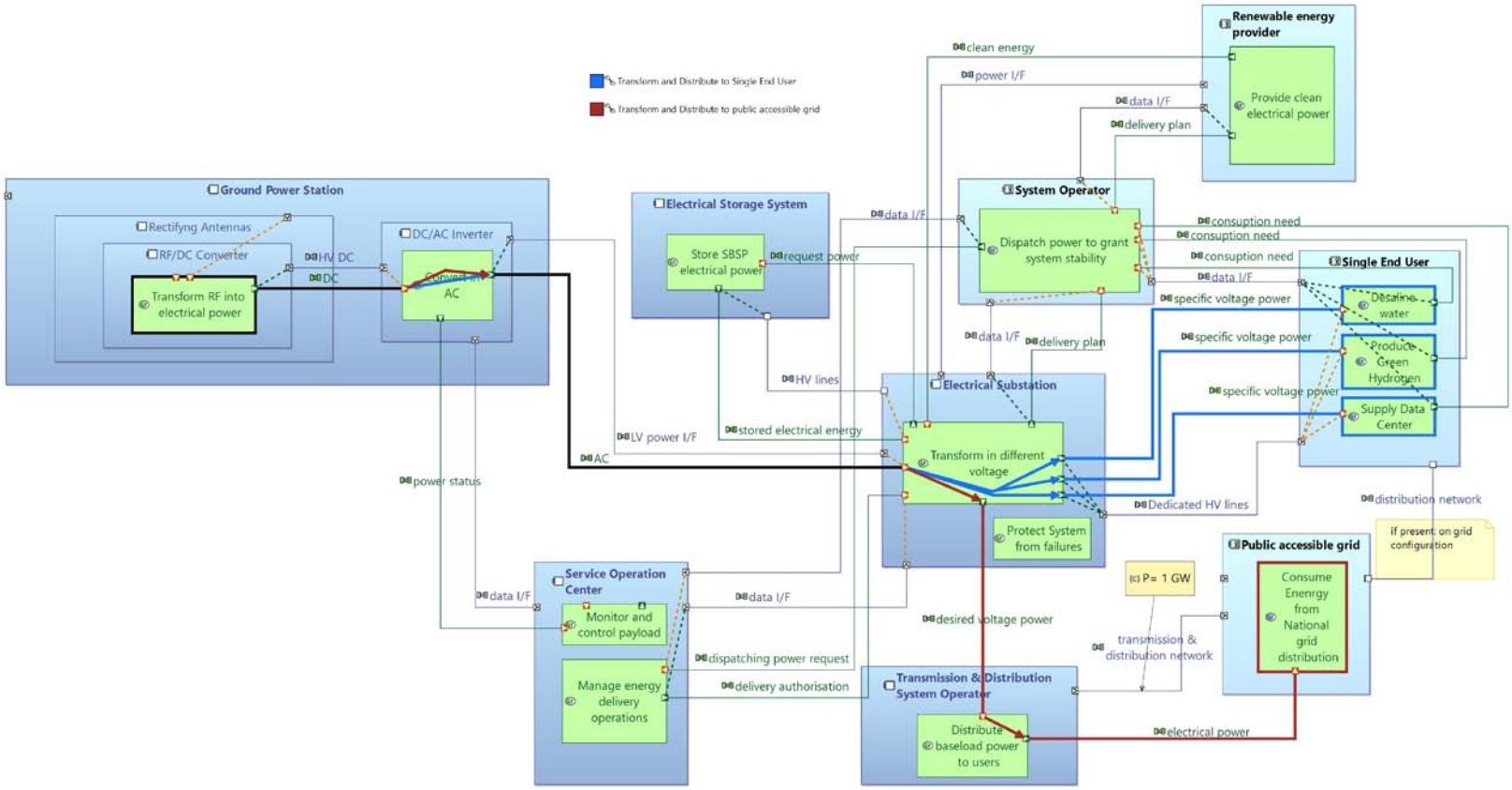

Figure 5-7 On-ground architecture

6 System Budgets

The mass budget of the proposed architecture is summarized in Table 6-1.

Item	Mass [tons]	Remarks
PVA	1870	This mass has been computed considering a PV area of 6 km2. We are considering Perovskite cells as the baseline solution with a weight of 0.08 kg/m2. Additionally, we are hypothesizing that the cell weight is only 25% of the full PV Assembly weight, which amounts to 0.3 kg/m2. The PVA density under consideration has been assesed as follows: • The photovoltaic layer of a perovskite cell is only 1-2 µm, which is equivalent on average to about 15 g/m². • Then, if electrical connections, an adapted packing factor, etc. are taken into account, an estimate of 80 g/m² as made by TAS-I seems realistic. • Similarly, at PVA level, assuming 0.3 kg/m² seems acceptable if a thin substrate and adequate encapsulation are taken into account; and in view of future technological developments. Refer to section 4.2.3
Phased Array Antenna	250	Considering Caltech ultra-lightweight phased array antenna technology [RD2]. The idea is to develop a lightweight RF IC (integrated circuit) glued on a foil of about 0,5 kg/m^2 of density (considering also SSPA and all the integrated circuit). Refer to section 4.2.3
Structure	3370	This mass has been computed considering a truss-like structure. Refer to section 4.2.3. This value is likely to fall considering the evolution of materials used.
AOCS	100	Thrusters + PPUs + Propellant for 1 year. Refer to section 4.2.4
EPS	1018	DC/DC converters + Harness. Refer to section 4.2.5
Mechanisms	30	Motorized rotary joints. Refer to section 4.2.2
TOTAL	**6640**	

Table 6-1 Mass budget

The power link budget is reported in Table 6-2.

Efficiency	Value	System efficiency	Power [MW]
Solar Power Generator (0.24)			8593
Photovoltaic cell efficiency	0.29	0.29	2492
Solar panel surface efficiency	0.86	0.25	2143
Illumination efficiency	0.99	0.247	2122
Power line efficiency	0.99	0.245	2100
Power conditioning efficiency	0.98	0.24	2058
Wireless Power Transfer (0.64)			
Power distribution network	0.98	0.235	2017
Power conditioning efficiency	0.98	0.23	1976
RF power generator	0.83	0.19	1641
Antenna efficiency	0.98	0.187	1608

Atmospheric attenuation	0.98	0.18	1575
Beam collection efficiency	0.833	0.153	1312
Ground Power Station (0.77)			
Rectenna panel surface efficiency	0.98	0.15	1285
Rectenna efficiency	0.833	0.125	1071
Power line efficiency	0.99	0.124	1060
Power conditioning efficiency	0.95	0.117	1007

Table 6-2 Power link budget

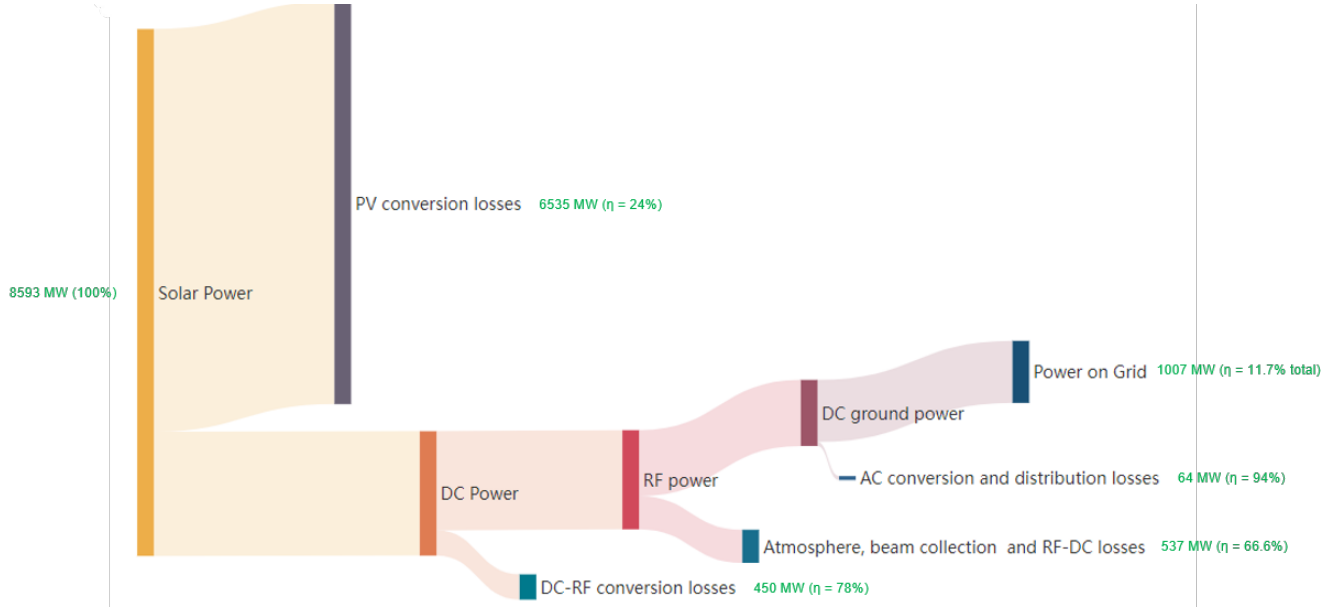

Figure 6-1 SBSP Sankey diagram

7 SPS Critical Areas & Technology Needs

The following table summarizes the SPS critical areas & technology needs.

S/S	Critical areas & technology needs	Remarks
PVA	Very-low cost, lightweight solar cells with ~30% efficiency and 30 yr lifetime are required	
Robotics & Mechanisms	Large Mechanisms (rotation of the Phased antenna structure)	Refer to section 4.2.2
	Assembly & Maintenance	The assembly and maintenance of big space infrastructures, performed by autonomous rendez-vous & Robotics systems is being tackled by ESA via the new Initiative on In-Orbit, Servicing, Construction and Recycling technologies (OSCAR). A workshop has been organized on 20/10/2023 and technology development activities will be pursued to raise the TRL of the necessary building blocks
Structure	Solar Arrays	Refer to section 4.2.3 **Boom:** development for 80 m boom either coilable or telescopic designs solutions **Flexible part with solar cells**: thin film e.g. Kapton internal joints and surface joining to flexible solar cells processes development **Deployment Mechanisms:** development of unrolling mechanism e.g. controlled unrolling of coilable boom or extension mechanism for telescoping boom
	Roll-out Modules	Refer to section 4.2.3 **Modules**: development of the modules to provide the above reported section inertia properties for target stiffness achievement as well as intra-modules joints
	Central Truss	Refer to section 4.2.3 **Modules:** development of the modules to provide the above reported section inertia properties for target stiffness achievement as well as intra-modules joints

AOCS	Actuators	Refer to section 4.2.4 Advancements in electric propulsion are required to support control.
	Structure/Control Interaction	Refer to section 4.2.4 Interaction with structure needs to be further investigated to ensure robustness of control concept.
EPS		Refer to section 4.2.5 The huge amount of power involved in SBSP applications makes necessary managing very high voltage ranges. Thus, highly performant power conversion technologies will be needed as well as high-power cables, which represent a big challenge in space. Another issue could be related to the power management of a complex high power space system like this.
Phased Array Antenna	Beam forming & pointing	Refer to sections 4.2.6.5 Methods for forming & pointing power beam within a very large phase array (millions of controls) to be developed and validated
	High Power Amplifier with very high Power Added Efficiency (PAE)	Refer to sections 4.2.6.2 and 4.2.6.6 Large technological effort is required to increase SSPA PAE to the expected efficiency.
	In-orbit assembly of very large planar phase array (from 10's of thousands of sub-panels)	Refer to sections 4.2.6
	Industrial mass production (millions of units) of space grade electronics for bricks and sub-panels (SSPA, EPC, phase shifter,…)	Refer to sections 4.2.6.10 Table 4-9.
TCS	New material to withstand extreme temperature	Refer to section 4.2.7
	New solutions to manage thermo-optical properties	
	New solutions to increase thermal capacitance	
Launch and deployment	In-Orbit Servicer	Refer to TN3 section 3.4.2.10 The Orbital Tug is a critical technology as it allows

		to bring the modules in the operative orbit and assemble the SPS
	Launcher Fairing	Refer to section 0
	In-Orbit Manufacturer	Refer to section 4.4.3 If a servicer satellite is capable to weld or glue modules there would be a great advantage in term of cost and overall mass, as well as maximize fairing capability

Table 7-1 Critical areas & technology needs

A preliminary TRL evaluation for the SPS platform systems has been provided in TN2. Considering the cutting-edge level of the project in question and the lack of specific relevant heritage, for the TRL projections, we can refer to the general assessment provided in [RD2] (TN3, chapter 7):

Years to TRL 9 from TRL:	Average (years)	Standard Deviation
1	16.3	11.4
2	14.5	10.9
3	13.1	10.6
4	11.3	10.6
5	9.7	10.7
6	7.0	5.6
7	5.0	3.9
8	2.2	3.1
9	0.0	0.0

Figure 7-1 Average duration to increase TRLs

8 Digital Model Overview

A digital model of a Space-Based Solar Power (SBSP) mission offers several significant advantages for analysis:

1. **Comprehensive Understanding:** it allows for a comprehensive and systematic analysis of the mission, taking into account various complex and interrelated parameters, such as orbit dynamics, solar energy collection, power beaming, and energy conversion.

2. **Simulation of Complex Scenarios:** digital models can simulate a wide range of scenarios, including different solar conditions, orbit variations, and equipment performance under various conditions. This enables a thorough examination of the system's behaviour in diverse operational environments.

3. **Data-Driven Insights:** by inputting real-world data and variables, digital models provide data-driven insights into the mission's performance, allowing for more informed decision-making.

4. **Efficiency Improvements:** it enables the optimization of system components and parameters, leading to more efficient and cost-effective mission design.

5. **Risk Mitigation:** by identifying potential challenges and vulnerabilities early in the design phase, digital models assist in risk assessment and mitigation strategies, reducing the likelihood of mission failures.

6. **Iterative Design:** digital models support an iterative design process, allowing engineers and scientists to refine and improve the mission design over time, ensuring it meets or exceeds performance targets.

7. **Cost and Resource Savings:** through virtual testing and analysis, digital models reduce the need for physical prototypes and experiments, ultimately saving time and resources during the development and testing phases.

8. **Communication and Collaboration:** digital models facilitate effective communication and collaboration among multidisciplinary teams working on different aspects of the SBSP mission, helping to ensure a unified and well-coordinated approach.

Due to these considerations, a comprehensive digital model has been developed in collaboration with MathWorks®, which has been denominated “SBSP Analysis Framework”. This digital model integrates multiple optimization and parametric models and includes a user interface, allowing for the simulation of various scenarios.

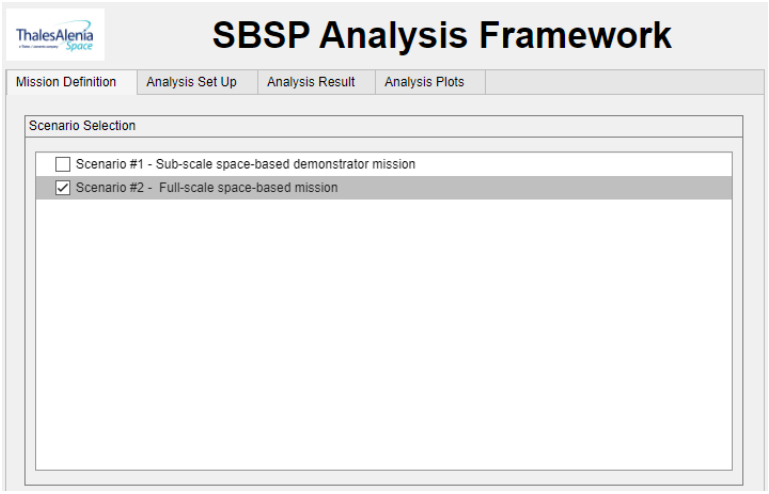

Figure 8-1 High-level scenarios of the SBSP Analysis Framework

8.1 Full-scale SBSP mission model

In the context of the full-scale SBSP mission, the framework allows for two types of analysis, each with distinct objectives:

- **Low-Fidelity Analysis**: an optimization model is used to assess the optimal combination of the three primary SBSP areas – the Photovoltaic (PV) area, antenna area, and GPS area. This evaluation is based on a range of variable inputs and user-defined optimization weight factors. All the analyses presented in chapter 3 have been conducted using this model.
- **High-Fidelity Analysis**: after selecting one of the optimized options derived from the low-fidelity analysis, the subsequent outputs are imported into a System Composer® architecture for the complete system. This architecture incorporates various models that enable different evaluations of the specific set of inputs derived from the low-fidelity analysis. These evaluations include high-level power simulations in various scenarios as well as preliminary assessments of mass and cost. The majority of the analyses presented in chapters 7 and 12 have been carried out using this particular feature of the tool.

8.1.1 Low-Fidelity Analysis

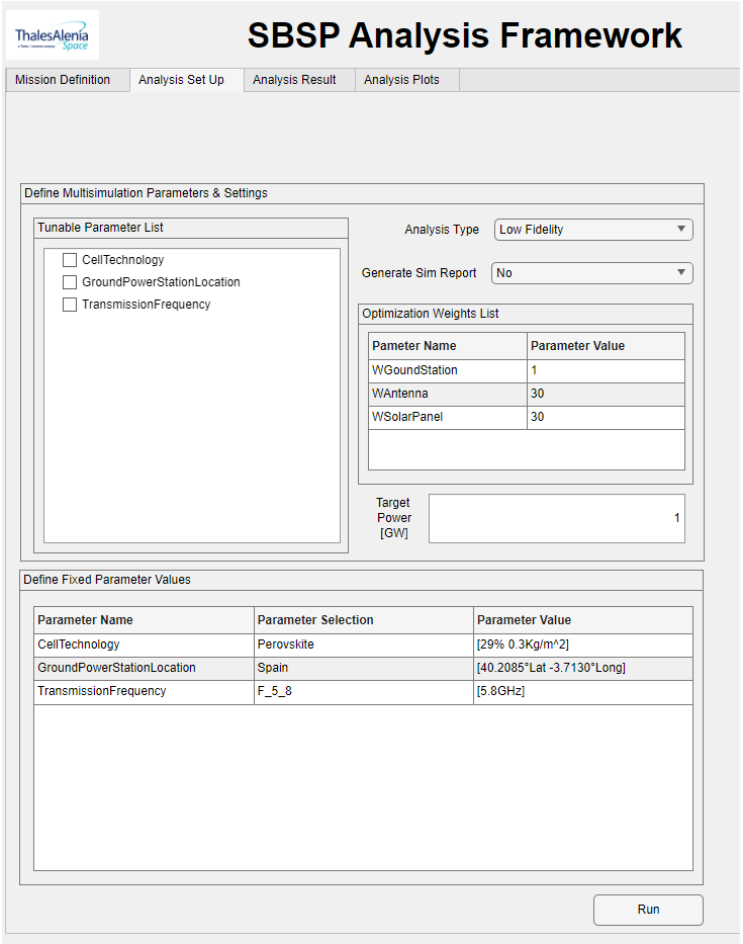

Figure 8-2 Low Fidelity analysis interface

The optimization model is used to assess the optimal combination of the three primary SBSP areas – the Photovoltaic (PV) area, antenna area, and GPS area. This assessment is conducted using a spectrum of variable inputs, which can be either set to specific values or left adjustable, allowing the tool to generate an optimized solution for each of these options.

The possible variables and their options (as already presented in chapter 3) are:

Parameter	Options
Cell technology	Thin Film 3 Junctions (Expected cell efficiency: 36 %)
	CIGS (Expected cell efficiency: 29 %)
	Perovskite (Expected cell efficiency: 29%)
Frequency	2.45 GHz

	5.8 GHz
GPS location	Spain (Latitude: 40.2°)
	Germany (Latitude: 51.1°)
	Sweden (Latitude: 60.1°)

Table 8-1 Possible options for every variable of the Low Fidelity analysis

Once, among all the optimized solutions, one of the possible configurations is selected, this can be exported to a SBSP high-level architecture transported from Capella MBSE tool in System Composer MathWorks® tool.

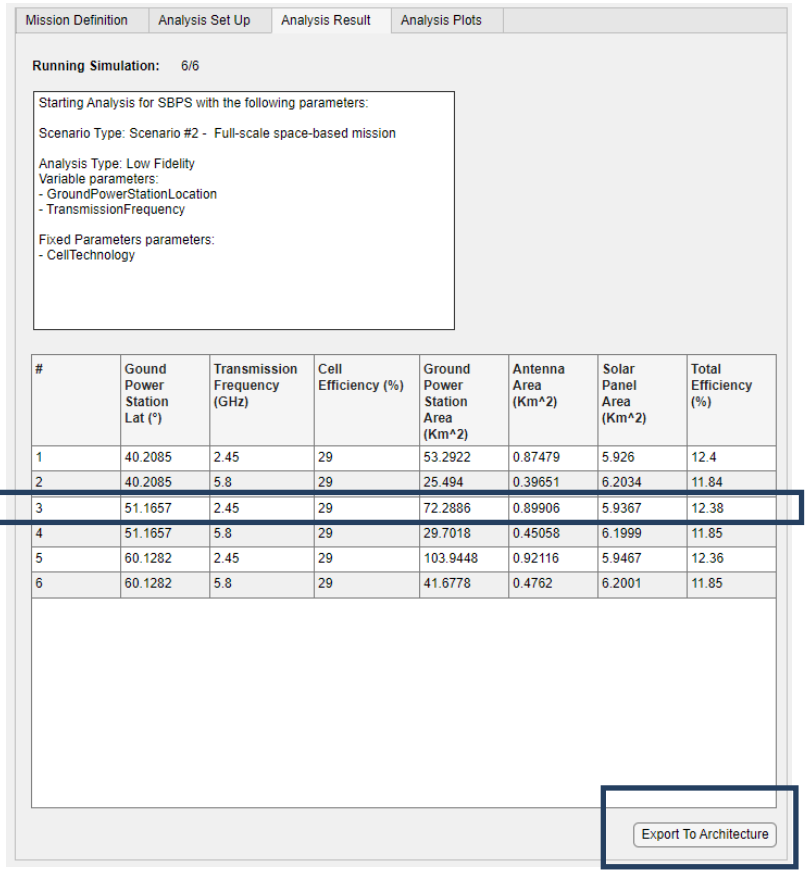

#	Gound Power Station Lat (°)	Transmission Frequency (GHz)	Cell Efficiency (%)	Ground Power Station Area (Km^2)	Antenna Area (Km^2)	Solar Panel Area (Km^2)	Total Efficiency (%)
1	40.2085	2.45	29	53.2922	0.87479	5.926	12.4
2	40.2085	5.8	29	25.494	0.39651	6.2034	11.84
3	51.1657	2.45	29	72.2886	0.89906	5.9367	12.38
4	51.1657	5.8	29	29.7018	0.45058	6.1999	11.85
5	60.1282	2.45	29	103.9448	0.92116	5.9467	12.36
6	60.1282	5.8	29	41.6778	0.4762	6.2001	11.85

Figure 8-3 Example of end simulation results with possibility to export to architecture

8.1.2 High-Fidelity Analysis

Once the desired solution is exported, these outputs are incorporated as inputs into the high-fidelity analysis. This process involves importing and saving all the relevant variables within the high-level architecture, which is used for detailed simulations and additional comprehensive system assessments.

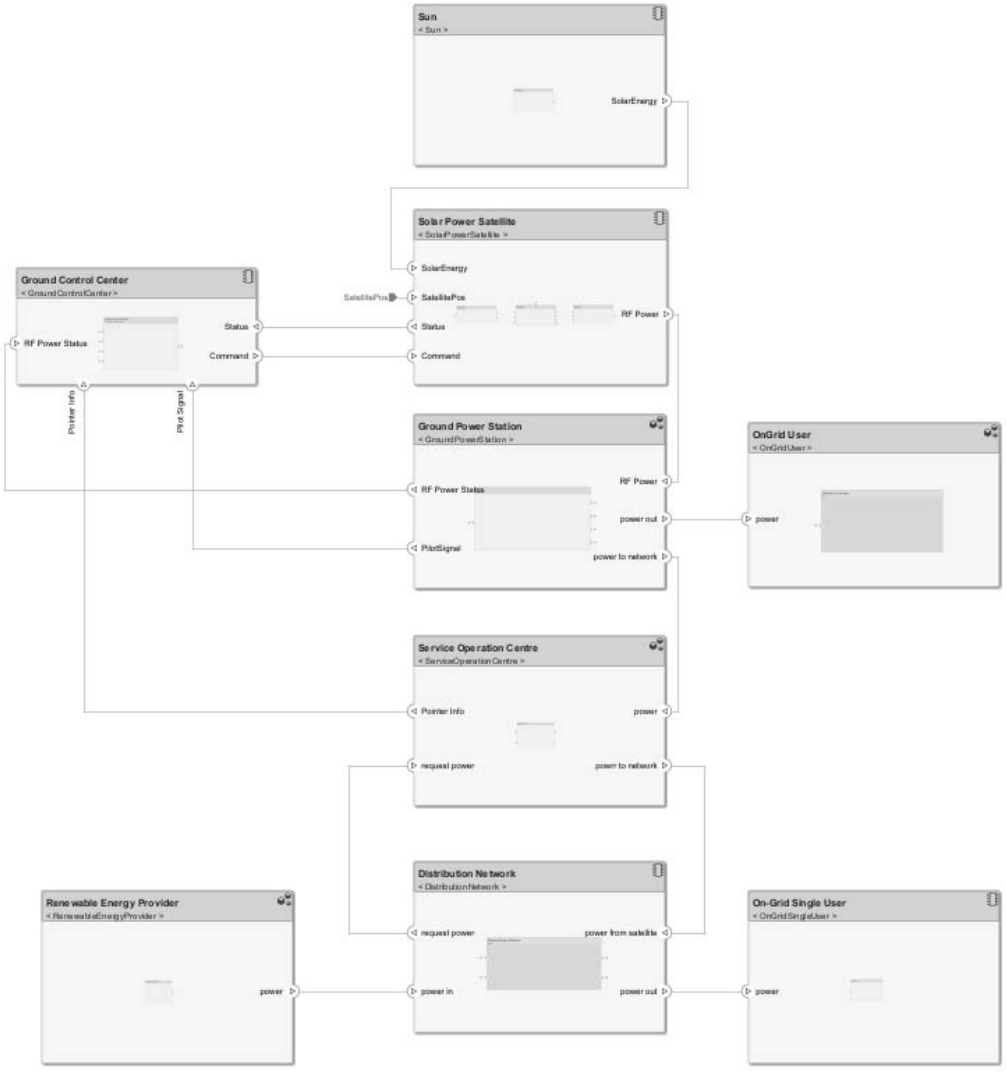

Figure 8-4 SBSP platform architecture in System Composer

With all the critical values now integrated into the architecture, we can proceed with the high-fidelity analysis. This set of functions allows us to:

- Assess the overall power transmission performance in various sections of the architecture throughout a simulation day;
- Evaluate the mass and total number of launches required for the chosen architecture;
- Calculate the mission cost and Levelized Cost of Energy (LCOE) for the selected architecture;
- Determine the Energy Return on Energy Invested (ERoEI) and Energy Payback Time (EPBT) for the selected architecture.

The assessments are based on the hypotheses outlined in chapter 12, and these evaluations can be conducted for any potential output architecture resulting from the Low-Fidelity analysis.

Similar to the Low-Fidelity case, certain parameters that serve as inputs (for either the power simulations and/or the mass and costs evaluation) can be either set as constants or adjusted among all the available options:

Parameter	Options	Main impact on the SBSP System
DC-RF technology	SSPA	DC-RF technology and the associated output power and mass per unit influence the mass (and all the related parameters) of the overall SPS
	Klystrons	
	Magnetron	
Simulation Day	Nominal day	The term "nominal day" refers to a day with uninterrupted 24/7 illumination of the solar panels, whereas the "worst day" represents the most challenging scenario with 71 minutes of eclipse during a day. It is important to note that the selection of the simulation day significantly affects the power profile throughout the day for different SBSP systems.
	Worst day	
Ecliptic inclination	Nominal	The term "Nominal" is used to describe a day with an average solar flux inclination toward the solar panels, while "Worst case" refers to the scenario with the maximum inclination of incident power, which is 23 degrees (ecliptic inclination).
	Worst case	
SPS alignment	Well aligned	A logical architecture has been established to simulate retro-directive beaming and implement potential safety measures associated with misalignment of the SPS. This architecture allows to model a scenario in which the antenna power beam is aimed at the designated target (Well aligned) and one with a certain error, that exceeds acceptable
	Bad aligned	

		safety threshold (Bad aligned).

Table 8-2 Parameters and options for the High Fidelity analysis

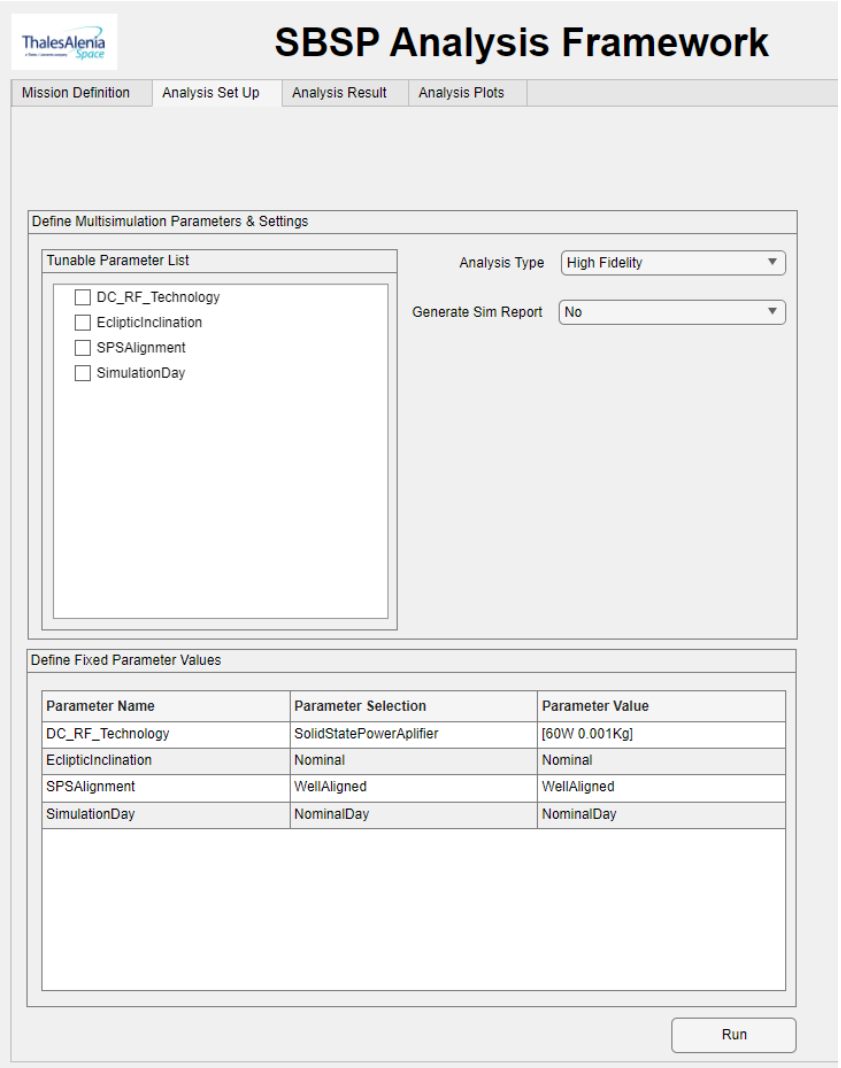

Figure 8-5 High Fidelity analysis interface

Once a specific combination of parameters is selected (or multiple combinations if certain parameters are left variable), the analysis produces various results, including those from the power transmission simulation and estimations of mass and cost (see Figure 8-6 and Figure 8-7). These results are invaluable for assessing and comparing different solutions, as seen also in the Low-Fidelity case.

#	DC_RF Technology	SPS Signal Alignment [-]	Simulation Day [-]	Ecliptic Inclination [-]	Average Transmission Power (MW)	Total Mass (T) & Total Launch(-)	Misson Cost (B$) & LCOE ($/MWh)	EROEI (-) & Energy Paybacktime (days)
1	SolidStatePowerAplifier	WellAligned	NominalDay	Nominal	• @PVA=2064 • @PMainBus=1979 • @On-board Antenna=1577 • @GPS=1051 • @Grid=993	• tot_mass=6591 • tot_launch=106	• miss_cost=14 • LCOE=191	• EROEI=42 • EPBT=219
2	SolidStatePowerAplifier	WellAligned	WorstDay	Nominal	• @PVA=1883 • @PMainBus=1805 • @On-board Antenna=1439 • @GPS=899 • @Grid=903	• tot_mass=6591 • tot_launch=106	• miss_cost=14 • LCOE=191	• EROEI=42 • EPBT=219

Figure 8-6 Example of High Fidelity analysis results 1/2

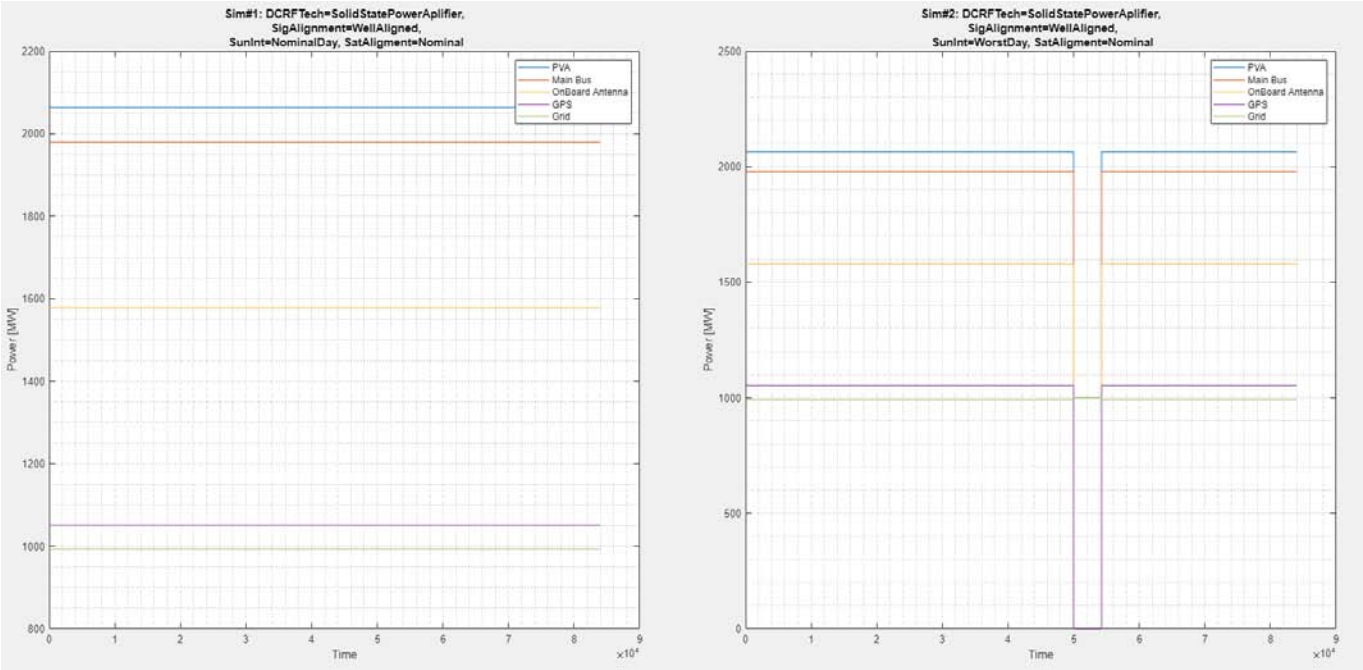

Figure 8-7 Example of High Fidelity analysis results 2/2

8.2 Sub-scale demonstrator mission model

As further elaborated in TN5, a dedicated parametric model has been developed and seamlessly integrated into the SBSP Analysis Framework for the sub-scale demonstrator (see Figure 8-8). In this context, the following inputs can be modified:

- Orbit Type: having the flexibility to choose between Low Earth Orbit (LEO), Medium Earth Orbit (MEO), and Geostationary Orbit (GEO) as potential operational orbits for the demonstrator;
- Ground Station Area: the tool performs parametric simulations for each Ground Power Station (GPS) area input provided in the section;
- Target Power Requirement: for each GPS area, the tool generates a dedicated curve for every specified target power on the ground, demonstrating the options included in that section.

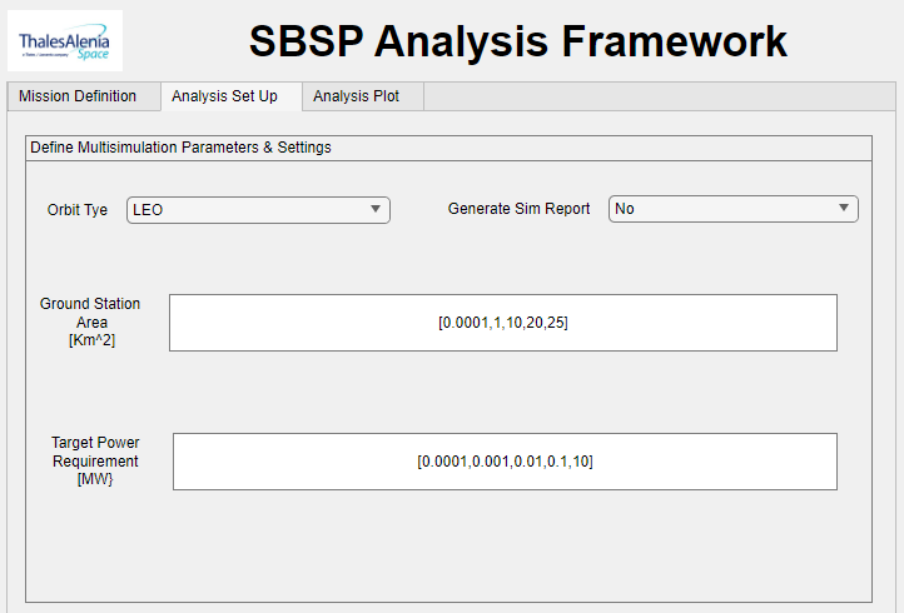

Figure 8-8 Sub-scale demonstrator mission scenario interface

The scenario has as results the plotting of a figure for every GPS inserted to be analysed (see Figure 8-9). In each plot is possible to observe a curve (that depends on the target power delivered) which correlates solar panel area and antenna area. These plots are fundamental to understand the expected scale of a demonstrator in function of the target power and other considerations.

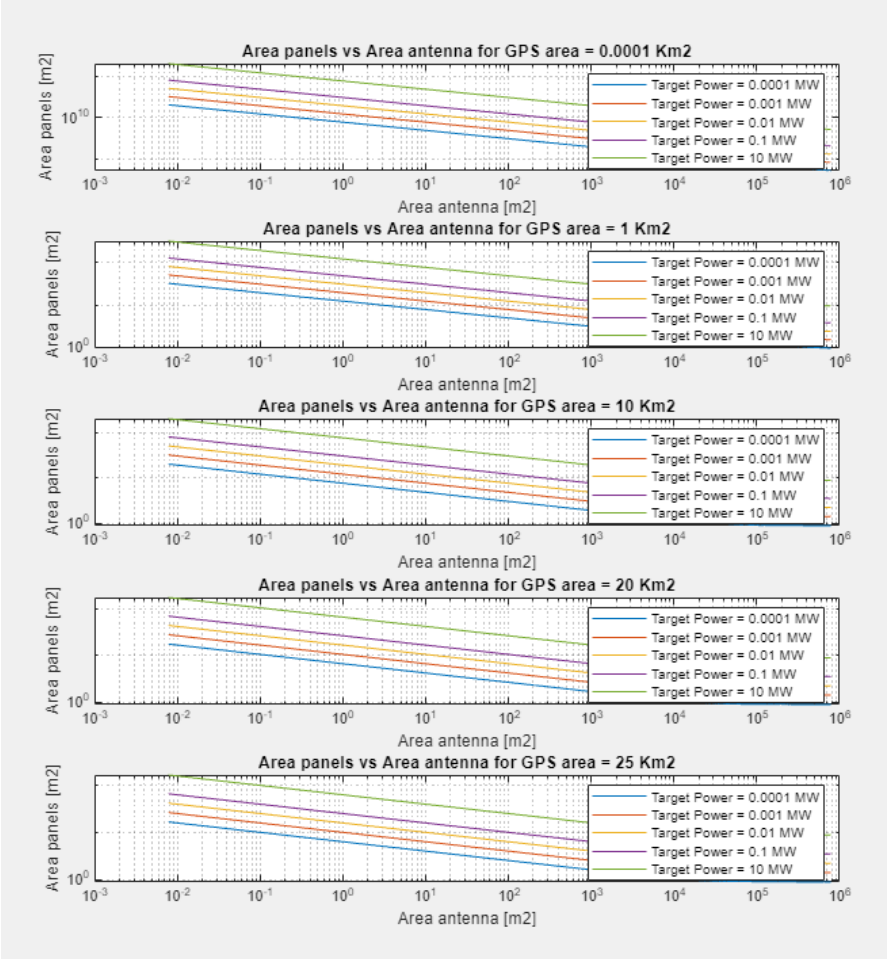

Figure 8-9 Example of Sub-scale demonstrator mission scenario interface results

9 System & Performance Simulations

The SBSP Analysis Framework, as elucidated in the preceding chapter, serves also the purpose of simulating the power link budget and wireless power transmission in different scenarios. This simulation takes into account the SBSP power link budget, which has been revised and updated following a more comprehensive analysis (see Table 6-2).

As previously elucidated in the SBSP Framework Analysis presentation on High-Fidelity simulations, the incorporation of the SBSP platform architecture within System Composer, replete with Simulink circuits, enables the power simulation of diverse high-level scenarios:

- Nominal day simulation;
- Worst day (71 minutes of eclipse) simulation;
- Worst case ecliptic inclination (23 deg) simulation;
- SPS alignment logic simulation.

9.1 Nominal Day Simulation

When discussing a typical operational day, it is plausible to assume a continuous 24-hour period of full nominal illumination for the Solar Power Satellite. Under these conditions, the on-board batteries and the ground-based super capacitors remain inactive because the solar power reaching the solar panels remains relatively constant, and there are no instances of eclipses. It is important to emphasize that, in addition to the energy supply, one must also consider the power requirements for various on-board systems, with a specific focus on the Attitude and Orbit Control System (AOCS) hall thrusters, and for the batteries recharge if needed.

In the following figures, it is possible to observe the power profile throughout the day at various critical points within the SBSP system:

- PVA power output;
- Main bus power;
- Antenna power output;
- GPS power output;
- Grid power.

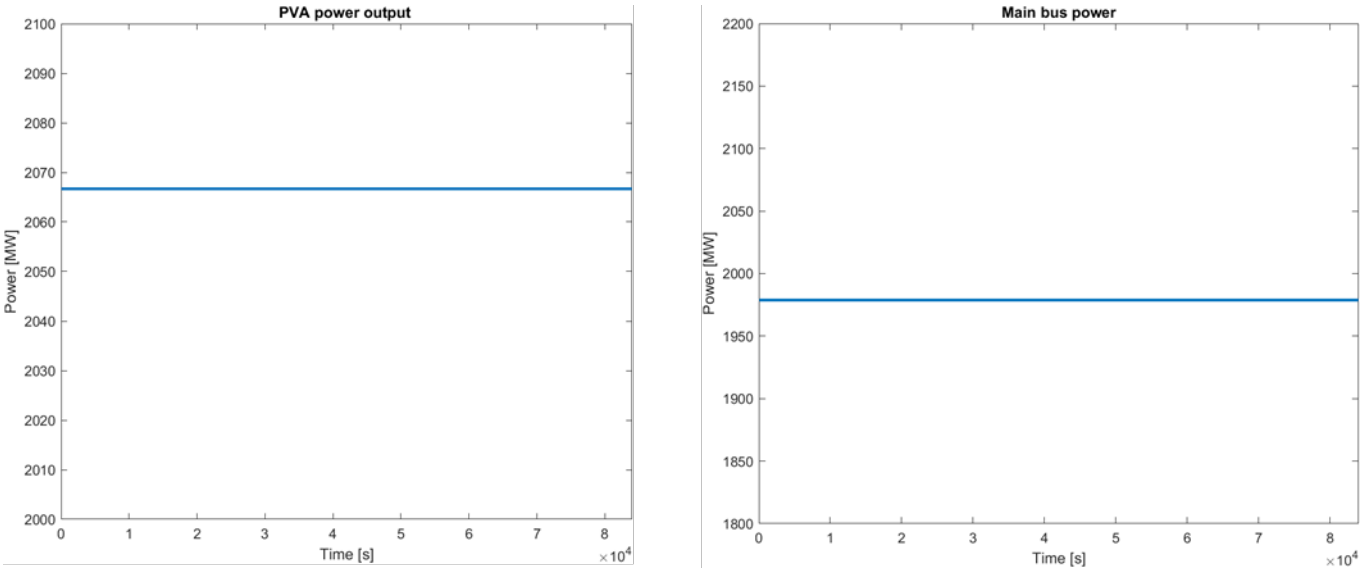

Figure 9-1 PVA power output (left) and Main bus power (right) during a nominal day

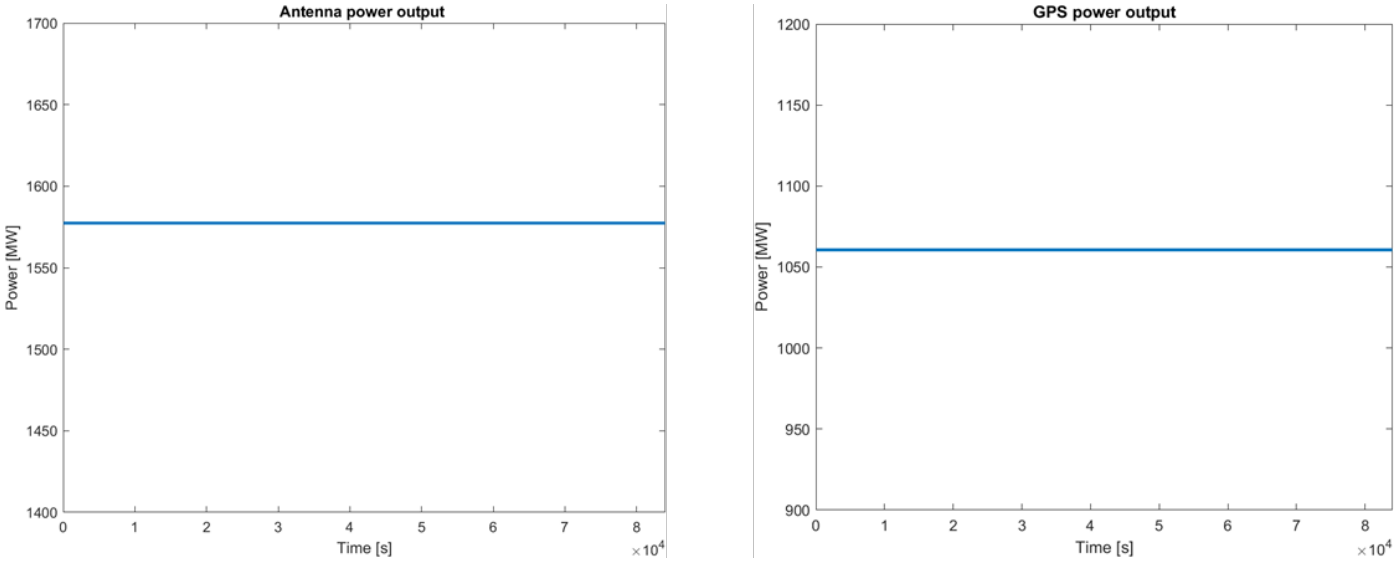

Figure 9-2 Antenna power output (left) and GPS power output (right) during a nominal day

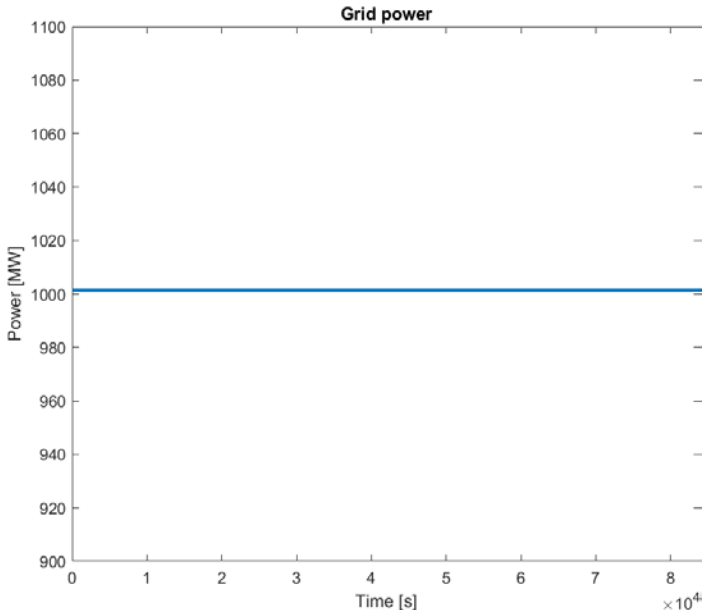

Figure 9-3 Grid power during a nominal day

As evident from Figure 9-3, the baseline of 1 GW of grid power is assured continuously throughout the day.

9.2 Worst Day Simulation (71 minutes of eclipse)

When examining the worst-case scenario, which occurs during equinoxes and involves the maximum duration of eclipses within a day (71 minutes), the tool's utility lies in high-level simulating the logic of compensations from on-board batteries and ground-based supercapacitors to address the absence of power generation during those brief periods.

In the following figures, it is possible to observe the power profile throughout the day at various critical points within the SBSP system:

- PVA power output;
- Main bus power;
- Other on-board loads power (with batteries compensation, it is observable how power does not arrive to zero in the eclipse period);
- Antenna power output;
- GPS power output;
- GRID power (with super capacitors compensation, it is observable how the grid power does not arrive to zero in the eclipse period).

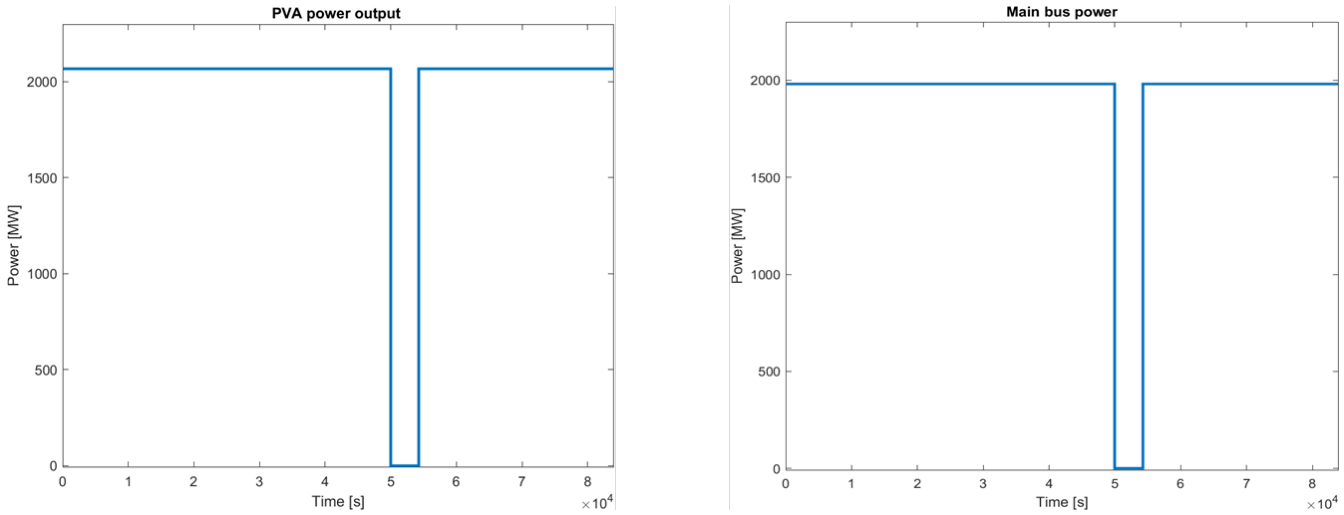

Figure 9-4 PVA power output (left) and Main bus power (right) during the worst day case

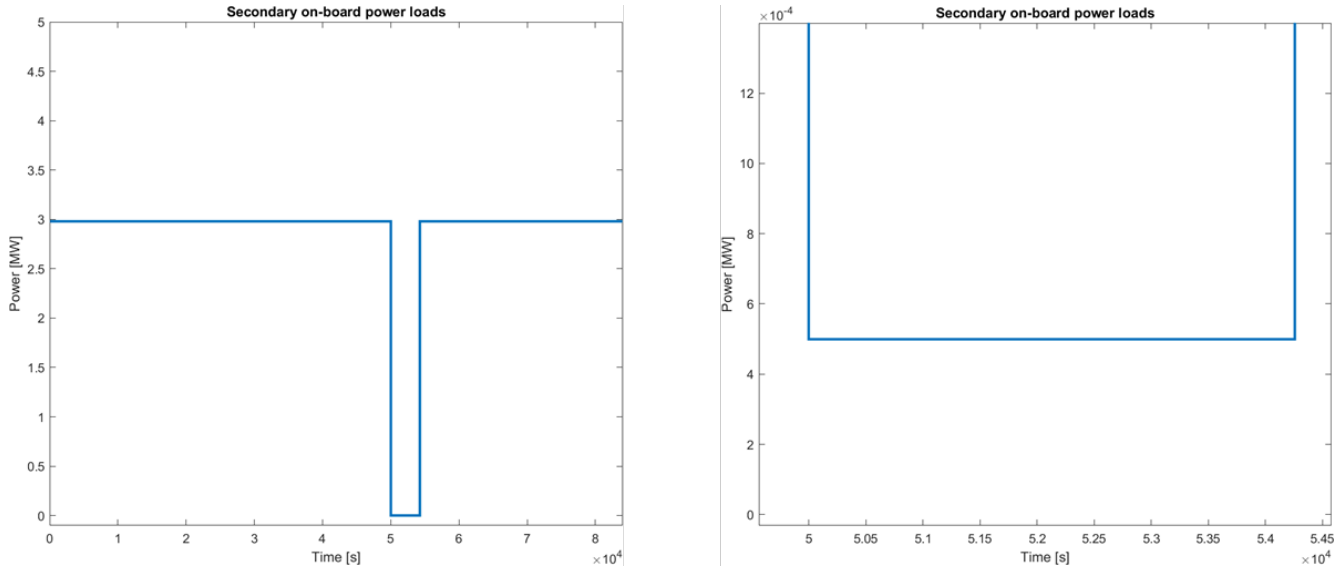

Figure 9-5 Secondary power loads on-board during the worst day case (right: detail of eclipse period)

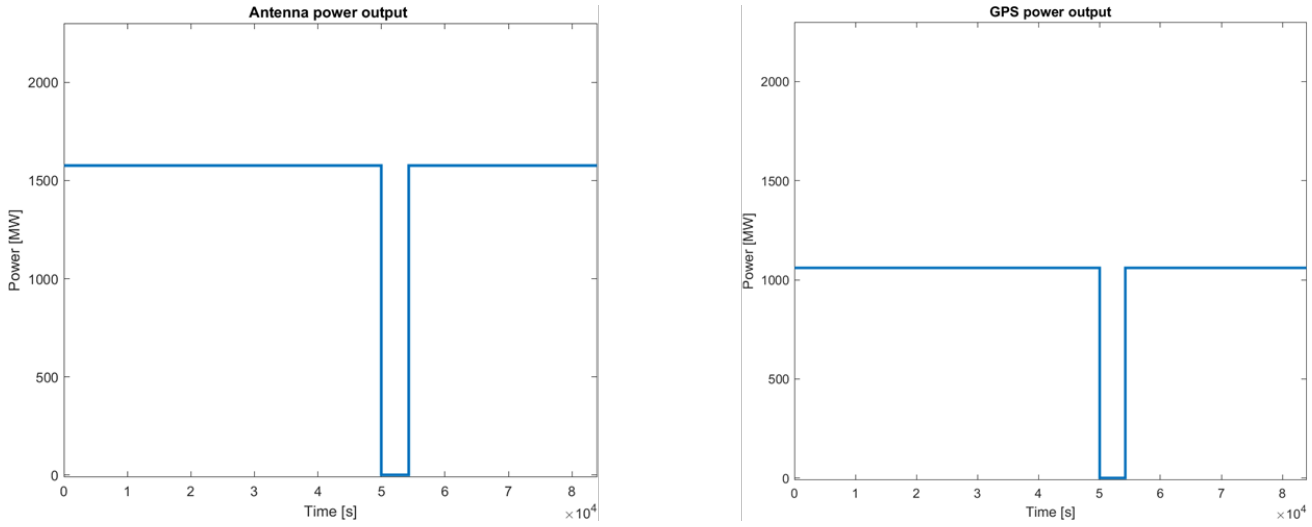

Figure 9-6 Antenna power output (left) and GPS power output (right) during the worst day case

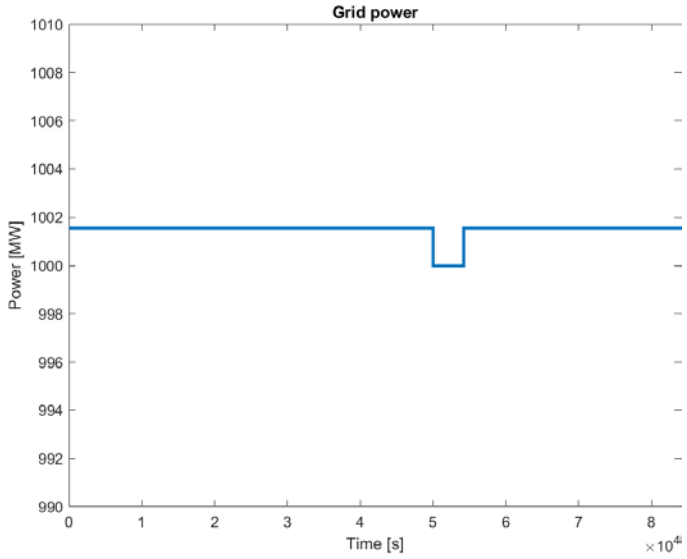

Figure 9-7 Grid power during a worst day case

Despite the 71-minute eclipse, as evident from Figure 9-7, the baseline of 1 GW of grid power is assured continuously throughout the worst day too. This is made possible by the ground-based super capacitors, which are activated when the SPS is not generating power.

9.3 Worst Case For Ecliptic Inclination

In Geostationary Orbit (GEO), the Solar Power Generator, represented by the solar panels, is positioned to continuously rotate around the North/South axis, ensuring it always directly faces the sun. The Solar Power Satellite, located on the celestial or equatorial equator, aligns the perpendicular to the plane of the solar panels with the equatorial plane. As a result, the angle at which the sun's rays arrive at the solar panels corresponds to the sun's declination.

The ecliptic plane, on the other hand, represents Earth's orbital plane around the Sun and is inclined to the equatorial plane at an angle of 23.4 degrees. This inclination causes the angle of incidence of the sun's rays on the solar panels to change with the sun's declination. For the purposes of this simulation, we have focused on assessing the impact on performance under the most challenging conditions, considering a 23.4-degree inclination.

In particular, in the subsequent figures, it is possible to observe the following power output profiles through a nominal day (but considering a 23.4-degree inclination of sun incident power):

- PVA output power;
- Grid power.

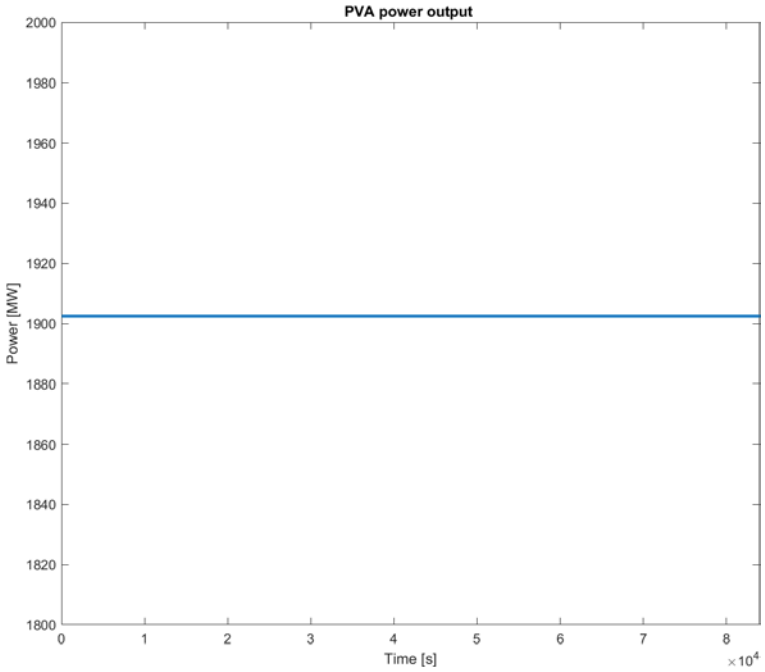

Figure 9-8 PVA power output in worst-case day for ecliptic inclination

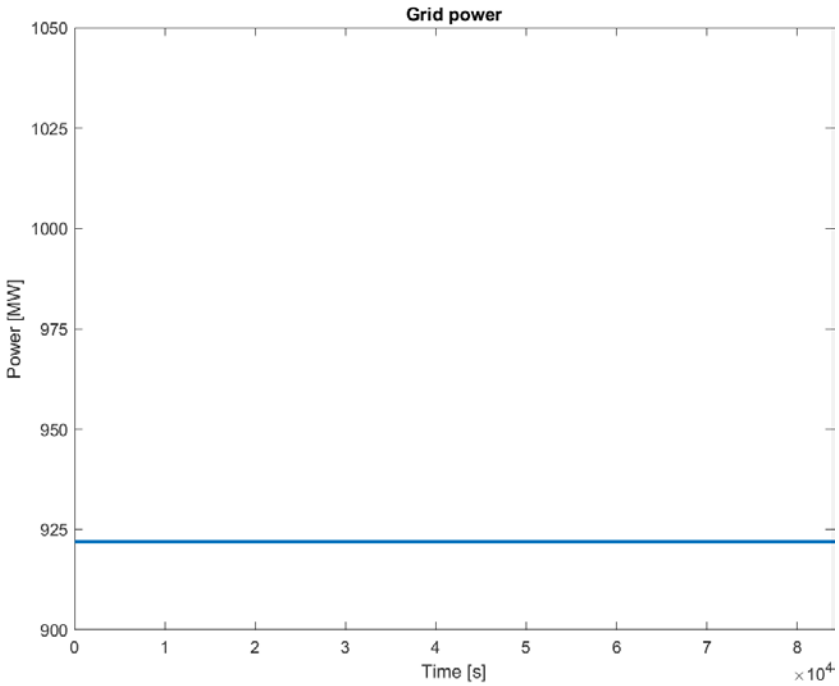

Figure 9-9 Grid power in worst-case day for ecliptic inclination

Looking at the last graph, one can see that the power loss is still acceptable and falls within the baseload power use-case definition of 1 GW + TBD%. In fact, this TBD can be quantified precisely by considering this worst-case as around 7%.

9.4 SPS Alignment Logic Simulation

Finally, a logical architecture has been established to simulate retro-directive beaming and implement potential safety measures associated with misalignment of the SPS. This architecture allows to model a scenario in which the antenna power beam is aimed at the designated target (a GPS) but with a certain error, that exceeds acceptable safety thresholds.

In such cases, the antenna's central unit and the phase shifters collaborate to interrupt the power beaming if the angle error surpasses specified safety standards. As evident from the graphs below, it is possible to observe that the power generated by the Photovoltaic Assembly (PVA) is no longer transmitted to Earth due to the antenna's disconnection (in this simulation this period is 10 seconds).

Nevertheless, at ground level, the baseline power requirements for the grid, easily during brief intervals, can be compensated by the utilization of super capacitors. This provision of additional power facilitates the SPS in its process of realigning with the GPS centre through retro-directive beaming and AOCS.

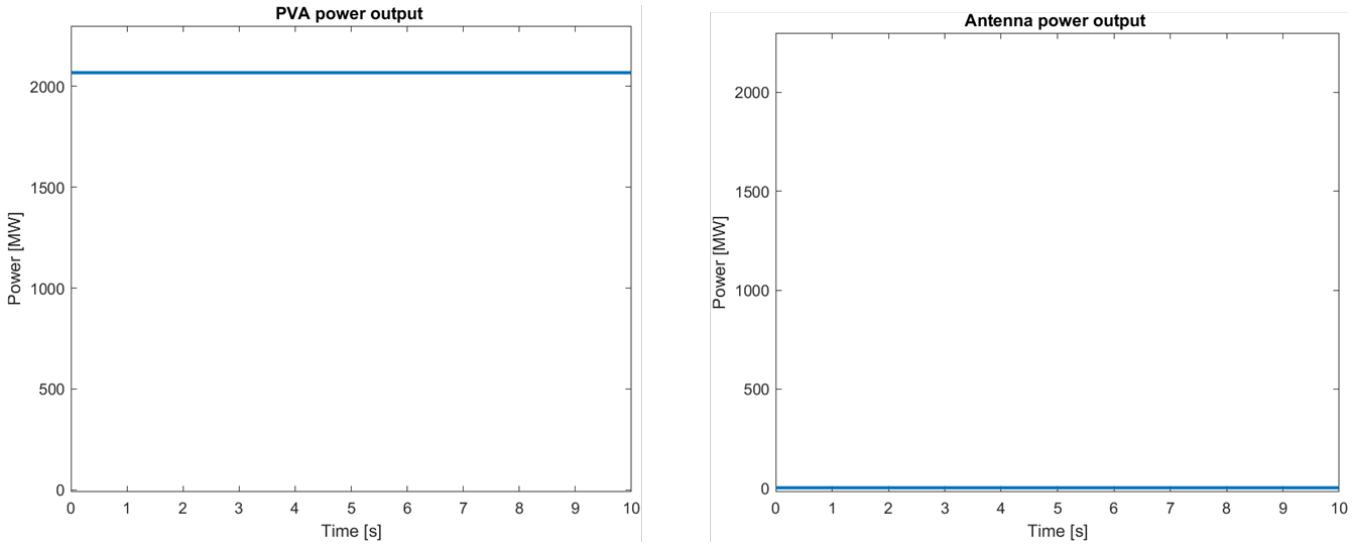

Figure 9-10 PVA power output (left) and antenna power output (right) during 10 seconds of SPS high misalignment

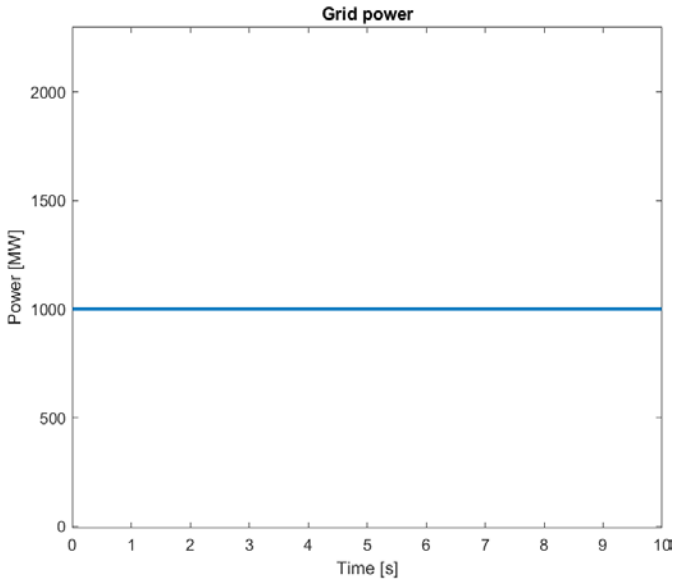

Figure 9-11 Grid power during 10 seconds of SPS high misalignment (compensated with super-capacitors)

10 Environmental Impact Analyses

Life Cycle Assessment (LCA) analysis is a comprehensive methodology used to evaluate the environmental impacts of a product, service, or system throughout its entire life cycle, from raw material extraction and production to use, and eventually disposal or recycling. When applied to a space-based solar power mission, LCA plays a crucial role in understanding the environmental implications of such a project. Here are some important considerations regarding the importance of conducting a preliminary LCA for a space-based solar power mission:

1. **Environmental Impact Assessment:** a preliminary LCA allows for the assessment of the potential environmental impacts associated with the entire life cycle of the space-based solar power mission. This includes the manufacturing of solar panels, launch and space operations, maintenance, and end-of-life disposal.

2. **Decision-Making Tool:** LCA provides essential information for decision-makers to understand the trade-offs and make informed choices. It helps in comparing different design and operational alternatives and identifying the most sustainable approach.

3. **Resource Efficiency:** analysing the life cycle helps in identifying opportunities to optimize resource use. This includes minimizing waste, reducing energy consumption, and choosing materials with lower environmental footprints.

4. **Mitigation of Negative Impacts:** early identification of environmental hotspots in the life cycle of a space-based solar power mission allows for the development of strategies to mitigate negative impacts, such as pollution, greenhouse gas emissions, or habitat disruption.

5. **Public Perception and Regulatory Compliance:** conducting an LCA can help enhance public perception by demonstrating a commitment to sustainability and environmental responsibility. It can also assist in complying with environmental regulations and international standards.

However, there are limitations when conducting a preliminary LCA without detailed information in the early phases of a project:

1. **Data Uncertainty:** preliminary LCA relies on estimates and assumptions, which can lead to a significant degree of uncertainty. The accuracy of the assessment increases with more detailed information becoming available as the project progresses.

2. **Incomplete Picture:** detailed data on specific materials, technologies, and processes may not be available during the preliminary phase, making it challenging to assess the entire life cycle accurately.

3. **Early Commitments:** decisions made based on a preliminary LCA can commit a project to certain technologies, designs, or processes that may not be optimal for sustainability. It is essential to remain flexible in the early phases.

4. **Limited Stakeholder Engagement:** A preliminary LCA might not capture all stakeholder concerns or values, as it is conducted before thorough stakeholder engagement. A more comprehensive assessment may be needed later in the project to incorporate these perspectives.

Additionally, the analysis will address potential risks related to EU regulations as REACH, RoHS, and CRM, promoting compliance and sustainability in the SBSP design and manufacturing.

In conclusion, conducting a preliminary LCA for a space-based solar power mission is essential for understanding and mitigating potential environmental impacts. While it has limitations due to data uncertainty and the incomplete picture of the project, it serves as a valuable tool for early decision-making and promoting sustainability. As the project progresses, more detailed and accurate LCAs should be conducted to refine sustainability strategies applying [AD2].

To obtain an initial approximation of the GHG parameter (greenhouse gas emission), it is necessary to conduct a preliminary evaluation of the CO_2 for SBSP deployment considering mainly material productions and launches. To achieve this, the energy expenses associated with the SBSP mission have been categorized into distinct macro-areas for estimation and the main formulas have been implemented into the parametric model used also for energy investment calculations.

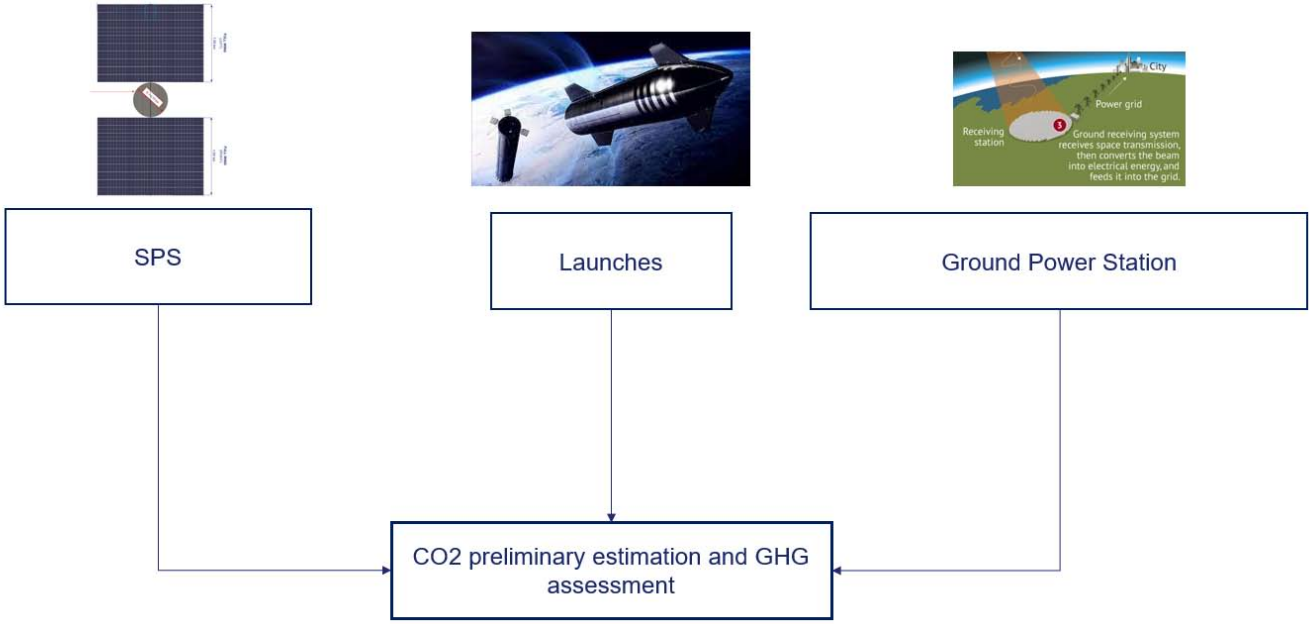

Figure 10-1 SBSP CO_2 production breakdown

10.1 Preliminary Assessment Of CO_2 Production For SBSP Mission

For what concerns the SPS, as for the energy investment calculations, it is plausible to assume that the platform predominantly consists of composites, aluminum or other more readily processed materials (60%), steel or materials akin to it (17%), silicon or similar materials (3%) and in the end perovskite for PV cells (20%). In particular, perovskite cells are surely greener solution when compared to other technologies such as Si-based solar panels.

With this foundation, considering the appropriate CO_2kg_{eq}/kg for every material, it is possible to calculate the preliminary estimated CO_2 production for the SPS parts production.

CO_2 for SPS materials production	**270 kt_{eCO2}**

Table 10-1 SPS materials production

The Ground Power Station, weighting approximately 2 kg per square meter, includes a steel mesh, minimal electronic components (e.g., diodes), and power cabling. For a 1 GW ground power station covering an area of approximately 25 km², this results in an estimated receiver mass of approximately 48000 tons. To simplify the calculation and avoid delving into intricate details, it is possible to assume that the GPS is primarily composed of steel or materials resembling it (80%), aluminum or other more easily processed materials (19%), and silicon or similar materials (1%). With this hypothesis, the CO_2 for the GPS materials production can be straightforwardly computed.

CO_2 for GPS materials production	**150 kt_{eCO2}**

Table 10-2 GPS materials production

Considering the input values provided by RFA as input to this study [RD31] it is possible to estimate the total amount of CO_2 for launches, which is the predominant factor.

CO_2 for Launches	**12109 kt_{eCO2}**

Table 10-3 Launches

10.2 Greenhouse Gas Emission Estimation For CO_2

Taking into account these preliminary evaluations, it is possible to calculate a first estimate of the GHG parameter for CO_2. This is evaluated as the total amount of CO2 divided for the energy provided during the entire SPS lifetime.

CO_2 for SBSP deployment	**12527 kt_{eCO2}**
GHG (CO_2)	56 g_e/kWh

Table 10-4 GHG emission estimation

The preliminary result obtained is surely compatible with other energy sources already avaible on the market.

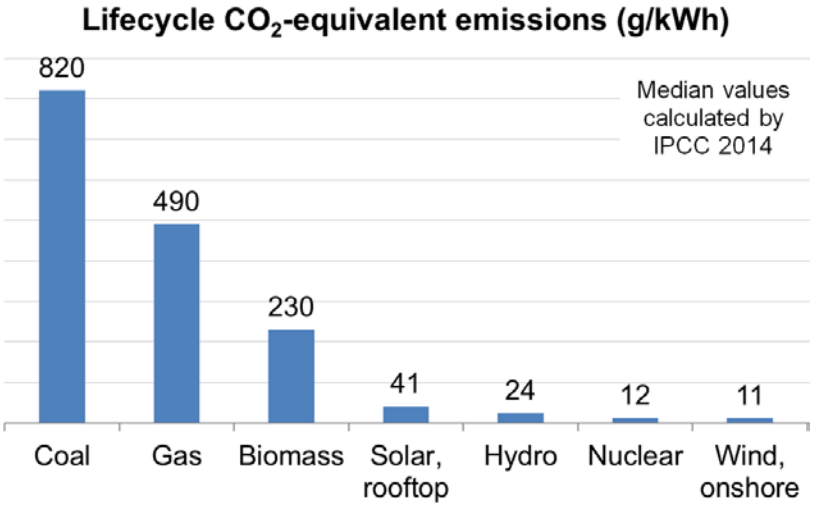

Figure 10-2 : GHG for other energy sources

Obviously, also this parameter, as the LCOE and the EROEI estimated previously, is sensitive to different values. In particular, two sensitivity analysis have been performed to assess the impact of SPS lifetime and SPS performance degradation ratio (%/year) on the GHG of CO_2, which are the main two parameters for the calculations of total energy delivered for an SBSP mission.

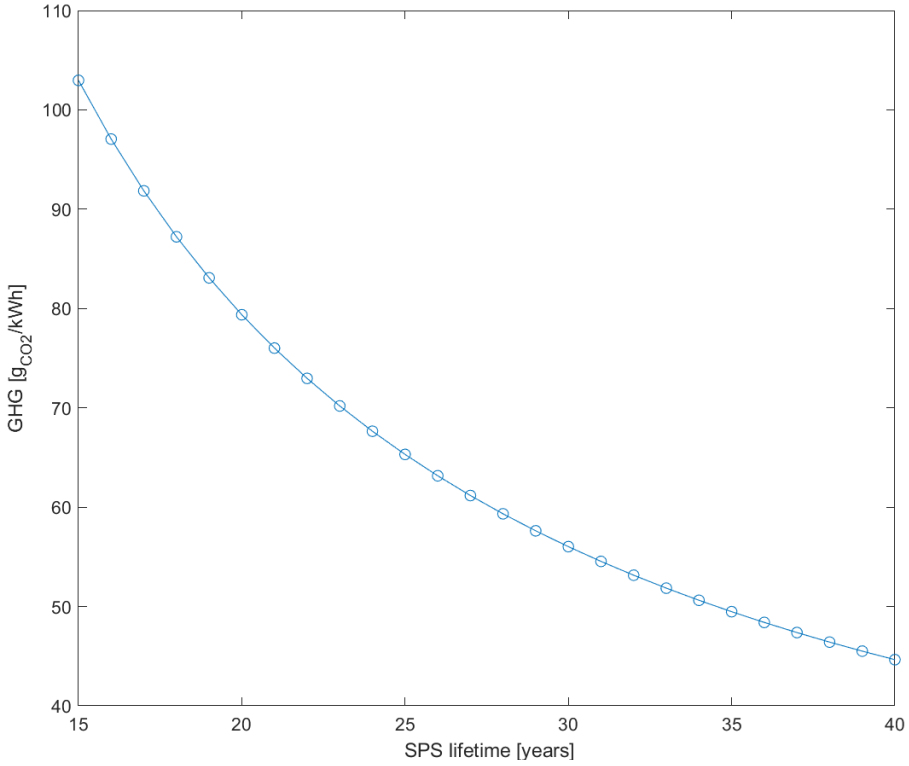

Figure 10-3 GHG of CO_2 as a function of SPS lifetime

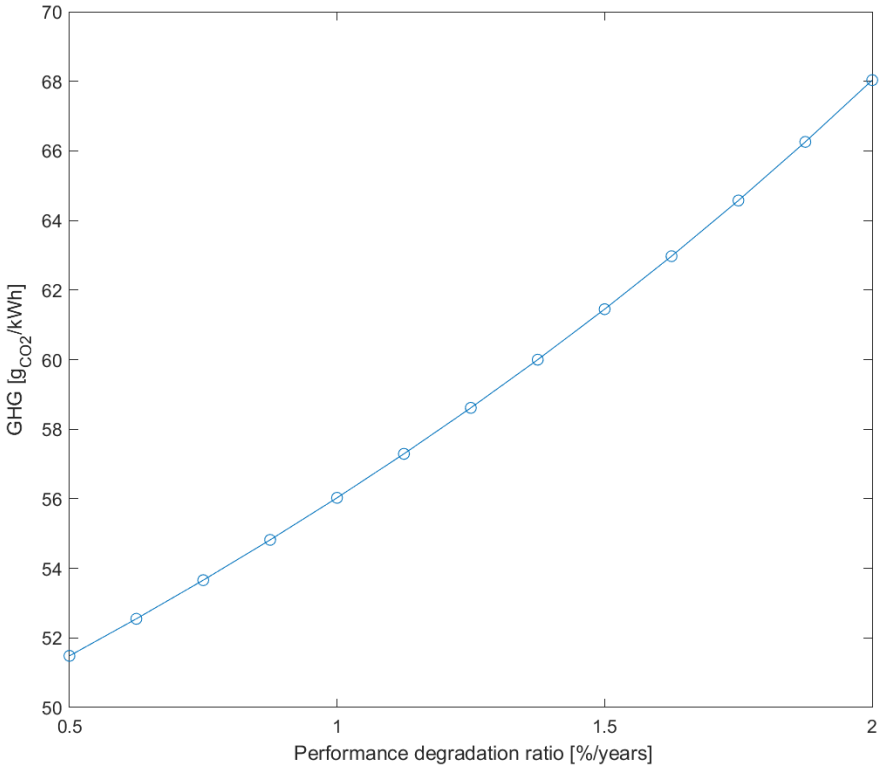

Figure 10-4 GHG of CO_2 as a function of performance degradation ratio

11 Energy & System Cost Analyses

All the cost evaluations reported in this chapter are based on assumptions taken from the relevant literature, including the cost-benefit analysis documents provided by ESA as input of the study (e.g. SOW RD1 and RD2). This cost assessment is not to be considered as a commitment on the part of Thales Alenia Space.

11.1 Methodology For SBSP Preliminary Cost Assessment

Many cost estimation methodologies employ mass-based (referred to as 'weight-based') cost estimation relationships (CERs), like the 'cost per kilogram' for a specific system or module. These CERs are influenced by various factors, including design complexity, similarities to other technologies and systems, etc.

Referring to the baseline CER mentioned above, the industrial history of the 20th century shows that, for a regularly produced item, there is a statistical correlation between the quantity of units manufactured and the anticipated change in the initial CER (for a single unit) as production quantities increase. This phenomenon, initially observed by Wright while employed at the Boeing Aircraft Company in the 1930s, is commonly referred to as the 'learning curve' (LC) or 'manufacturing curve.'

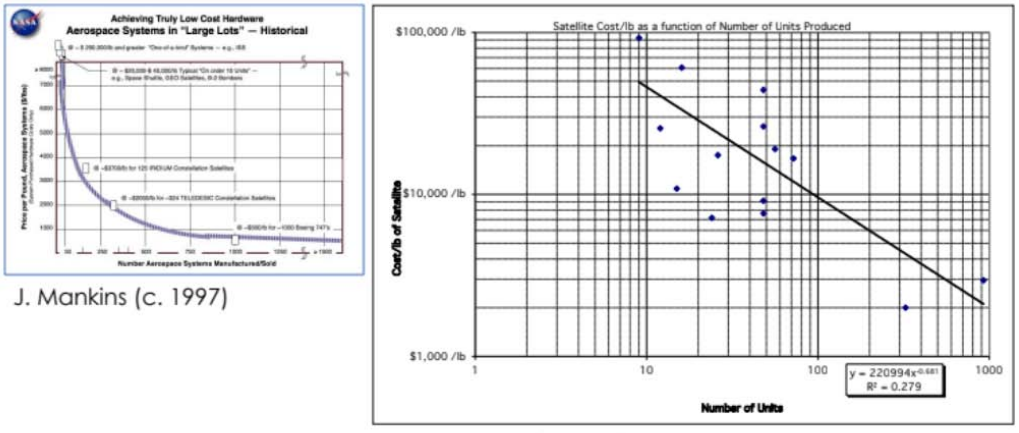

Figure 11-1 Examples of learning curve approach in space applications

The learning curve is a mathematical relationship that takes into account productivity improvement for larger number of produced units considering cost reductions due to the economics of scale, setup time and human learning as the number of units increase. The total production cost for N units (as showed in Figure 11-1) is modelled as follows [RD2]:

$$\text{Production Cost} = \text{TFU x L}$$

$$L = N^{B}$$

$$B = 1 - \frac{\ln(\frac{100\%}{S})}{ln2}$$

Where:

- TFU: Theoretical first unit cost;
- L: Learning curve factor;
- S: Learning curve slope, represents the percentage reduction in cumulative average cost when the number of production is doubled (it depends on the number of equal items is considered).

This approach, already used in several cost assessment for SBSP missions [RD1] [RD2], is the most suitable when considering very big and complex systems.

The SBSP mission costs can be divided in four areas as shown below.

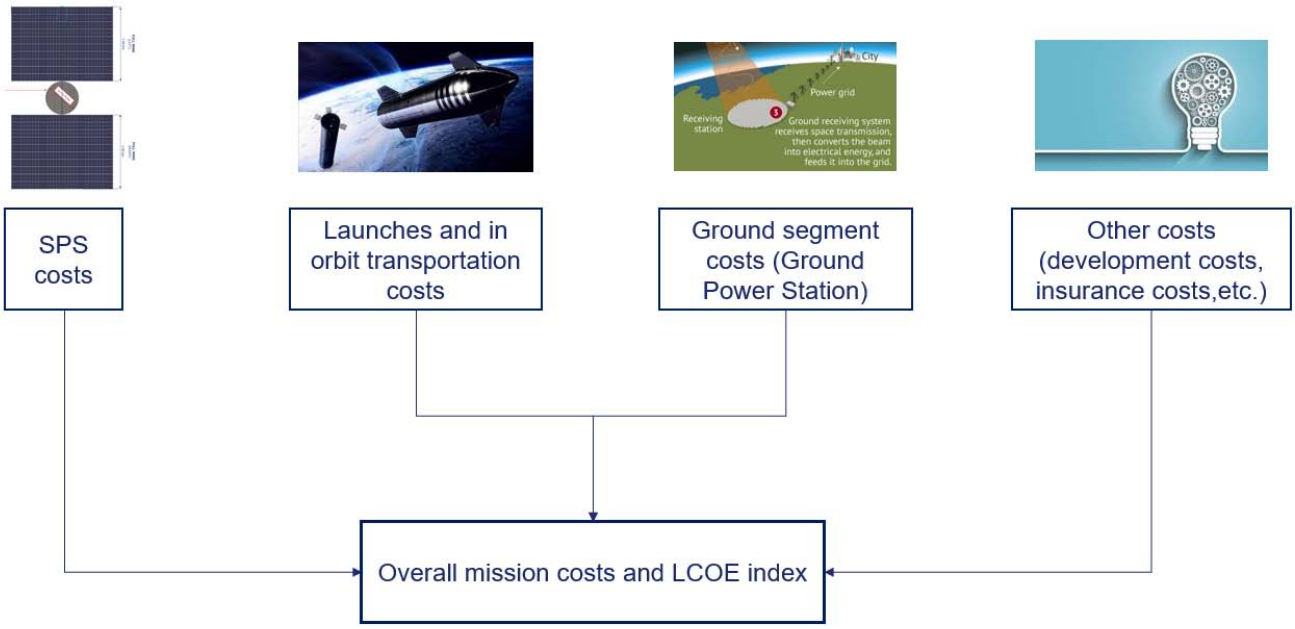

Figure 11-2 High level cost division

11.2 Costs Breakdown

The four main cost areas have been analyzed considering for each area the different subdivisions and specializations. All the relationships have been implemented in a parametric cost model (integrated within the SBSP Analysis Framework) allowing different sensitivity analysis for the main parameters affecting the overall mission costs.

Regarding the SPS costs, an high-level bottom-up approach has been utilized to estimate the cost of each component type comprising the entire SPS.

Various cost estimation relationships (CERs) as cited in [RD1] and [RD2] have been used to evaluate the expenses associated to each unit type. Subsequently, the learning curve approach has been applied to derive an overall cost for each group of similar units within the system (which are listed in Table 11-1).

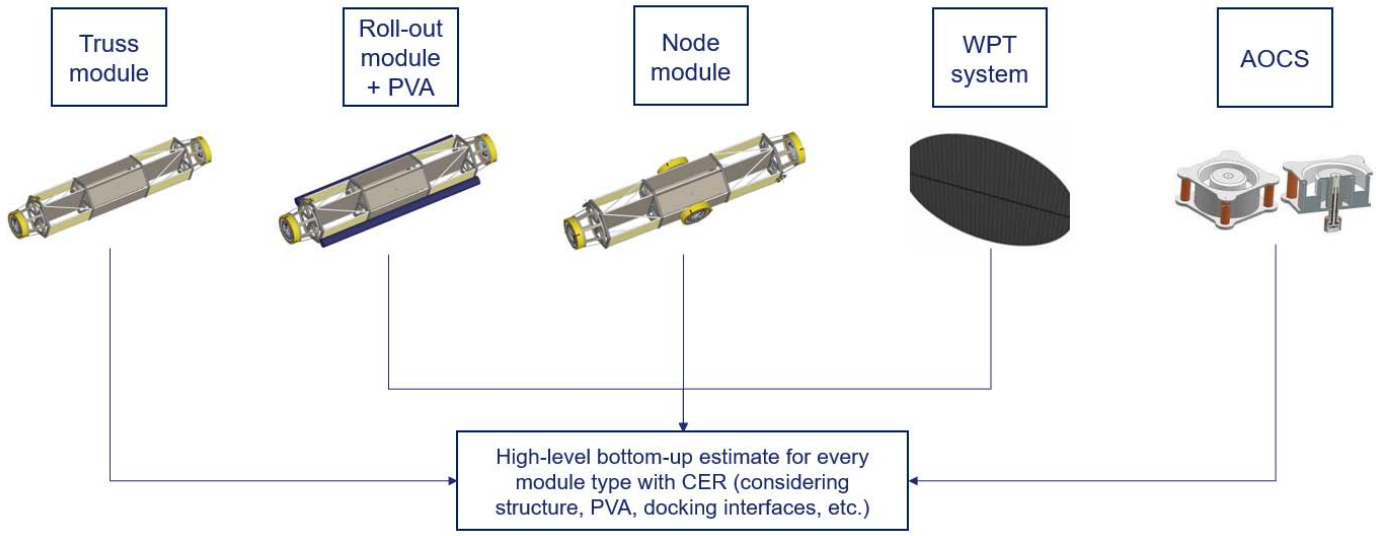

Figure 11-3 Main unit groups composing the SPS system

Unit Group	Cost
Truss modules	0.01 B$
Roll-out modules (with PVA)	0.18 B$
Node modules	0.002 B$
WPT system	0.50 B$

AOCS	1.43 B$
SPS cost	**2.06 B$**

Table 11-1 Summary results for SPS costs

Launch costs are, on the other hand, one of the crucial cost areas, contingent upon the assumptions under consideration. Extensive sensitivity analyses have been conducted in the relevant section to account for various parameters that could substantially influence launch expenses. A few notable factors include:

- Launch cost per kg [$/kg];
- Usable volume of the launcher fairing (considering 100 tons of maximum mass capability);
- Orbital tug mass;
- Type of manoeuvre considered for LEO-GEO transfers (impulsive or continuous);
- Specific impulse of propellant considered for the LEO-GEO transfer.

Launch costs	**3.31 B$**

Table 11-2 Launch costs

This value is computed considering the following assumptions on the driving parameters listed before:

- Launch cost per kg = 200 $/kg;
- Usable volume of the launcher fairing (considering 100 tons of maximum mass capability) = 100 %;
- Orbital tug mass = 60% of the launcher transportable mass;
- Type of manoeuvre considered for LEO-GEO transfers = continuous;
- Specific impulse of propellant considered for the LEO-GEO transfer = 1000 s (it could be possible considering higher values, however the assumption would be very strong in particular when considering time constraints in the problem for in-orbit transportation and assembly).

For in-orbit transportation from LEO to GEO a cost per kg of 100$/kg for the orbital tug utilization is estimated.

In-orbit transportation costs	**1.65 B$**

Table 11-3 In-orbit transportation costs

For Ground costs a series of values have been considered in order to compute the final cost. The most relevant are:

- Land occupation costs

- Rectenna mesh costs
- GPS power control costs

Ground costs	**682 M$**

Table 11-4 Ground costs

Finally, a list of other costs are included in the SBSP cost model such as:

- Insurance costs (considering both launch insurance and satellite insurance [RD1]);
- OM costs (the yearly operational expenses of the system comprise two components: ground operation and satellite operation. These expenses are determined by applying the O&M Factor to the respective construction costs. [RD1]);
- AOCS refuelling launches;
- Assembly costs (considering a $/kg relationship for every robotic system needed on-board for assembly).

Other costs	**3.66 B$**

Table 11-5 Other costs

11.3 Cost Assessment & LCOE Results

Considering the cost breakdown presented above and a plausible estimation for launch costs (which will be further elaborated in appropriated sensitivity analyses), the total cost for a FOAK (First Of a Kind) SBSP system has been evaluated.

Also the CAPEX (capital expenditure) and the OPEX (operational expenditure) have been estimated considering an appropriate cost grouping showed below with the correspondent values (see Table 11-6).

Parameter		Composition and value		
CAPEX	SPS costs	Truss module costs	0.01 B$	7.71 B$
		Roll-out modules (with PVA) costs	0.18 B$	
		Node modules costs	0.002 B$	

		WPT system costs	0.50 B$	
		AOCS costs	1.43 B$	
	Launch and in-orbit transportation/assembly costs	Launch costs	3.31 B$	
		In-orbit transportation costs	1.65 B$	
		Robotic hardware costs for assembly	0.004 B$	
	GPS costs	Land occupation costs	0.06 B$	
		Rectenna mesh costs	0.17 B$	
		GPS power control costs	0.36 B$	
OPEX	Insurance costs		1.7 B$	3.66 B$
	OM costs		1.6 B$	
	AOCS thrusters refueling costs		0.36 B$	
TOTAL SBSP MISSION COST	**11.4 B$**			

Table 11-6 : Cost assessment results

Considering these values, the LCOE was calculated, and its fluctuations have been scrutinized in response to changes in the primary cost-driving parameters.

The levelized cost of electricity (LCOE) serves as a metric to assess the average net present cost of electricity generation for a given generator throughout its operational life. It proves very useful for investment planning and facilitates a consistent basis for comparing various electricity generation methods.

$$\mathrm{LCOE} = \frac{\text{sum of costs over lifetime}}{\text{sum of electrical energy produced over lifetime}}$$

While the sum of costs over lifetime has already been discussed, the total amount of energy produced over lifetime has not been discussed yet.

Considering a BOL (beginning of life) power delivered of 1 GW 24/7/365 (apart from the very short eclipse periods) and 30 years of SPS lifetime (UR-REQ-0070), the annual performance degradation rate has been estimated to 1% in order to have a plausible estimate of the evolution of power produced over this timespan. This value has been considered due to:

- 0.1-0.5 %/year expected radiation degradation ratio for perovskite cells (ref. TN3). This value is based on recent laboratory tests assessing perovskite radiation resistance. Notably, research conducted by Sydney University highlights the remarkable potential and viability of "self-recovery" in perovskite cells through the strategic use of specific dopants. The selection of the right dopant could have the dual benefit of limiting radiation damage and enabling cells to undergo a "self-healing" process through TV treatment, ultimately restoring their Power Conversion Efficiencies (PCEs), as documented in [RD27]. Further exploration of this potential could mark a pivotal moment in PV space applications, such as SBSP, by curbing the rate of system performance degradation;
- Possible system failures, debris impacts or space weather events, which could affect system performances. However, it is to be expected that a fully developed system will have a comprehensive in-orbit maintenance and resupply programme. This should be fundamental to reduce the impact on system capacity factor in a long lifespan such as the one considered for an SPS.

According to the above considerations and given the assumptions taken for system costs (further LCOE sensitivity analyses will be showed in the paragraph 11.6) the following results are obtained for a FOAK SBSP system:

Parameter	Value	
Expected energy generated over the system lifetime	Lifetime = 30 years 1 %/year degradation rate 1 GW 24h 365 days BOL	**223.4 TWh**
LCOE	**158 $/MWh (≈ 15.8 ¢/kWh)**	

Table 11-7 : Total energy delivered and LCOE results

The LCOE for the 10th of a kind SBSP system is also computed and reported in Table 11-8

Parameter	Value
LCOE for the 10th of a kind SBSP system	**143 $/MWh (≈ 14.3 ¢/kWh)**

Table 11-8 : LCOE result for 10th of a kind system

The resulting LCOE are calculated using a 15% discount rate, a reasonable choice given the complexity and uncertainties associated with the SBSP project. Nonetheless, a dedicated sensitivity analysis will be performed to assess the impact of this value, considering that various studies have explored a range of discount rates from 10% [RD2] to 20% [RD1].

A discount rate is a financial metric used to evaluate the present value of future cash flows or benefits. It represents the rate of return required to make an investment or project's net present value equal to zero. In other words, it reflects the opportunity cost of allocating resources to a specific project or investment rather than pursuing alternative opportunities with a similar level of risk. The discount rate is a critical component in financial decision-making, cost-benefit analysis, and investment appraisal, helping to account for the time value of money and assess the attractiveness of an investment or project over time. It is typically expressed as a percentage or a decimal.

The results obtained for the LCOE are competitive with respect to other energy sources now available:

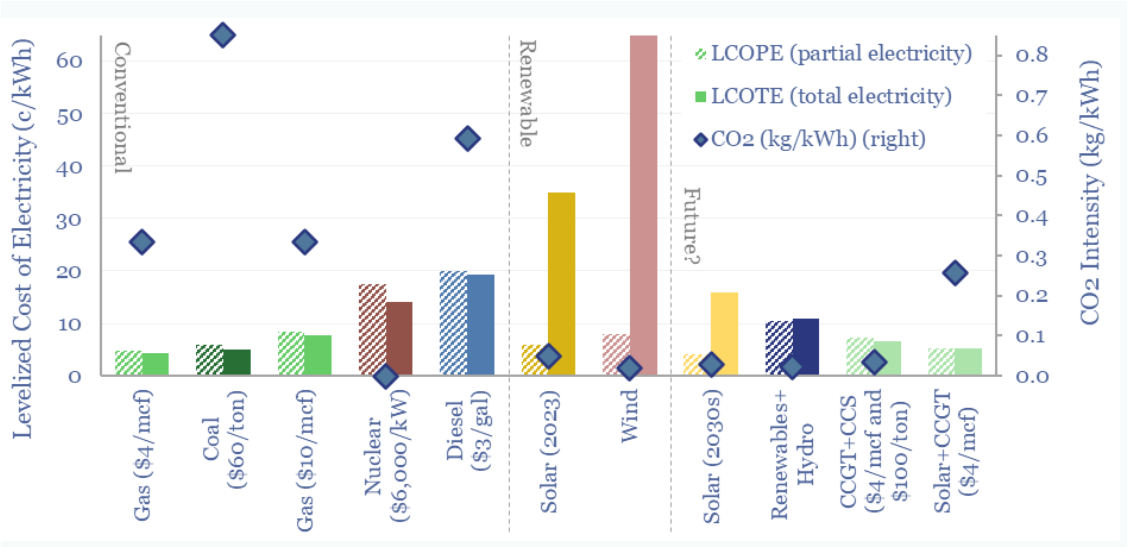

Figure 11-4 : LCOE/CO2 of several energy sources (Credits: Thunder Said Energy)

11.4 FOAK vs NOAK System Costs

To attain the baseload objectives for achieving net zero emissions in Europe by 2050, multiple SBSP system need to be deployed. It is reasonable to anticipate that, as the number of SPS deployed increases, the cost per satellite is likely to decrease so as the cost per SBSP mission.

The learning curve approach has been applied to assess a preliminary estimation of what could be the cost for an n-of-a-kind (NOAK) system with respect to a first-of-a-kind (FOAK), which have been calculated in the section 11.3. The slope of the curve applied for these calculations is 0.90 [RD2], which is a credible assumption based on the experience gained from more than 10 SPS deployments. Consequently, for cases involving fewer than 10 systems, a slightly more conservative curve slope of 0.95 has been adopted (see Table 11-9). For what concerns the cost per SBSP mission for the NOAK, the learning curve is applied only to the hardware costs (and not for example launch or orbit transportation costs).

Number of SPS	Cost per SPS [B$]	Cost per SBSP mission [B$]
1	2.06	11.4
5	1.81	11.0
10	1.43	10.5
30	1.25	10.3
50	1.15	10.1
86	1.05	10

Table 11-9 Results of learning curve approach for multiple SPS deployment

11.5 Energy Investment & ERoEI assessment

After having calculated the energy delivered during SPS lifetime, a critical performance indicator for sustainable energy systems revolves around the speed at which the energy needed to manufacture and install the system can be recovered once the system becomes operational; this metric is commonly referred to as the "energy payback time" (EPBT).

Furthermore, the comprehensive energy commitment required to establish a SBSP mission in comparison to the energy yield over the SPS's operational lifespan serves as a pivotal measure for evaluating the feasibility of the concept in relation to alternative energy sources. This parameter is commonly known as ERoEI (Energy Return on Energy Invested). This value is a derivation of the RoI economic parameter for energy investment applications.

To obtain an initial approximation of these two metrics, conducting an essential preliminary evaluation of the energy investment for SBSP is imperative. To achieve this, the energy expenses associated with the SBSP mission have been categorized into distinct macro-areas for estimation and the main formulas have been implemented into the parametric cost model (see Figure 11-5).

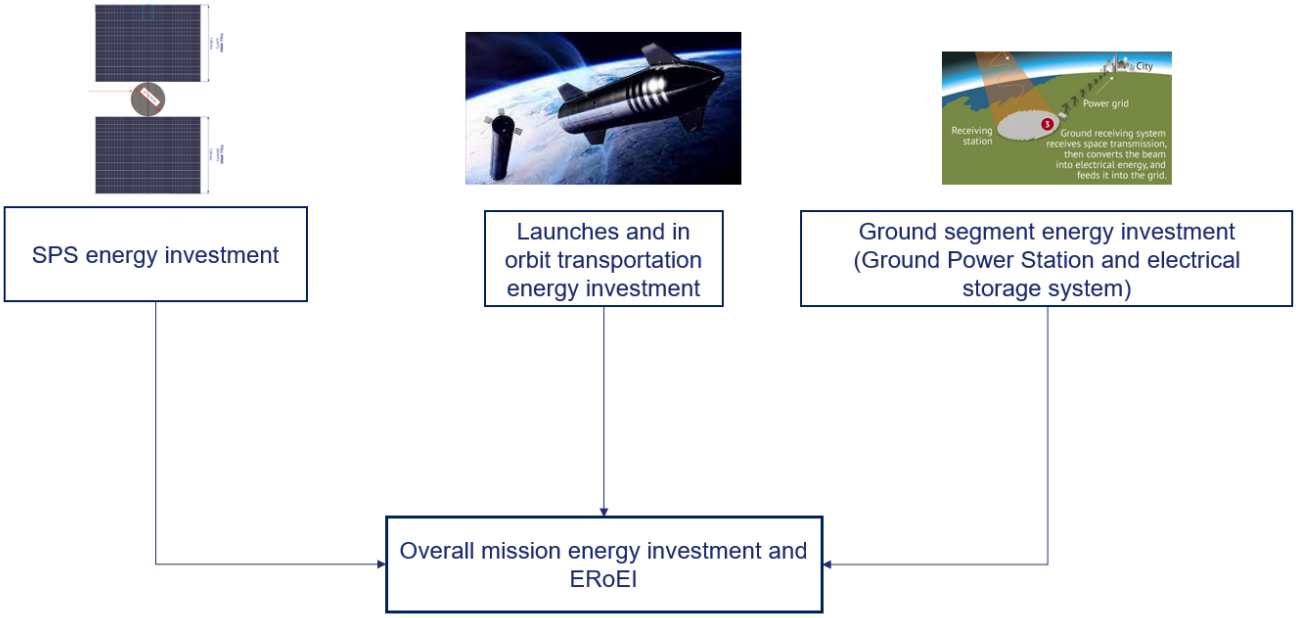

Figure 11-5 SBSP energy investment breakdown

For what concerns the SPS, without delving into intricate specifics, for the purpose of this computation, it is plausible to assume that the platform predominantly consists of composites, aluminum or other more readily processed materials (60%), steel or materials akin to it (17%), silicon or similar materials (3%) and in the end perovskite for PV cells (20%).

With this foundation, considering the appropriate kWh/kg for every material, it is possible to calculate the estimated energy cost for SPS.,

SPS energy investment	**789 GWh**

Table 11-10 SPS energy investment

The Ground Power Station, weighting approximately 2 kg per square meter, includes a steel mesh, minimal electronic components (e.g., diodes), and power cabling. For a 1 GW ground power station covering an area of approximately 34 km², this results in an estimated receiver mass of approximately 70000 tons. To simplify the calculation and avoid delving into intricate details, it is possible to assume that the GPS is primarily composed of steel or materials resembling it (80%), aluminum or other more easily processed materials (19%), and silicon or similar materials (1%). With this hypothesis, the estimated energy cost for the GPS can be straightforwardly computed.

GPS energy investment	**3209 GWh**

Table 11-11 GPS energy investment

In the available literature, it is well documented that the production of each kilowatt-hour (kWh), equivalent to approximately 10 kg of Lithium-Ion battery, requires around 55-65 kWh of energy. For a system with the capacity to store approximately 1,120,000 kWh (equal to 1 GW for 71 minutes, the maximum duration of shadowing of GEO at the Equinox) the energy investment can be calculate with the previous numbers.

Electrical storage system energy investment	**58 GWh**

Table 11-12 ESS energy investment

As mentioned earlier, the cost model includes a dedicated section aimed at assessing the number of launches required for the entire payload and the propellant necessary for transferring and assembling the SPS in GEO. This evaluation takes into account various inputs such as the type of maneuver for LEO-GEO transfer, specific impulse, and the mass of the propulsion system.

Utilizing the preliminary estimation, and considering Methane and LOX as the launch propellants (with quantities of 1000 tons and 3600 tons per launch for a heavy reusable two-stage launcher with a maximum cargo capacity of 100 tons), along with the established energy content values for these propellants in kWh, the launch energy investment required has been estimated. This calculation is based on the total number of launches and follows the same assumptions applied in calculating the LCOE.

Launches energy investment	**3179 GWh**

Table 11-13 Launches energy investment

Finally, the last energy investment area is the in-orbit transportation. It is plausible to consider the kinetic energy of every single transfer from LEO to GEO (about 4.5 km/s for Edelbaum approximation in case of continuous maneuver) of the orbital tug with the correspondent payload and an inefficiency of about 50% of the overall energy produced. Considering this approach, it is possible to have a preliminary estimate of the in-orbit transportation energy investment needed (considering the same assumptions as for the LCOE calculations).

In-orbit transportation energy investment	**62 GWh**

Table 11-14 In-orbit transportation energy investment

After having analyzed the entire energy cost breakdown, the main results are showed below:

Parameter	Formula	Value

SBSP Energy investment (e.i)	SPS e.i + GPS e.i + Electrical storage system e.i + Launches e.i + In-orbit transportation e.i	**7.30 TWh**
EPBT	SBSP Energy investment / Energy delivered per day	**300 days**
ERoEI	SBSP Energy returned / SBSP Energy investment	**31: 1**

Table 11-15 Final energy analyses results

With respect to other renewable technologies such as PV farms, the EPBT is minimal, making clear the possible advantages of SBSP and its economic potential:

Energy Investment Item	Winter Case (Overcast 7 day)	Summer Case (Overcast 1 day)
Ground PV System		
PV Array	– 756,800,000,000 kWh	– TBD kWh
Energy Storage System	– 336,000,000 kWh	– TBD kWh
Energy Produced per Day	+ 48,000,000 kWh / day	+ 48,000,000 kWh / day
Energy Payback Time	~40 Years	~6 Years

Figure 11-6 EPBT example for solar farms on Earth

11.6 Cost & Energy Investment Sensitivity Analyses

The LCOE value presented for our SBSP concept is very sensitive to certain parameters, which make the final mission costs quite complex to assess.

For this reasons, it becomes fundamental to have some cost sensitivity analysis taking into account the main cost driving parameters and the ones with the largest uncertainty. These parameters are listed below (with the respective plausible ranges) and a sensitivity analysis have been performed for each one:

- SPS mass [20% +100%] (with respect to baseline mass)
- Usable volume of the launcher fairing : [10% - 100%];
- Tug mass percentage with respect to transportable mass : [10% - 200%];
- Tug propulsion system specific impulse [400 s – 3000 s];
- Specific cost per launch [100 $/kg – 1500 $/kg];
- System Lifetime [15 years – 40 years];
- Performance degradation rate during SPS lifetime [0.1% - 2%];
- Learning curve slope for roll-out module group cost estimation [0.75 - 0.95];

- Discount rate [10% - 20%].

In the following sensitivity analyses the LCOE and/or ERoEI variations w.r.t. the parameters listed above will be shown in a graph. When selecting a parameter to be analyzed the others will be fixed according to the assumptions reported in section 11.2 and 11.3.

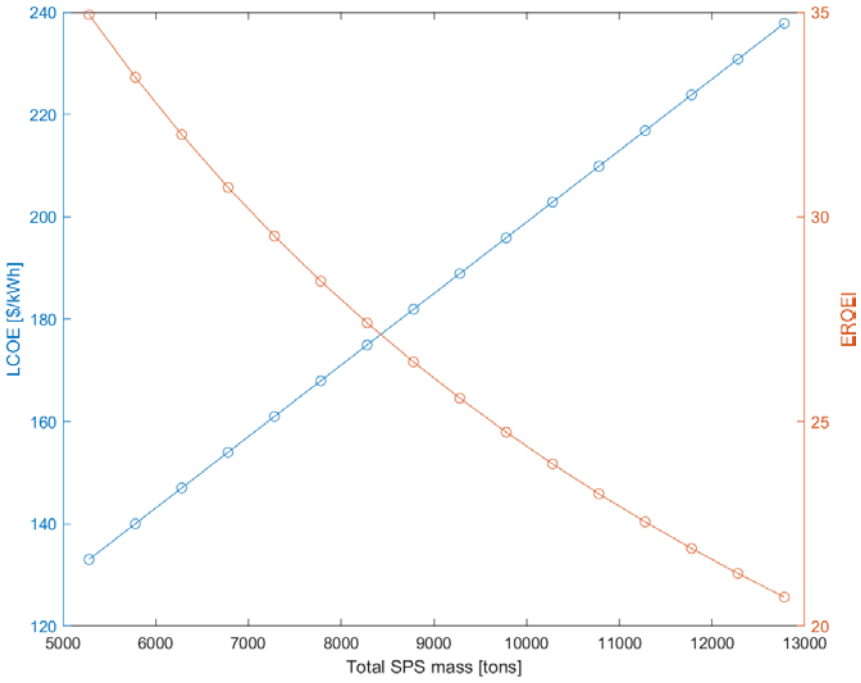

Figure 11-7 LCOE and EROEI as functions of SPS mass

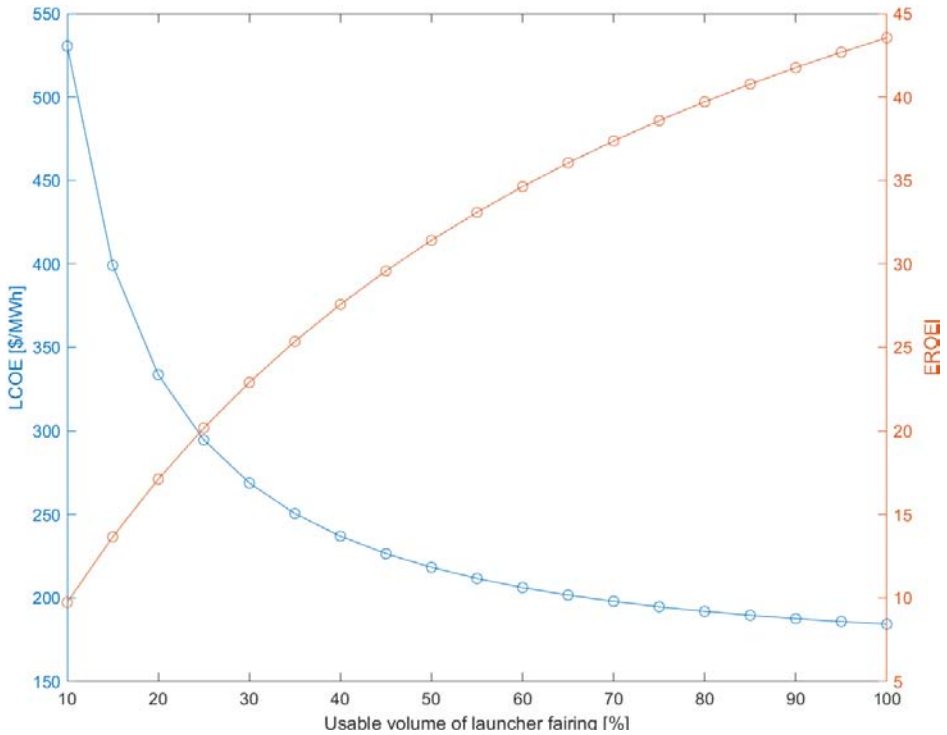

Figure 11-8 LCOE and EROEI as functions of usable volume of the launcher fairing

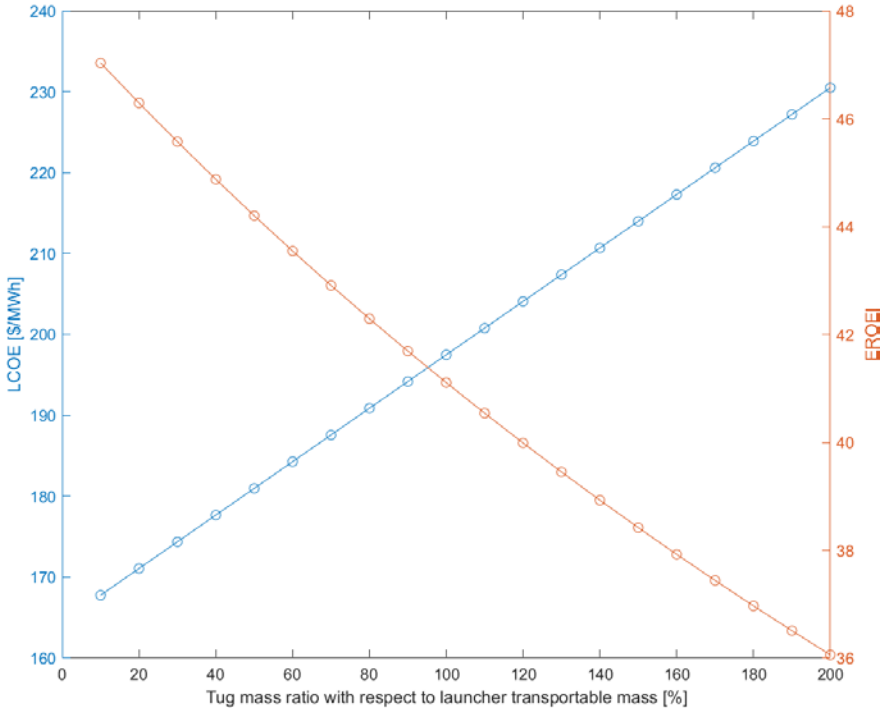

Figure 11-9 LCOE and EROEI as functions of Tug mass ratio with respect to transportable mass

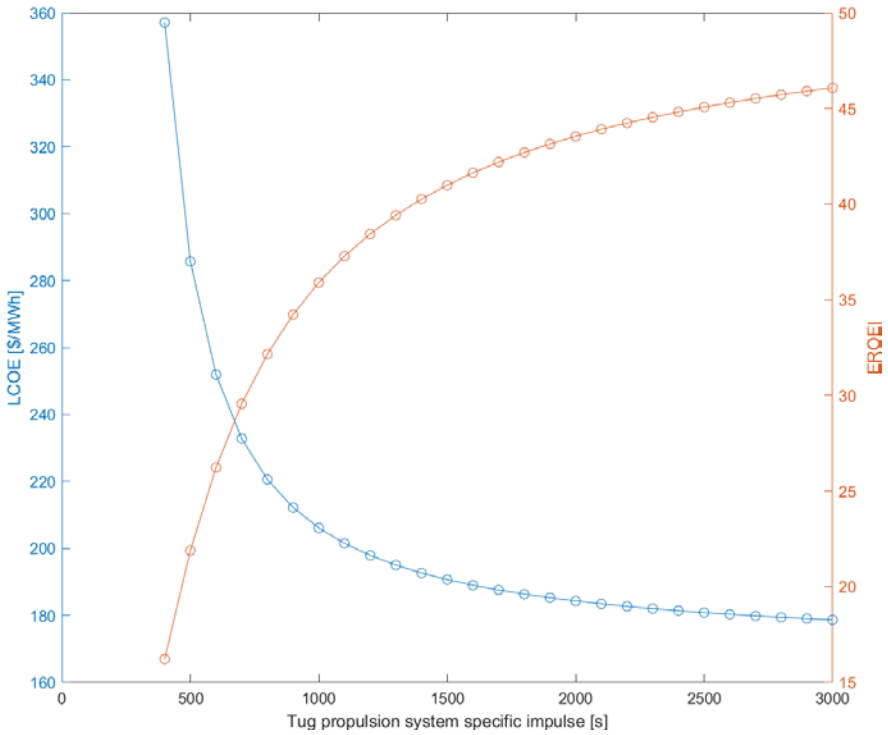

Figure 11-10 LCOE and EROEI as functions of Tug propulsion system specific impulse

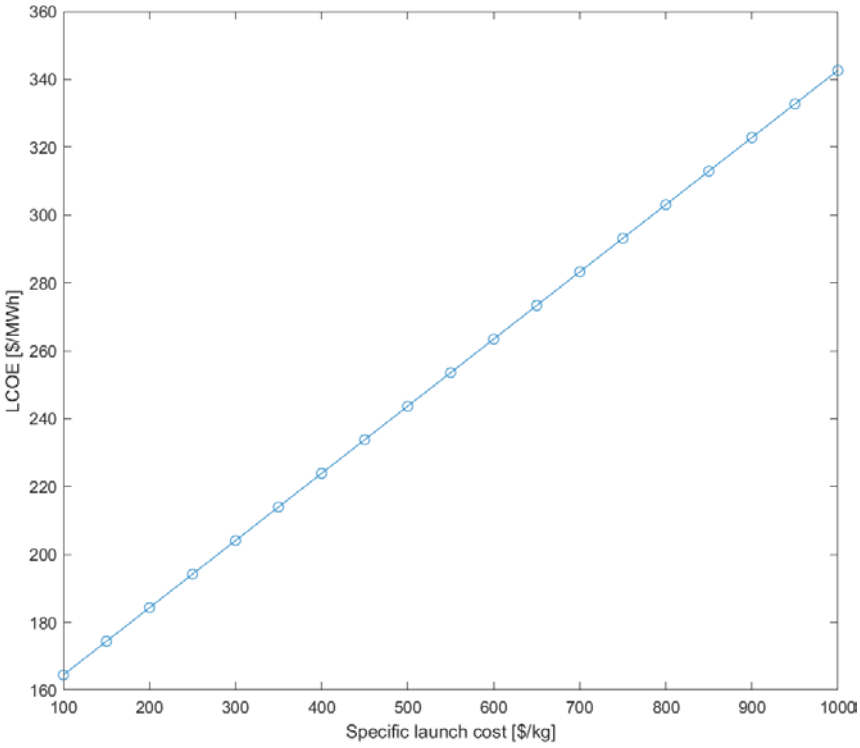

Figure 11-11 LCOE as a function of specific cost per launch (considering launch cost to LEO)

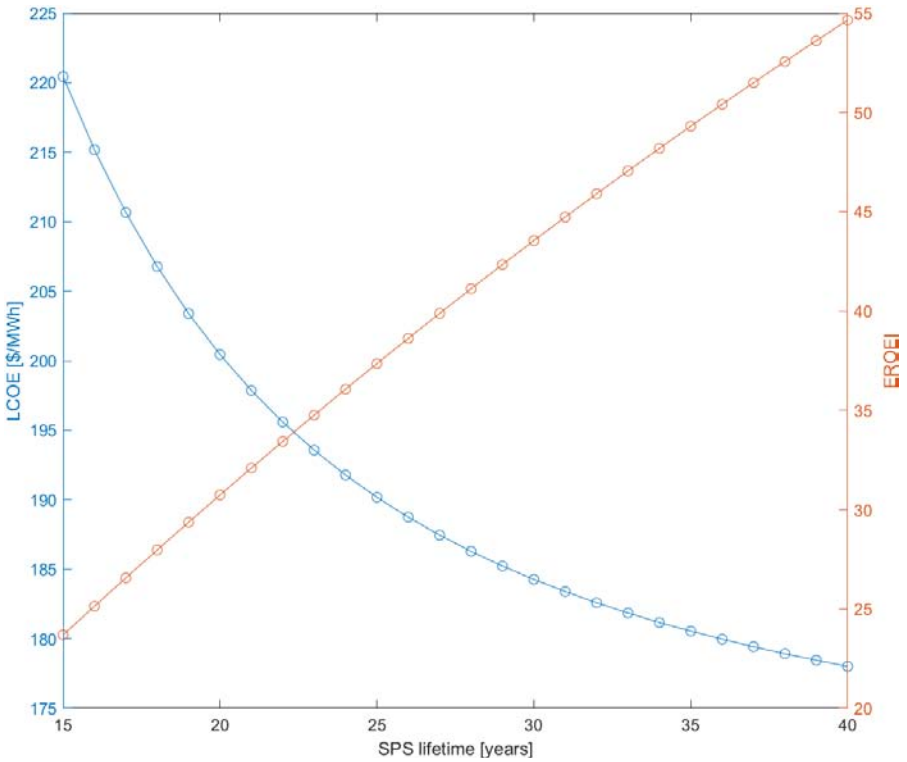

Figure 11-12 LCOE and EROEI as functions of SPS lifetime

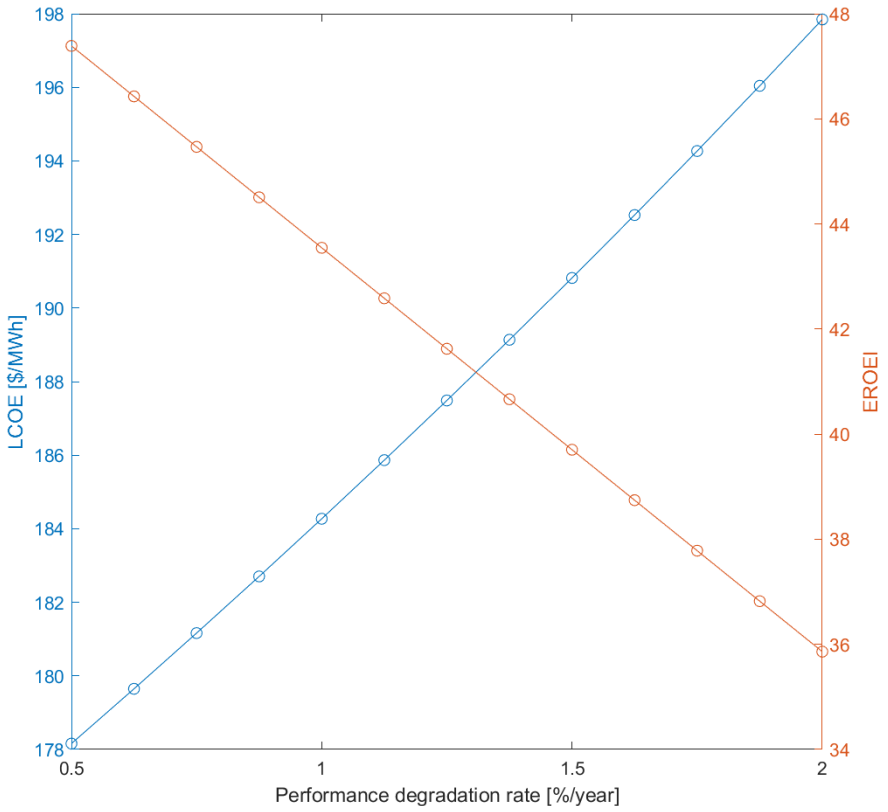

Figure 11-13 LCOE and EROEI as functions of SPS performance degradation rate

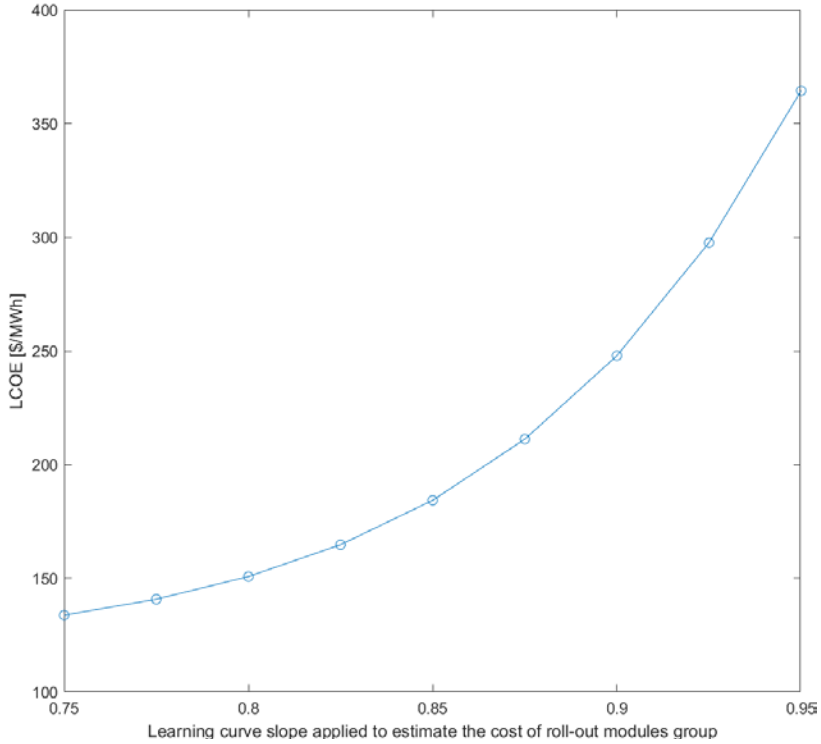

Figure 11-14 LCOE as a function of learning curve slope applied to estimate the cost of roll-out modules group

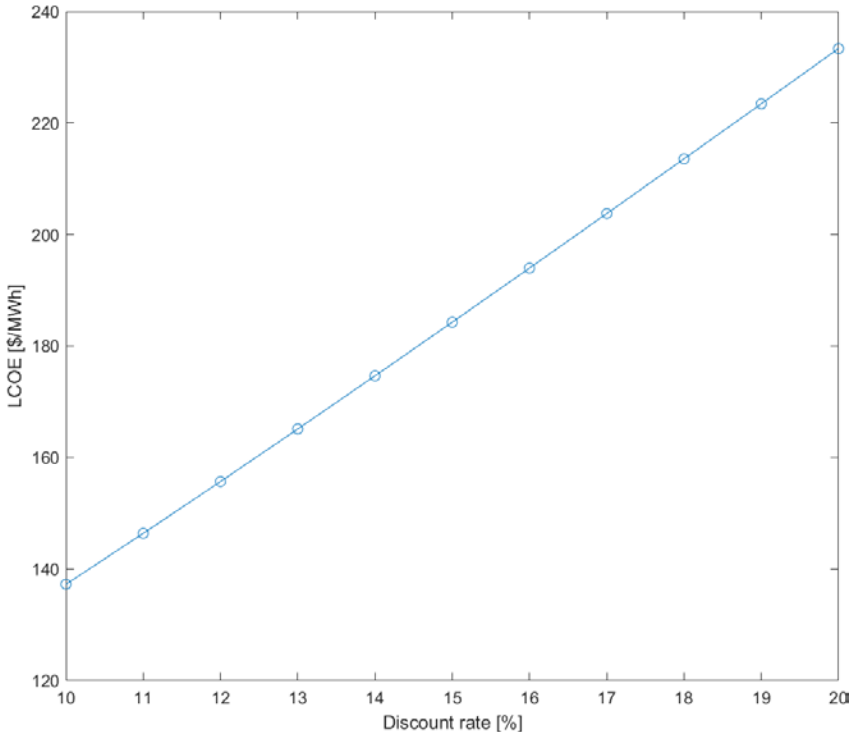

Figure 11-15 LCOE as a function of discount rate

12 Programmatic Aspects

12.1 Business Case Confirmation

The System proposed is compliant with the reference use case agreed with the stakeholders and reported in the TN1 section 3.3. Moreover the competitive LCOE proves that the technology can be technically and economically viable in the future energy mix.

12.2 SBSP Roadmap

The SBSP development roadmap towards a commercial scale SBSP system development, including major demonstrators along the way, proposed by our Consortium is shown in Figure 12-1.

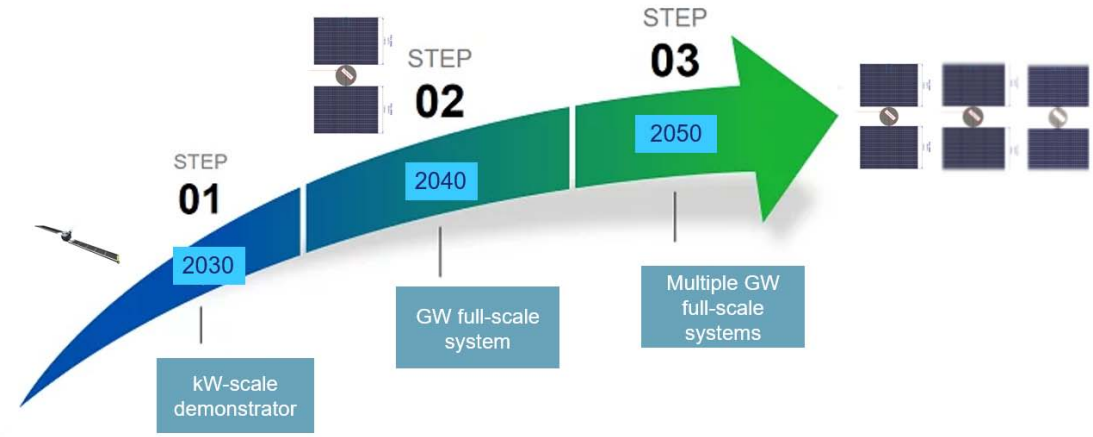

Figure 12-1: SBSP Roadmap

12.3 Risk Management

“Risks are a threat to project success because they have negative effects on the project costs, schedule and technical performance, but appropriate practices of controlling risks can also present new opportunities with positive impact. The objective of project risk management is to identify, assess, reduce, accept, and control space project risks in a systematic, proactive, comprehensive and cost effective manner, taking into account the project’s technical and programmatic constraints” [RD25].

The objective of the SBSP risk management is to identify risks and propose actions to mitigate these risks.

In order to improve the identification and further processing of the risks the following source of risks and risk domains are identified:

Source of risks:

1. Procurement;
2. Program Schedule;
3. Technical.

Risk domains:

- Performance Impact;
- Schedule Impact;
- Cost Impact.

12.3.1 Risk Management Process

The risk management process is performed within the project management structure during the life cycle of the project, ensuring a systematic identification, assessment and follow-up/reduction of risks.

The risk management is implemented as a team effort, with tasks and responsibilities being assigned to the functions and individuals within the project industrial organization on the basis of the relevant expertise in the areas concerned by a given risk. The results of the risk management process are considered in the routine project management process and in the decisions relative to the project baseline evolution.

Risk management is an iterative process that will be applied during the whole SBSP Project Life Cycle. The steps of the risk management process consist of the following main activities:

- Identification of the risks;
- Assessment of the risks;
- Acceptability evaluation of the risks;
- Reduction of the risks, performed by mitigation actions;
- Monitoring and Communication.

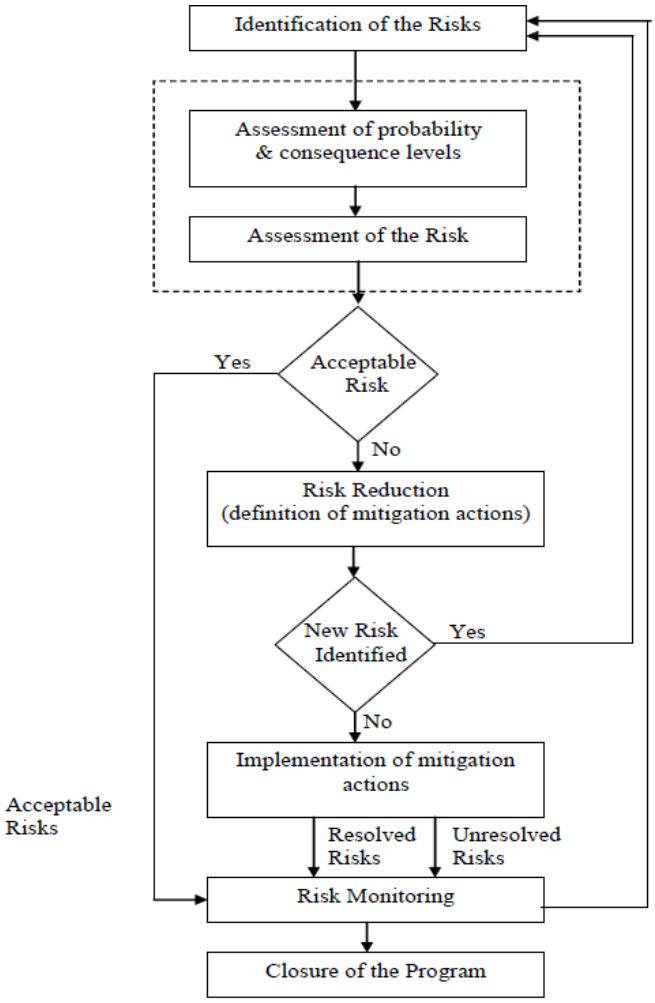

Figure 12-2 Risk management process flow

- **Identification of the risks**: the first activity is the identification of the possible risks; this is an activity that involves all the project team; the result of this activity is the compilation of a risks list which is submitted to the risk management team.
- **Assessment of the risks**: the risk management team will assess the impacts and the probability of occurrence of risks. During the assessment of the risk and its evaluation, each risk will be assigned to a risk owner, or, if necessary, the risk will be apportioned to more responsible persons. In case that the apportionment involves also the Customer, the relevant apportionment shall be discussed and agreed.
- **Acceptability of the risks**: the risk management team will evaluate, by the computed risk ranking, the opportunity to apply mitigation actions or accept the risks as they are, limiting the activities to the monitoring of the events in order to control that the risk criticality remains negligible.

- **Reduction of the risks**: performed by mitigation actions. The risk management team will evaluate and define the mitigation actions; the actions, after approval by Program Management, will be implemented, monitored and controlled.
- **Monitoring and Communication**: the risks and the status of mitigation actions will be continuously monitored, by updating the risk forms. From these, the ranked risk status will be extracted to give the visibility to the Customer, if needed. The ranked risk status will be provided to the Customer according to the needs of the project (to be defined in agreement with the Customer).

12.3.2 Risk Management Implementation

12.3.2.1 Risk identification

The first step in risk management is the identification of all individual risks that can affect the SBSP Project. The Project objectives are analyzed in terms of the risk domains of Technical Performances, Schedule and Cost.

12.3.2.2 Risk assessment

The purpose of this phase is to determine the magnitude (severity and likelihood) of the individual risks identified in the previous activity and to rank them. The Risk register (RR) and Ranked Risk Log (RRL) are used. The following scoring schemes have been adopted to fill the Risk Register (RR).

Scoring schemes

Score	Severity	Severity of consequence: impact on performance	Severity of consequence: impact on schedule	Severity of consequence: impact on cost
5	Catastrophic	Unacceptable, no alternative exist	Cannot achieve major project milestone	Leads to termination of the project
4	Critical	Major reduction, workarounds available	Project milestone slip > tbd month(s) or project critical path impacted	Project cost increase > tbd %
3	Major	Moderate reduction, workarounds available	Project team milestone slip < tbd month(s)	Project cost increase > tbd %
2	Significant	Moderate reduction, some approach re-	Additional activates required, able to meet	Project cost increase < tbd %

		tained	need dates	
1	Negligible	Minimal or no impact	Minimal or no impact	Minimal or no impact

Table 12-1 Severity of consequence

Score	Likelihood	Likelihood of occurence
E	Maximum	Certain to occur,
D	High	Will occur frequently
C	Medium	Will occur sometimes
B	Low	Will seldom occur
A	Minimum	Will almost never occur

Table 12-2 Likelihood of occurrence

Risk index diagram and mitigation scheme

The risk index diagram adopted to denote the magnitudes of the risks of the various risk scenarios is shown in Table 12-3.

Severity / Likelihood	1	2	3	4	5
E	Index = 5 Low	Index = 10 Medium UNACCEPTABLE	Index = 15 High UNACCEPTABLE	Index = 20 Very High UNACCEPTABLE	Index = 25 Very High UNACCEPTABLE
D	Index = 4 Very low	Index = 8 Low	Index = 12 Medium UNACCEPTABLE	Index = 16 High UNACCEPTABLE	Index = 20 Very High UNACCEPTABLE
C	Index = 3 Very low	Index = 6 Low	Index = 9 Low	Index = 12 Medium UNACCEPTABLE	Index = 15 High UNACCEPTABLE
B	Index = 2 Very low	Index = 4 Very low	Index = 6 Low	Index = 8 Low	Index = 10 Medium UNACCEPTABLE
A	Index = 1 Very low	Index = 2 Very low	Index = 3 Very low	Index = 4 Very low	Index = 5 Low

Table 12-3 Risk index diagram

Mitigation actions may already be identified and proposed in the Risk Form.

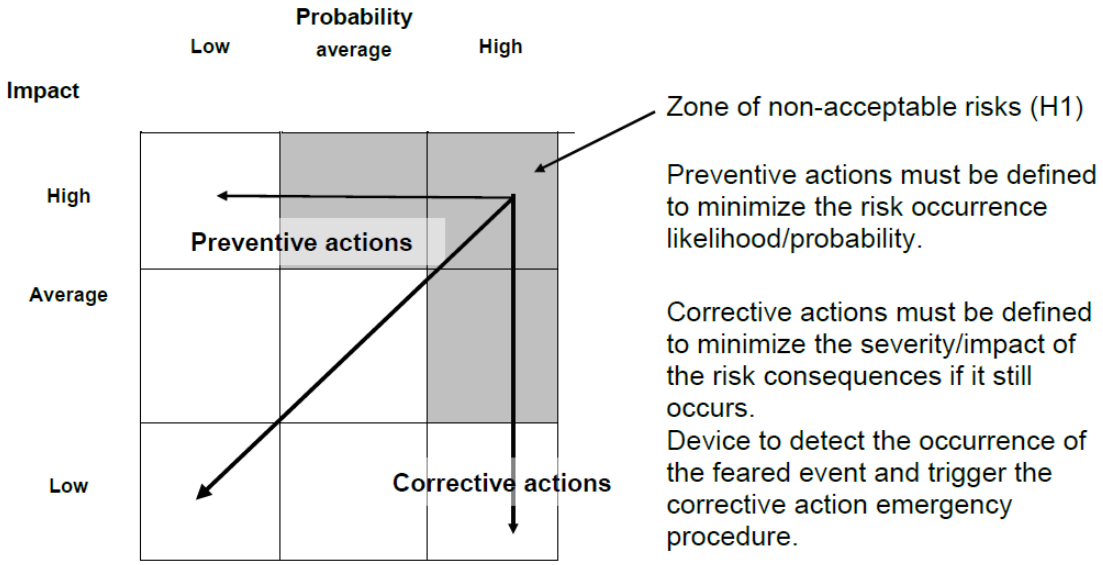

Figure 12-3 - Risk mitigation scheme

Each risk owner draws up a summary of the risks evaluated and actions proposed. The decisional hierarchy may become involved when the risks associated with the activity have causes or consequences outside the Program activities.

Risk monitoring and communication

All identified risks, associated risk avoidance, or mitigation actions, as well as identified contingency planning actions will be tracked and reported, by the risk owner, to the Risk management team.

The Risk management team will produce the Ranked Risk Status in accordance to the Risk Register. This is the primary form of reporting to the Customer.

12.3.2.3 Action criteria

For what concerns the actions to be taken on risks the following policy is adopted:

- risk marked in **green**: not managed
- risk marked in **yellow**: mitigation strategy and outlined contingency plan
- risk marked in **red**: mitigation strategy and detailed contingency plan

12.3.3 SBSP Preliminary Risk Analysis

This preliminary risk assessment is based on the SBSP architecture elaboration performed in chapter 4.

The risk register contains the following details for each risk:

- Risk ID/number;
- Risk title and scenario description;
- Risk evaluation in terms of Severity and Likelihood and resulting Risk Index;
- Type of Risk;
- Mitigation/recovery actions (“Pr” when the action is intended for reduction of probability, “Gr” when the action is intended for reduction of gravity/severity).

Additional non technical risks to be considered (not part of the risk register provided in Table 12-4) are the following:

- *The safety of the system and equipment* – for example the effects on other spacecraft (in lower orbits) of passing through the RF power beam and the tolerance of the satellite to debris, including the prevention of debris shedding;
- *Safety of people and wildlife* – agreements on acceptable safe RF beam intensity, both above and outside the rectenna, and strategies to ensure safety if beam lock lost and beam wanders off the rectenna will be required;
- *Environmental* – the effects of microwaves on flora, fauna, and the atmosphere, as well as carbon intensity will need to be better understood;
- *Standards* – a new energy generation technology will require new standards, especially the formation of international standards to allow interoperability between sub-system elements;
- *Security* – to maintain control of the satellite and the beam, ensuring security of a critical national infrastructure;
- *Public acceptability* – There will need to be a properly coordinated information programme to that the public receive the appropriate information so they can make informed decisions rather than be influenced by conspiracy theories.

Risk Number	Risk Title	Risk Scenario	Severity	Likelihood	Index	Type of Risk	Actions
Risk 3	Modular large-scale phased array antenna for highly efficient wireless power transmission	Technology to build large phased array antenna in-orbit not able to be achieved in time.	5	B	10	Technical	Pr: extensive technology development and demontrations required
Risk 1	Perosvkite development and qualification	Perovskite cell technology development delay resulting in schedule impact. So more massive cell techology need to be adopted resulting in mass increase and impact on economic feasibility.	5	B	10	Technical	Pr: extensive technology development and demontrations required Gr: identify alternative design solution
Risk 6	On-orbit robotic assembly technology	Capability to perform large-scale robotic assembly efficiently and affordably is not achieved	5	B	10	Technical	Pr: extensive technology development and demontrations required
Risk 7	Development of flexible structure that can be controlled by AOCS	Controllable lighweight flexible structure cannot be achieved resulting in mass increase for stiffness	5	B	10	Technical	Pr: extensive technology development and demontrations required Gr: identify alternative design solution
Risk 2	Launcher availability	If high cadence heavy-lift low-cost launcher is not available the concept cannot be economically viable.	5	A	5	Technical	Pr: start development of new european launcher as soon as possible
Risk 4	Succeptibility to orbital debris and production of debris	Design solution to protect against orbital debris and production of debris may result in substantial mass cost increase	4	B	8	Technical	Pr: extensive technology development and testing required
Risk 5	Cyberattacks actions	Cyberattack resulting in taking control of the SBSP system inducing off-nominal power beaming or interruptions	4	A	4	Technical	Pr: implement cybersecurity policies in SW/HW design for both space and ground segment Gr: monitor the System and plan contingency operations (e.g. switch-off power beaming) if any attack is detected

Table 12-4 Risk Register

A.1 Annex 1: DM4/DM5 model

Attached file: *Annex1_TN4 Digital Model-MBSE* including:

1. *capella132.zip*: Capella software
2. *HTML_export_18122023.zip*: model export in HTML format
3. *README.txt*: HTML export location instruction
4. *Solaris_18122023.zip*: Capella model

A.2 Annex 2: DM8 model

Attached file: *Annex3_SBSP_CAD_models.zip* including:

- *SBSP - Space Based Solar Power 20231030.stp*
- *SBSP - Space Based Solar Power 20231030.smg*
- *SBSP - Space Based Solar Power 20231102 - simplified.stp*
- *SBSP - Space Based Solar Power 20231102 - simplified.smg*

The simplified models include only details of the first half-wing for each side of the S/C, the phased array antenna and a portion of the central truss. These models require lower computational effort to be visualized.

The .stp and .smg files attached have been exported from CATIA V5.

END OF DOCUMENT